UNITED STATES DEPARTMENT OF COMMERCE
JESSE H. JONES, Secretary

NATIONAL BUREAU OF STANDARDS
Lyman J. Briggs, Director

✦

Journal of Research

of the

National Bureau of Standards

✦

Volume 26, Number 5

May 1941

[Published with approval of the Director of the Budget]

UNITED STATES
GOVERNMENT PRINTING OFFICE
WASHINGTON : 1941

For sale by the Superintendent of Documents, Washington, D. C. - - - - - Price 30 cents
$3.50 per year on subscription

The prices of the separate Research Papers appearing in this JOURNAL are given on the front cover page. If 100 or more copies of any separate are ordered, a discount of 25 percent is allowed. Those who desire copies of separate Research Papers should send their orders and remittances without delay to the Superintendent of Documents, U. S. Government Printing Office, Washington, D. C. This will aid him to determine the number of copies to be printed for sale. Research Papers are not printed from electrotypes, and usually no more reprints can be had when the first and only printing is exhausted.

MATHEMATICAL TABLES

A list of the mathematical tables now obtainable from the National Bureau of Standards is printed on page 3 of the Journal cover. New tables will be announced from time to time as they become available.

U. S. Department of Commerce National Bureau of Standards

RESEARCH PAPER RP1383

Part of Journal of Research of the National Bureau of Standards, Volume 26, May 1941

HAZARD OF MERCURY VAPOR IN SCIENTIFIC LABORATORIES

By Martin Shepherd and Shuford Schuhmann, and Robert H. Flinn,* J. Walter Hough,* and Paul A. Neal*

ABSTRACT

This paper is divided into two parts. The first part reports the determination of the amounts of mercury vapor found in the air of various ventilated and unventilated laboratories at the National Bureau of Standards and elsewhere. The new optical mercury-vapor detector devised by Woodson and produced by the General Electric Co. was used to secure this information. The concentrations found ranged up to 70 micrograms of mercury per cubic meter of air. Various sources of mercury vapor are described, as well as some measures taken to lower the concentration.

The second part, by members of the staff of the National Institute of Health, reports the results of extensive physiological and psychological examinations of 38 laboratory men who were exposed to the various concentrations of mercury vapor noted in part 1. The examinations of these men were made 3 months after the severest exposures had been terminated.

CONTENTS

Part 1. Mercury Vapor in the Air of Scientific Laboratories

Martin Shepherd and Shuford Schuhmann

	Page
I. Introduction	358
II. Detector and its operation	359
1. Detector and the sampling modification	359
2. Calibration of the detector	360
3. General behavior of the detector	362
III. Local sources of mercury vapor found in laboratories	363
IV. Amount of mercury vapor found in the air of various laboratories	365
V. Reduction of mercury vapor in the air of several laboratories tested	368
1. Effect of ventilation	368
2. Removal of local sources	369
3. Cleaning and reflooring	369
4. Removal of mercury vapor by iodized charcoal	369
VI. Respiratory experiment—retention of inspired mercury vapor	370

Part 2. Medical Examination of Thirty-Eight Workers

Robert H. Flinn, J. Walter Hough, and Paul A. Neal

I. Introduction	371
II. Examination of employees	372
III. Conclusions	374
IV. References	375

*From the Division of Industrial Hygiene, National Institute of Health, Public Health Service, Federal Security Agency.

Part 1. Mercury Vapor in Air

By Martin Shepherd and Shuford Schuhmann

I. INTRODUCTION

The danger of breathing mercury vapor has long been known. Considerable information concerning the physiological effects of this vapor is afforded by the researches of the United States Public Health Service and others.[1] The symptoms associated with mercury poisoning have caused many a moment's reflection on the part of imaginative laboratory workers. For instance, the long and interesting list of symptoms includes forgetfulness, a strong disinclination to work, mental fatigue, irritability, excitability, and other such matters associated with the daily history of normal people—both in and out of laboratories. Other symptoms such as headaches, digestive disturbances, and bad teeth are scarcely specific, but may furnish the excuse for a self-diagnosis which may cause unnecessary worry.

In real cases of chronic mercurialism such general symptoms as those mentioned are often present; but there are other more definite symptoms. However, no one wishes to observe these other symptoms in himself, and for this reason may be entitled to an occasional flurry of healthy concern over the condition of his laboratory with respect to the mercury hazard. There are then two direct questions to be answered:

1. What is the amount of mercury vapor in the air of various typical laboratories?
2. What is the permissible limit of mercury vapor in inspired air, *especially for daily exposure over long periods*?

Part 1 of this paper will confine itself entirely to the first of these two questions. Information concerning the second question is given in part 2.

While the two reports comprising this paper do not constitute a final answer to all cases, nevertheless they do give a general idea of what may be expected with regard to the hazard of mercury vapor in typical scientific laboratories. They are accordingly of interest to laboratory workers who have no clear idea of how much mercury vapor they may be dealing with, and what to expect from it.

The first question concerning the amount of mercury vapor to be expected is at least partially answered in this portion of the paper by the results of the examination of various typical laboratories, ventilated and unventilated, and containing different amounts of mercury (as liquid) of varying degrees of cleanliness. Among the laboratories examined were many devoted to typical as well as to special chemical and physical work. The laboratories were located at the National Bureau of Standards, the United States Department of Agriculture Experimental Station at Beltsville, Md., and the Geophysical Laboratory of the Carnegie Institution. Considerable concentrations of mercury vapor were found in some laboratories, although the general picture was not alarming. Remedial measures were taken where it was considered advisable.

[1] An excellent bibliography of this subject is given by Clark Goodman, Rev. Sci. Instr. 9, 233 (1938). Of particular interest are U. S. Public Health Bulletin 234, A study of chronic mercurialism in the hatters' fur-cutting industry, by Neal, Jones, Bloomfield, Dallavalle and Edwards; and U. S. Public Health Bulletin 263, Mercurialism and its control in the felt-hat industry, by Neal, Flinn, Edwards, Reinhart, Hough, Dallavalle, Goldman, Armstrong, Gray, Coleman, and Postman.

II. DETECTOR AND ITS OPERATION

1. DETECTOR AND THE SAMPLING MODIFICATION

Such a survey as that reported here could not have been successfully made without some such instrument as the GE optical detector. The various chemical methods that have been proposed are distinctly unsatisfactory. They are not only exacting and time-consuming, but are often inaccurate, usually because of the loss of mercury through volatility of its salts. One chemical method proposed by Nordlander,[2] based upon the reaction of mercury vapor with selenium sulfide, is successful for higher concentrations of this vapor in air. According to measurements made during the calibration of the optical detector, the lower limit of sensitivity of the Nordlander instrument is approximately 150 micrograms (μg) of mercury vapor per cubic meter of air. Since lesser amounts are of definite interest, the instrument was entirely unsuitable for a general survey of laboratories.

The new optical detector sponsored by the General Electric Co. was developed by Woodson.[3] Air to be examined is drawn by a motor-driven pump through a section of iron pipe, at one end of which is an ultraviolet lamp, and at the opposite end a photoelectric tube sensitive to the radiation from this lamp (2537 A). According to Woodson, the response of the phototube decreases when mercury vapor is present and scatters the radiation. The phototube is connected to a triode amplifier whose plate current is indirectly measured as an indication of the amount of mercury vapor present.

The particular instrument used in this investigation was intended for permanent installation rather than for portable use, and it was accordingly mounted on the laboratory equivalent of a tea cart. Only one modification of the instrument was made—and this without changing a single part of the original apparatus. In order to be certain of the result obtained, the instrument must be used virtually as a differential device—that is, air containing no mercury must be compared with the air to be examined. Instead of making this comparison simultaneously, which would be desirable, but for which the instrument was not designed, it was made by repeatedly switching from the mercury-free air to the laboratory air. This was done with a two-way steel cock connected to the inlet of the apparatus. The large (10 mm) bores of this cock offered no appreciable restriction to air flow. One inlet of the cock admitted air to be tested; the other admitted air which must pass through Hopcalite,[4] which quantitatively removes mercury vapor from air, and so provides the reference air needed. To prevent the Hopcalite from offering significant restriction to air flow, a relatively thin layer (15 mm) of this material with comparatively large surface area (about 20 cm^2) was supported on a screen within the glass tube acting as the absorbing vessel. The Hopcalite absorber has been tested from time to time by comparing air drawn through it with air taken directly from outdoors. No difference in composition was observed. The procedure used eliminated any effect of the rate of flow, to which the detector is somewhat sensitive.

[2] B. W. Nordlander, Ind. Eng. Chem. **19,** 518 (1927).
[3] T. T. Woodson, Rev. Sci. Instr. **10,** 308 (1939).
[4] Hopcalite is a proprietary catalyst for the oxidation of carbon monoxide. Hopcalite may now be obtained under the name Mercurysorb.

2. CALIBRATION OF THE DETECTOR

The detector was calibrated with air saturated with respect to mercury vapor at 0° C and known pressure. The amount of mercury in the air was calculated from the total pressure at the exit of the saturator and the known saturation pressure of mercury.[5] The calculated percentage by volume was reduced to milligrams of mercury per cubic meter of air, assuming the density of mercury vapor at 25°C to be 8.2 g/liter. Proper saturation with respect to mercury was shown to have been attained by approaching the desired equilibrium from opposite directions—that is, air containing no mercury was passed through a saturator at 0°C, and thereafter air containing more mercury than corresponded to saturation at 0°C was passed through the same saturator now acting as a condenser. Concordant results were obtained. The amount of mercury in the air used for calibration was varied by diluting the saturated air with air containing no mercury.

The apparatus used for this calibration is shown schematically in figure 1. Air containing no mercury entered the apparatus at the left under a pressure of 8 lb/in.[2] The stream was divided and passed

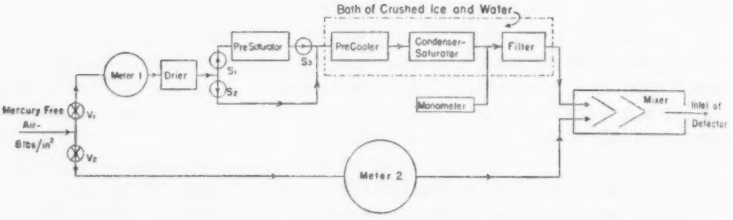

FIGURE 1.—*Flow diagram of apparatus used for calibrating the detector.*

at controlled rates through the two special needle valves, *V1* and *V2*. The portion entering the apparatus through *V1* was metered by a 1/20 ft.[3] wet test meter, and was then passed through a drier containing calcium chloride, which removed excess water that otherwise would have condensed in the saturator. After leaving the drier, one of two routes could be used. The air might be passed through a presaturator with stopcocks *S1* and *S3* opened and stopcock *S2* closed; or the presaturator might be bypassed by reversing the setting of the stopcocks. This operation could be accomplished without changing the rate of flow through meter 1. The presaturator was a 500-ml glass flask with inlet leading to the bottom, its walls completely coated with freshly condensed mercury. Air leaving the presaturator contained enough mercury vapor to correspond to approximate saturation at temperatures ranging from 40° to 25°C. Depending upon the procedure selected, air containing such amounts of mercury vapor, or no mercury vapor at all, next passed through a cooling coil, a condenser-saturator, and a filter. All three of these units were immersed in a bath of crushed ice and water held in a D'Arsonval tube. The condenser-saturator was a tall gas-washing bottle whose inlet terminated in a sintered glass disk which effectively subdivided the air stream. The disk was immersed in clean mercury, so that the air bubbled

[5] Int. Crit. Tables **3**, 205-206 (1928).

through a 5-mm layer of this continually stirred liquid. The filter was a pack of glass wool about 3 cm thick. No mercury could condense beyond the filter, since there the temperature was above 0°C. A manometer registered the pressure at the inlet surface of the filter. When air entering the precooler contained more mercury than corresponded to saturation at 0°C, the condenser-saturator acted as a final condenser; and when air entering the precooler contained no mercury, the condenser-saturator acted as a final saturator.

The air which contained mercury vapor was finally passed to the mixer, where it joined a stream of air containing no mercury. The latter stream, entering through *V2* and metered by a 1 ft³ wet test meter (No. 2), formed by far the larger percentage of the total air entering the mixer. The system was thus designed to insure proper equilibrium, since only a small portion of the total air need be saturated, and this resulted in relatively small rates of flow through the

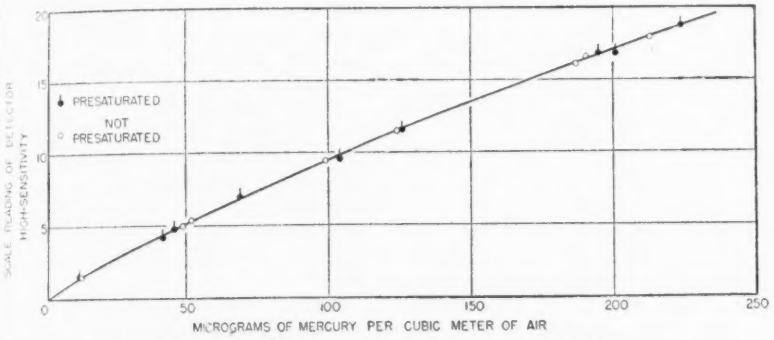

FIGURE 2.—*Calibration curve for high sensitivity setting.*

saturator. The mixer was a glass tube of about 6-cm diameter and 2 m long, provided with baffles. The inlet of the mercury-vapor detector projected about 20 cm into the mixer at the exit end. The total flow of air through the mixer always exceeded the amount drawn by the detector.

The two meters were compared under the actual experimental conditions which existed during the calibration of the detector. This was done by connecting meter 2 at the exit of the filter and making simultaneous observations of volume at different rates of flow.

During the actual process of calibration, the detector was repeatedly adjusted to zero reading with reference air containing no mercury, and a series of readings were taken, both with and without the presaturator in the line, with each definite setting of *V1* and *V2*. The two meters were read simultaneously. The data are plotted in figure 2. It will be seen that concordant results were obtained between the two methods of approaching equilibrium with respect to saturation with mercury. The sensitivity of the instrument may be varied, but the data given were all obtained with the detector adjusted to maximum sensitivity and a rate of flow of 0.5 ft³/min. At the lower concentrations, 1 scale division corresponds to approximately 9 μg of mercury per cubic meter of air. The full range of the scale is 20 divisions, and tenths of a division may be estimated without difficulty.

The highest sensitivity claimed by Woodson is 10 micrograms per cubic meter ($\mu g/m^3$), but our experience justifies the statement that an indication of half this amount can be relied upon under ordinary test conditions, and ± 0.1 of a scale division is usually significant under carefully controlled laboratory conditions.

3. GENERAL BEHAVIOR OF THE DETECTOR

During the entire progress of this work, the detector gave an excellent account of itself and repeatedly proved itself trustworthy. There were times when its indication was regarded with a moment's doubt, but in the end it always turned out that the operators and not the instrument had been fooled. A homely example will suffice to illustrate. Before the sampling device was installed, outside air was being compared with air in a hallway by alternately connecting and disconnecting a glass sampling tube by hand. No difference was observed between the two atmospheres; but when a chance observer made the test, there was an indication of mercury immediately upon his removing the fresh-air inlet. This was observed to vary as he repeated the operation, and it was apparent that the distance between his hand and the sampling inlet determined the extent of the response of the detector. It was then recalled that, a short time before, this observer had been left in the act of cleaning mercury from his bench, following a test of his laboratory. His right hand, which had been so employed, gave the upscale reading; his left hand, which had not been as industrious, gave no reading. From that time on, the operator's hand was required to show a clean blank, and actually touching the sampling inlet was avoided.

The response of the indicator to various substances other than mercury was examined. The list included all of the organic solvents to be found upon the shelf of the various well-equipped laboratories visited during the survey, as well as water vapor, carbon dioxide, illuminating gas, ozone, dust, tobacco smoke, and even some aqueous solutions of mercury salts. Marked responses to high concentrations of some organic solvents, ozone, and illuminating gas were noted. However, the use of the detector as specifically related to mercury vapor was in no way limited thereby, since the nose was always more sensitive than the detector. A room filled with a blue haze of tobacco smoke gave an indication of three times as much mercury vapor as was actually present; therefore, smoking was avoided in laboratories to be examined. The dust ordinarily present will not interfere. A comparison of mercury-free air, taken from outside and from inside of a building whose air was cleaned with an electrostatic precipitator, showed no difference. Insofar as our extended experience goes, the detector can be trusted to indicate mercury vapor alone if the nose can detect no organic vapors, ozone, etc., and no dust or smoke can be seen.

The detector is somewhat sensitive to changes in temperature and to rate of flow. The two effects are associated, although a second factor, namely, the catalytic oxidation of mercury by the *UV* lamp, influences the response, particularly at the lower rates of flow. The detector is designed to operate at a fixed rate. However, calibrations were obtained at 0.25, 0.5, and 0.75 ft^3/min, and were notably different. Changes in either temperature or rate of flow will cause a drift from

the zero adjustment, and our greatest difficulty with the instrument arose from this fact. The difficulty was overcome by the sampling unit already described. This permitted such rapid intercomparison of the reference air with that to be tested that temperature equilibrium was no longer a primary consideration, and the effect of rate of flow was eliminated by making the sampling rate equal to the reference rate.

It was suspected that the possible accumulation of dust upon the glass walls of the *UV* lamp and photo tube might alter the calibration of the instrument, but no such change was measured after several months of use. However, it is possible that changes from this or other sources may sometimes occur; therefore, the instrument should be recalibrated periodically until its behavior is better established.

III. LOCAL SOURCES OF MERCURY VAPOR FOUND IN LABORATORIES

The General Electric Optical Detector is admirably adapted to ferreting out local sources of mercury vapor, and many of these sources were explored during the survey of various laboratories. They will be noted now, since this will serve to give a general picture of laboratory conditions, which will later assist in understanding and interpreting the results reported for the average atmosphere of the same laboratories. It may be mentioned in this connection that many people seem to think that if mercury is exposed in a laboratory, the concentration of vapor within the entire room will be equivalent to saturation at the existing temperature. Fortunately, this is very far from true, since the mercury vapor from relatively small sources is quickly diluted by the air supplied by normal ventilation.

Mercury spilled upon a bench or floor is perhaps the commonest source of its vapor in most laboratories. The following example shows what happens after mercury is spilled. Nearly 100 ml of mercury was discharged from the top of a buret and fell about 1 meter to the bench below. Most of it collected as a pool upon the bench (designed to trap mercury), although some reached the floor and the side of an adjacent bench. The room was 20 by 18 by 11 ft., and was ventilated with eight complete changes of fresh air per hour. The room temperature was approximately 25° C. The air was examined at nose level 6 ft. from the bench. Fifteen minutes after the mercury was spilled, the air contained 120 μg of mercury per cubic meter. Twenty-four hours later the concentration had decreased to 60 $\mu g/m^3$, and after another 28 hours to 35. The bench top was then shaken by blows of a mallet. Ten minutes thereafter the concentration in the air was again 120 $\mu g/m^3$ cubic meter. This effect seems quite typical. Exposed mercury surfaces gradually collect a protective film of oxide, sulfide, grease, dirt, etc., which diminishes the amount of mercury vapor escaping. When the surfaces are freshened, the mercury again escapes in greater amounts. Another example of this effect was found in a small unventilated room, a portion of whose sheet metal (tinned) floor was amalgamated. The air of this room had repeatedly indicated 60 μg of mercury per cubic meter. The concentration had been so uniform and reproducible over a period of several months that the room had been used for brief experiments associated with respiration and with a reagent for

removing mercury vapor. One day the air of this room indicated almost no mercury vapor. While the senior author was pacing the floor wondering what had gone wrong with the detector, he remembered that the room had not been used during the past month. The pacing was continued at an accelerated tempo, and soon fresh surfaces of mercury had been rubbed up, and the air of the room again contained 60 μg of mercury per cubic meter. The higher concentration of mercury vapor usually found at floor level is reasonably explained by the fresh surfaces and elevated temperatures following the brisk massage applied by the sole of a shoe.

A bench top may hold mercury that cannot ordinarily be seen. For example, mercury was spilled upon a smoothly finished maple bench top. It was then brushed off, the bench top was carefully wiped off with a damp cloth, and no mercury could be seen. For months thereafter, the hand could first be held near the inlet of the detector to insure no response, then rubbed over the bench top and so made to give a high response. The microscope disclosed ample reason for the response of the detector; viewed so, the bench top was splattered with small globules of mercury.

Mercury kept in open containers is probably the second most common source of its vapor in most laboratories. If the mercury is left undisturbed over long periods and is visibly dirty, it may not yield much vapor. The air within a radius of 20 in. of open bottles containing such mercury indicated less than 10 $\mu g/m^3$; but when the mercury was disturbed by moving the container, the concentration increased immediately. The air at nose level near the mercury switch used with a resistance bridge and platinum resistance thermometer contained 20 $\mu g/m^3$ when the switch was at rest between readings, and 40 $\mu g/m^3$ for a moment after the position of the switch had been altered. The air at the atmospheric opening of a leveling bulb containing mercury showed 20 to 30 $\mu g/m^3$ at nose level 20 in. from the bulb, when mercury was flowing into the bulb. These observations were made in ventilated laboratories.

Mercury may sometimes fall upon surfaces which are heated at times. Often its presence in such spots is not suspected. During the survey of various laboratories, cylindrical rheostats, thermal insulation of diffusion pumps, ovens and such devices, and even electric lamps were found to be sources of mercury vapor. Amounts varying from 30 to 200 $\mu g/m^3$ were found at respiratory levels in the immediate vicinity of such apparatus. This concentration was greatly reduced at distances greater than 2 or 3 ft. from the source.

The exhaust of ordinary vacuum pumps of the oil-immersed type is often a source of mercury vapor. This happens if the pumps are drawing air across mercury surfaces, or acting as backing pumps for mercury-vapor pumps. The air within 10 in. of the exhaust of such pumps indicated mercury vapor in amounts varying from 60 to 200 $\mu g/m^3$.

Some types of high-frequency electric furnaces are prolific sources of mercury vapor.[6] The present practice is to place the furnace under a hood and remove the vapor by strong suction. Of various units so equipped, all but one examined in this survey were satis-

[6] Turner has reported a very serious case of this sort. The amounts of mercury vapor he found were much too low, because of the extremely large error inherent in the analytical method available at that time. U. S. Public Health Service Report 39, No. 8 (1924); and B. W. Nordlander, Ind. Eng. Chem. **19**, 522 (1927.)

factory; in the exceptional case, 30 $\mu g/m^3$ was found in the air immediately outside of the screen guard of the furnace.

In one laboratory, hot bituminous material was poured onto amalgamated brass plates. With the wind in the proper direction, 200 $\mu g/m^3$ was easily detected during the pouring process. The air immediately around a stack of the amalgamated plates, at room temperature, contained 20 $\mu g/m^3$.

While the following source does not strictly contribute mercury vapor to the laboratory air, it certainly does to the inspired air. It may therefore be included as important. A cigarette was tapped upon the maple top of a bench upon which mercury had been spilled and brushed off. No mercury was apparent on the bench top except by careful scrutiny through a magnifying glass. The end of the cigarette was examined under a low-power microscope. The tobacco held many small globules of mercury. Since tapping the cigarette prior to lighting it is a habitual practice with smokers, and a laboratory bench is often used for the purpose, this hazard should be realized.

IV. AMOUNT OF MERCURY VAPOR FOUND IN THE AIR OF VARIOUS LABORATORIES

In the report which follows, the amounts of mercury vapor noted are expressed in micrograms per cubic meter of air, and represent the average of three or more observations made at significant respiratory levels. Comparison with reference air was always made. When necessary, a glass tube with short rubber connection was placed so that its inlet was, as nearly as could be judged, in the space most frequently occupied by the laboratory worker's nose. The glass-rubber sampling inlet was repeatedly tested with mercury-free air to insure its freedom from contamination. (Rubber tubing is not to be trusted without such tests. It may have picked up organic solvents or even mercury. For this purpose, it must be free from talc.)

The survey was made during the winter months, and the laboratory windows were always closed. The room temperatures were approximately 25° C. Mercury had been spilled at one time or another in all of the laboratories examined. In many cases, it had been cleaned up and was no longer apparent; in other cases, more or less spilled mercury was visible.

The observations are given in table 1. The laboratories are divided into four groups with respect to the amount of mercury vapor found. A rough appraisal of the amount of spilled mercury, and specific sources of the vapor, are given for each laboratory. Ventilation is specified in somewhat general terms. "Natural" refers to steam-heated rooms, with ordinary unsealed doors and windows, and without forced ventilation. "None" refers to rooms without windows or vents, or rooms which have been reasonably closed for the purpose of maintaining constant temperature and humidity, where the ventilation occurs by occasionally opening and closing a door, or by seepage through materials of construction. Room 0 C was actually the nearest approach to a sealed airtight compartment. When forced ventilation was used, the number of changes of fresh air per hour is noted. The amount of mercury vapor found is expressed in micrograms per cubic meter of air.

TABLE 1.—*Survey of various typical laboratories with respect to mercury vapor in respiratory air*

Laboratory number	Type of laboratory	Kind of work done	Appraisal of mercury spilled on benches and floor	Other sources of mercury vapor	Ventilation—Numerals specify changes of air per hour. "Natural" means natural building ventilation	Micrograms of mercury vapor per cubic meter of air
GROUP I LABORATORIES—The air in all of these laboratories contained less than 4 μg of mercury per cubic meter. Mercury had been spilled on benches or floor some time prior to test. In some cases none of this mercury was apparent at time of test						
312 C	Chemical	Inorganic analysis	None apparent	None	8 to 10	<4
405 C	do	do	do	Several mercury seals	8 to 10	<4
221 L		Organic analysis	Very little	None	Natural	<4
208 M	Metallurgical	Chem., phys., and metall. research	Small amount	Two ventilated induction furnaces	do	<4
300 M	Physical	Barometry	None apparent	Barometers stored in sealed cabinet	do	<4
103 R	do	Office	do	None	4	<4
111 R	do	Radio wave meters	None	Amalgamated contacts	4	<4
112 R	do	Shop	do	None	4	<4
203 R	do	Electrolytic	do	do	4	<4
211 R	do	Radio frequency meters	do	do	4	<4
212 R	do	Radio piezo-oscillators	None apparent	Open manometers	4	<4
12 E	do	Batteries	None	None	4	<4
13 E	do	Current balance	do	do	4	<4
15 E	do	do	Very little	Amalgamated contacts	4	<4
16 E	do	Batteries	do	None	4	<4
18 E	do	do	do	do	4	<4
211–12 M	do	Metallurgical	do	Ventilated furnace	Natural	<4
308–10 M	do	Aeronautical instruments	Fair amount	Open manometers	do	<4
212 E	do	Capacitance and inductance	None	None	4	<4
214 E	do	Capacitance	do	Amalgamated contacts	4	<4
216 E	do	Insulation	do	None	4	<4
305 E	do	Radioactivity	do	do	4	<4
403 E	do	Standard cells	do	One open manometer	4	<4
408 E	do	do	do	None	4	<4
G 3	Phys.-Chem	Microscopy	do	do		<4
G 10	do	Gases and rocks	Considerable amount	Mercury in glass open to air		<4
G 12	Chemical	Gas analysis	Fair amount	Mercury in glass open to air		<4
G 23	Physical		None	None		<4

GROUP II LABORATORIES—The air in all of these laboratories contained 4 to 12 μg of mercury per cubic meter. Mercury had been spilled on benches or floor in all of these

GROUP II LABORATORIES—The air in all of these laboratories contained 4 to 12 μg of mercury per cubic meter. Mercury had been spilled on benches or floor in all of these laboratories some time prior to test. In all cases except one, some of this was apparent

103 I	Engineering	Mechanics	Small amount	None	Natural	4 to 8
236 B–I	Physical	Rubber	do	Dilatometer	do	6
323 I	do	Leather	do	Mercury in glass open	do	4
326 I	Phys.-Chem		do	Mercury regulator	do	4
211 W	Physical	Pyrometry	do	None	4	4 to 8
210 C	Chemical	Physical-Chemistry	do	Open manometers and vac. pumps	8 to 10	4 to 8
12 E	Dark room	Dry cells	None apparent	None	4	4
207 E	Physical	Soil corrosion	Small amount	Mercury open to air	4	5
312 E	do	Photometry	do	Vacuum pumps	4	5
209 C	Chemical	Distillation of gases		Mercury open to air, vacuum pumps and mercury in thermal insulation.	8 to 10	8 to 12
213 E	Physical	Condensers and inductance	do	Amalgamated contact	4	12
215 E	do			Oven with broken thermometer	4	8
308 E	do	Photometry	None apparent	Apparatus with small shaft revolving in mercury.	4	8
212 W	Office		Very little	None	Almost none	8 to 12
216 I	Physical	Textiles	None apparent	do	None	8
236 I	Shop	Mechanical	Fair amount	do	Natural	8

GROUP III LABORATORIES—The air in all of these laboratories contained up to 20 μg of mercury per cubic meter. In addition to spilled mercury, some special apparatus or unusual condition contributed mercury vapor

108 C	Chemical	Preparing pure compounds—purifying mercury.	Very little	Hg switch on Mueller bridge. Hg stills in special cabinet under hood. Hg switch used with resistance bridge. Latter responsible for highest local concentration in room.	8 to 10	4 to 20
208 C	Chemical	Gas analysis	Considerable	Gas analysis apparatus	8 to 10	12 to 20
406 C	do	Bituminous	Very little	Heated amalgamated brass plates	8 to 10	16 to20
23 B	Shop	Mechanical	Considerable			16
139 I	Ceramic	Porosity of ceramic bodies	Large amount	Immersion pans	Natural	20
336 I	Physical	Constant temperature room	Fair amount	Electrodes—contacts	12 ft³/min	16
	Shop	Glass blowing	Almost none	Hg on warm thermal insulation inside special oven of barometer-filling apparatus.	Natural	20

GROUP IV LABORATORIES—The air in these laboratories contained up to 70 μg of mercury per cubic meter. Some of the rooms were unventilated. All contained mercury spilled on floors and benches, but in general the lack of ventilation was the predominant factor involved

G 27	Physical		Small amount	Some of spilled mercury on warm bench top under heated furnace.		4 to 28
209 W	do	Pyrometry	do	Induction furnace—ventilated	4	6 to 24
244 I	Ceramic	Porosity of ceramic bodies	Large amount	Immersion pans (covered)	Natural	20 to 30
307 C	Photographic	Dark room	Small amount		do	24 to 40
111 E	Physical	Electrical resistance measurements	Considerable		do	20 to 50
23 B	do	Gas analysis	Large amount	Pools of mercury under cupboards	do	35 to 45
112 E	do	Electrical resistance measurements	Considerable	Mercury switches	do	16 to 56
0 C	do	Polarograph	Very small amount	Amalgamated tinned floor	do	60
00 E	do	Electrical resistance measurements	Very little		do	70
0 E	do	Gravity measurements	Small amount		do	60

A brief study of the table gives the following information. Of the 61 laboratories tested, 28 yielded less than 4 μg of mercury per cubic meter of air, 16 yielded amounts varying from 4 to 12 μg, 7 yielded up to 20 μg, and 10 yielded up to 70 μg. The amount of mercury vapor found depended primarily upon ventilation and thereafter upon the number and types of local sources, and the degree to which mercury surfaces were disturbed by mechanical means or mercury was vaporized by heating. The survey was not sufficiently extensive to justify any statistical correlation between the type of laboratory, in terms of physical or chemical, with the amount of mercury found, even though the largest amounts were found in physical laboratories. If such a correlation exists, it would probably find its natural explanation in the fact that chemical laboratories are generally very well ventilated, and special physical laboratories may not be. The total amount of mercury actually *used* is not the important factor. This is illustrated by comparing room 209 C, which yielded 8 to 12 $\mu g/m^3$ of air, with room 0 C, which yielded 60 μg. At least 500 lb of mercury is regularly used in room 209 C, and only a few grams in room 0 C. Although most of the mercury in the former laboratory is kept within closed glass vessels, the surface exposed to air far exceeds that exposed in the latter room, and in addition there are other local sources not present in the latter room. The difference lies in the ventilation.

In general, the survey should be comforting to those who work in well-ventilated laboratories and are not careless with their mercury. It may give a moment's pause to those who are too careless, and should cause some real reflection on the part of those who work with even small amounts of mercury in unventilated rooms. Whether such reflection is entirely justified is a problem for medical agencies. Until sufficient data have been collected to answer this question, the experiments outlined in the following two sections will be of interest.

V. REDUCTION OF MERCURY VAPOR IN THE AIR OF SEVERAL LABORATORIES TESTED

1. EFFECT OF VENTILATION

By far the most effective means of reducing the mercury content of laboratory air is ventilation. The effect of ventilation is illustrated in the following experiments.

Room 209 C was examined under the same conditions of temperature and exposure to mercury, but with varying degrees of ventilation. With approximately 6 changes of air per minute, the air contained 12 μg of mercury per cubic meter. With 8 to 10 changes of air per minute, 8 $\mu g/m^3$ was found. With 2 windows open and a slight breeze blowing in, the concentration dropped to 3.

Room 0 C contained 60 $\mu g/m^3$; with a small blower forcing in fresh air, the concentration dropped to 32.

Room 23 B contained 16 $\mu g/m^3$; with 2 windows open, the concentration dropped to 6.

2. REMOVAL OF LOCAL SOURCES

An example of what may be expected if local sources of mercury vapor are at least partially removed is afforded by the following experiment. The air of room 209 C contained 15 μg of mercury per cubic meter under the following conditions: A few globules of mercury were trapped in the asbestos insulation surrounding a mercury-vapor pump, which was operating and therefore hot; three Hyvac pumps were operating, drawing air over mercury and discharging into the room; a few globules of mercury were on the surface of a lighted 60-watt electric lamp; a few globules of mercury were visible on the floor and upon benches; the ventilation was 8 to 10 changes of air per hour; the laboratory temperature was 25° C. Then the exhaust from the Hyvax pumps was piped outside; the mercury was removed from the two heated surfaces, and partially (it can never be completely) removed from the floor and benches. Under these new conditions, and at the same temperature and degree of ventilation, the concentration was lowered from 15 to 4 μg of mercury per cubic meter.

3. CLEANING AND REFLOORING

Room 112 E, an unventilated physical laboratory, contained a great deal of spilled mercury. Much of this had collected in cracks of the wooden floor, and had even run under baseboards. Walking across the floor would raise the concentration of mercury vapor considerably. The room was subjected to a thorough house-cleaning. The mercury was carefully cleaned up, the baseboards were removed and the hoarded supply removed, the floor was treated with sulfur, oiled, and thereafter a sealed linoleum floor was installed. Previous to this work, the concentration of mercury vapor in this room was 16 to 60 $\mu g/m^3$ of air. After the cleanup, the concentration was lowered to 4 to 6 μg.

In this connection, it is well to remember that when mercury is spilled upon the floor of an unventilated room, enough will remain in cracks and uneven places, even after cleaning up, to yield a considerable amount of vapor if the floor is walked upon. This suggests the advisability of a mercury-free duckboard. A rubber mat which can be discarded when contaminated is one means of avoiding difficulty.

4. REMOVAL OF MERCURY VAPOR BY IODIZED CHARCOAL

Room 0 C, the small unventilated room lined with tinned sheet metal, which was previously mentioned, consistently showed the presence of 60 μg of mercury per cubic meter of air. A large ceiling fan circulated the air, and the concentration of mercury vapor was uniform throughout the room. A commercial device was installed which circulated air at the rate of approximately 250 ft^3/min over

(not through) iodized charcoal. The lowering of the amount of mercury vapor with time was as follows:

Minutes of operation of the purifier	Concentration of mercury vapor in micrograms per cubic meter of air
0	64
10	32
20	10
30	5
40	4
60	<4

VI. RESPIRATORY EXPERIMENT—RETENTION OF INSPIRED MERCURY VAPOR

The following simple experiment was performed by the senior author and H. Matheson of this Bureau. As noted previously, room 0 C was a tightly sealed space in which known concentrations of mercury vapor could be uniformly distributed. With the ceiling fan operating and an open surface of clean mercury (approximately 4 in.^{2} in area) placed within the room, it was possible to raise the concentration of mercury vapor to 200 $\mu g/m^3$ of air within 5 minutes. When the source of mercury was removed, the concentration remained nearly constant for 20 to 30 minutes.

Using this well-suited environment for the experiment, air containing known amounts of mercury vapor was inhaled and then exhaled through the mercury-vapor detector. The rate of exhalation was measured by a flowmeter, so that the detector was supplied at its normal sampling rate. When air containing 60 μg of mercury vapor per cubic meter was thus inhaled, the exhaled air contained no mercury vapor. When air containing 200 μg was inhaled, the exhaled air contained 8 to 12 μg in the case of one man and 0 to 8 μg in the case of the other.

It is true that the conditions of the experiment do not represent normal respiration, since inspiration was deep and the respiratory rate was not normal. Nevertheless, the ability of the lung area to quickly and almost completely absorb these amounts of mercury vapor is startling. If absorption during normal respiration is of the same order of magnitude as indicated by these direct experiments, it would be entirely possible for a worker, occupied 8 hours per day, in a laboratory containing 15 μg of mercury vapor per cubic meter of air, to absorb 72 μg of mercury in the course of a day's work. (This assumes a respiratory volume of 10 liters/min, slightly in excess of the average for activity corresponding to "standing" and less than corresponds to the average for "walking 2 miles per hour.")

With the absorption of anything like this amount of mercury, one would expect to be able to detect it in the urine of workers so exposed. It is worthy of note that mercury was found in the urine of three men,

whose exposures (before the laboratories were cleaned and reconditioned) were as follows:

Case 1.—Thirty-nine hours per week in room 208 C. About 30 hours per week working with gas analysis apparatus where the respiratory air contained 12 to 20 μg of mercury per cubic meter. Total period involved about 10 years.

Case 2.—Approximately 2 hours per week with same exposure as case 1. About 37 hours per week in room 209 C at a concentration of 8 to 12 $\mu g/m^3$. Total period involved about 20 years.

Case 3.—Exposure to 60 $\mu g/m^3$ in room 0 C was intermittent, the maximum periods being approximately 2 hours, with a total of about 6 hours per week. Total period involved about 2 years.

Urinary analyses in cases 1 and 2 were made by the Chemical Laboratory of the United States Army Medical Center, Walter Reed Hospital, in charge of Col. C. J. Gentzkow; tests in case 3 were made at this Bureau. The urinalyses were not quantitative, but in each case mercury was definitely isolated as the metal from the specimens. The physiological significance is not established, but it is suspected that such exposures had best be avoided if possible. These exposures were complicated, since in all three cases there was also opportunity for absorption through the skin, and in addition likelihood of contaminated cigarettes, particularly in the first two cases.

About 3 months after the concentration of mercury vapor had been reduced (as previously noted) in the worst of the laboratories reported in this survey, the National Institute of Health conducted a comprehensive series of physiological and psycological tests on 38 men from this Bureau who had previously been exposed to the various concentrations noted in table 1. The result of this investigation is given in part 2 which follows.

Part 2. Medical Examination of Thirty-Eight Workers

By Robert H. Flinn,[1] J. Walter Hough,[1] and Paul A. Neal [1]

I. INTRODUCTION

In recent years interest in industrial mercurialism has increased. This interest has been stimulated by United States Public Health Service studies of chronic mercurialism among workers engaged in the preparation of fur [1] and its fabrication into fur felt hats [2] and by a study by Markwith and his associates [3] in Ohio dealing with the problem of mercurialism among men engaged in the manufacture of copper amalgam. In connection with these investigations, attention has been attached naturally to the possibility of mercurialism occurring among workers in scientific laboratories, where often large quantities of mercury are used in such analytical procedures as gas analysis.

Turner [4] in 1924 made an investigation of mercurialism at the National Bureau of Standards. Nordlander [5] in 1927 showed the fallacy of earlier methods of measuring atmospheric mercury concentrations and presented a new method. Christensen [6] in 1937 warned of the danger of mercurialism in unventilated or poorly ventilated rooms. Goodman [7], Eltenton [8], and Giese [9] have dis-

[1] From the Division of Industrial Hygiene, National Institute of Health, United States Public Health Service, Federal Security Agency.

307823—41——2

cussed methods of control of the mercury hazard in laboratories. McCarroll [10] in 1939 published the results of a United States Bureau of Mines investigation of the hazard of mercury vapor in analytical laboratories of the petroleum industry and presented detailed recommendations for the control of this hazard.

In the Public Health Service study of the hatting industry [2], 59 cases of chronic mercurialism were found on medical examination of 534 hatters employed in 5 representative felt hat factories. These workers were engaged in the fabrication of felt hats from fur that had been previously treated with a mercury carrot. Four of the 21 mixers and blowers, 8 of the 34 coners, 6 of the 29 hardeners, and 33 of the 179 starters and sizers were so diagnosed. These men were working at processes that offered an average mercury exposure of 500, 270, 250, and 210 μg of mercury per cubic meter of air, respectively [1], as measured by the Nordlander instrument. The incidence of mercurialism was found to increase with increasing intensity and duration of mercury exposure. From these data it was concluded that 100 μg of mercury per cubic meter of air probably represents the upper limit of safe exposure. In the report of the hatting study, these values were stated in terms of *milligrams* per *10* m^3 of air.

Early in 1940 the Division of Industrial Hygiene, National Institute of Health, of the United States Public Health Service, received a request from the Medical Director of the United States Employees Compensation Commission to investigate the possibly harmful effects of working conditions on health in certain laboratories at the National Bureau of Standards, where large quantities of mercury were used as a confining fluid in gas analysis. A request was made for recommendations regarding any necessary steps to protect the employees who might be exposed to hazardous mercury concentrations.

In compliance with this request, the National Bureau of Standards was visited and it was found that mercury was being used in large quantities in the gas analysis laboratories, in laboratories for the testing of dental amalgams, and in certain other laboratories as described by Shephard and Schuhmann in the preceding part of this paper dealing with the environmental exposure of workers in these laboratories.

By means of a newly designed mercury detector [11], they were able to identify lower atmospheric concentrations of mercury in the workrooms than was possible with the Nordlander instrument, the range being from less than 4 to 70 μg of mercury per cubic meter of air. As stated in part 1 of this report, about 3 months prior to this visit an attempt had been made to control the atmospheric mercury exposure of these workers. This had resulted in a material reduction of such exposure.

II. EXAMINATION OF EMPLOYEES

In order to ascertain the possible effects of exposure to mercury, 38 employees of the National Bureau of Standards were examined, who had had varying degrees of exposure to mercury in the workrooms previously described. These examinations were made between June 28 and July 12, 1940. The duration of employment in such laboratories

varied from 1 year to 33 years and averaged 9.1 years. These medical examinations included a complete medical and occupational history and a physical examination with special attention to signs of mercurialism, such as intention tremor, abnormal psychic changes, vegetative changes such as abnormal blushing, sweating, and dermographia, and increased tendon reflexes. Intention tremor was also sought for by objective methods including a Porteus maze test, a handwriting test, and a psychologic test for hand steadiness. In addition to this, tests were given to determine reaction time, reaction-coordination time, and speed of tapping, as described in a recent study of the Public Health Service of fatigue among truck drivers [12]. Clinical laboratory examinations included hemoglobin determination (Newcomer), erythrocyte and leucocyte counts, differential white-cell counts, and determinations of stippled cells and reticulocytes. Routine urinalyses were made on all subjects. A chemical analysis was made for mercury in certain 24-hour urine specimens, using the method described by Goldman [2]. In addition, spectrographic determinations for mercury were made by the method described by Armstrong [2] on all 24-hour samples as well as on single specimens. A Kahn test was made on the blood of all persons examined, and the examination included an X-ray film of the chest.

Two previous studies of the Public Health Service in the fur-cutting and hatting industries had revealed 102 cases of chronic mercurialism among a group of 1,063 workers exposed. The average exposure of these workers varied from 20 to more than 700 μg of mercury per cubic meter of air. The symptoms observed in these examinations included complaints of tremor, psychic disturbances and nervous disorders, headache, drowsiness or insomnia, and weakness. The outstanding physical findings in this group of 102 cases included fine intention tremor; psychic disturbances, particularly irritability, excitability, timidity, apprehension, and restlessness; vaso-motor disorders as indicated by readiness to blush, excessive perspiration, and dermographism; increased tendon reflexes; gingivitis; and slight abnormalities of speech. The hatters with mercurialism tended to be underweight, to have increased systolic blood pressure, and to show albumin and red cells in the urine. At low atmospheric mercury exposures, the urinary mercury values were low and the range narrow. In successively higher atmospheric exposure groups, both the average value and the range of values increased, varying from 0 to 2.7 mg of mercury per liter. Many hatters with mercurialism were found to have measurable amounts of mercury in the urine, but these samples contained on the average slightly less mercury (0.297 mg of mercury per liter) than similarly exposed but nonaffected workers (0.413 mg of mercury per liter). No association was found between mercurialism and the hemoglobin content of the blood or reticulocyte and differential white-cell count.

It is known, of course, that any of the above symptoms and signs may occur in apparently healthy persons among the general population. Such was found to be the case in this study of 38 laboratory workers and in other studies of the Public Health Service among industrial populations not exposed to mercury. No individual was

found, however, in this study, with a sufficient combination of the above symptoms and signs of mercurialism to warrant a diagnosis of this disease, and those isolated symptoms observed were not of the degree of severity seen in hatters with mercurialism.

As a group, these 38 men were in good general health. The occurrence of tremor, psychic disturbances, abnormal reflexes, vegetative changes, and other abnormal physical findings was infrequent and was thought to be in about the same proportion as that for men of similar ages in industries with no mercury exposure. In no instance was more than a slight degree of tremor observed. This observation was substantiated by the results of the maze test, the hand steadiness test, and the handwriting test. As a group, they made good scores on the psychologic tests which measured manual steadiness, simple reaction time, reaction-coordination time, and speed of tapping. Spectrographic analysis of single and 24-hour specimens of urine revealed no measurable quantities of mercury (spectrographic threshold about 0.05 mg/liter). Spectrographic analysis of blood samples revealed no measurable mercury. Chemical analysis of fourteen 24-hour samples of urine revealed no mercury. X-ray examinations of the chest revealed two cases of healed, minimal tuberculosis. Clinical examination of the blood and urine revealed no findings of interest.

One subject differed notably from the others in that on the first of three examinations, he showed evidence of intention tremor and psychic disturbances and had a history of excreting measurable amounts of mercury in the urine several months previously. He was suffering from a serious and painful vascular disease, however, that may have contributed to these symptoms as they were much improved on subsequent examinations. On the other hand, the possibility of a previous attack of mercurialism with a few intermittent residual symptoms could not be excluded. In this one case, previous exposure to mercury vapor had terminated 7 months before the physical examination.

III. CONCLUSIONS

In conclusion, there was no medical evidence of mercurialism manifested by these 38 laboratory workers exposed to concentrations of from less than 4 to 70 μg of mercury per cubic meter of air. These findings are in agreement with those made in other studies on mercurialism by the United States Public Health Service. Those studies showed that only with exposure to concentrations of more than 100 μg of mercury per cubic meter, cases of mercurialism were found.

If working conditions in other laboratories are such that there is considerable doubt whether control measures for mercury exposure are adequate, it would be desirable to have an experienced industrial physician and industrial hygiene engineer evaluate the hazard and recommend suitable measures for its control.

IV. REFERENCES

[1] P. A. Neal, R. R. Jones, et al. A study of chronic mercurialism in the hatters' fur-cutting industry, U. S. Public Health Service Bul. No. 234.
[2] P. A. Neal, R. H. Flinn, T. I. Edwards, et al, Mercurialism and Its Control in the Felt-Hat Industry, U. S. Public Health Service Bul. 263.
[3] R. H. Markwith, Industrial Mercurialism. Report of an Investigation. Ohio Department of Health (mimeographed) 1940.
[4] J. A. Turner, Mercurial Poisoning. A Report on Poisoning from Small Quantities of Mercurial Vapor. Reprint 903, from Public Health Reports (Feb. 22, 1924).
[5] B. W. Nordlander, *Quantitative methods for the determination of mercury vapor*, Ind. Eng. Chem., Anal. Ed. **19,** 522 (1926).
[6] H. Christensen, et al. *Acute mercury poisoning in a respiration chamber*, Nature **139,** 626 (1937).
[7] Clark Goodman, *Mercury poisoning*, Rev. Sci. Instr. **9,** 233 (1938).
[8] G. C. Eltenton, *Note on mercury poisoning*, Rev. Sci. Instr. **10,** 68 (1939).
[9] A. C. Giese, *Mercury poisoning*, Science **91,** 476 (1940).
[10] C. F. McCarroll, Hazard of mercury vapor in analytical petroleum laboratories. Report of Investigations No. 3475, U. S. Bureau of Mines (October 1939).
[11] T. T. Woodson, *A new mercury vapor detector.* Rev. Sci. Instr. **10,** 308 (1939).
[12] B. F. Jones, R. H. Flinn, E. C. Hammond, W. H. Wulfeck, R. H. Lee, D. D. Donahue, H. Specht, H. D. Baernstein, R. C. Channell, J. W. Hough, R. R. Jones, R. R. Sayers: Fatigue and Hours of Service of Interstate Truck Drivers. U. S. Public Health Service Bul. 265.

WASHINGTON, December 20, 1940.

U. S. Department of Commerce National Bureau of Standards

RESEARCH PAPER RP1384

Part of Journal of Research of the National Bureau of Standards, Volume 26, May 1941

FIELD EQUIPMENT FOR IONOSPHERE MEASUREMENTS

By Theodore R. Gilliland and Archer S. Taylor

ABSTRACT

Field equipment for the automatic recording of virtual heights and critical frequencies of the ionosphere layers is described. Such equipment is useful for special investigations, such as during solar eclipses, to supplement the systematic recording which has been in progress at Washington since 1932. A frequency range from 790 to 14,000 kc/s is covered. Only 1 minute is required for the recording cycle. Records are made on 35-mm positive film. The transmitter is pulsed by means of a Thyratron and resistance-capacitance network controlled by a magnetic synchronizing device. The equipment is mounted in an automobile trailer and is complete, including a primary source of power.

CONTENTS

		Page
I.	Introduction	377
II.	Transmitter	379
III.	Antenna system	380
IV.	Pulsing circuit	380
V.	Receiver	382
VI.	Recorder and control equipment	382
VII.	Power	384
VIII.	References	384

I. INTRODUCTION

The need for ionosphere recording apparatus that could be readily transported from place to place has been apparent since the beginning of systematic recording of ionosphere characteristics at Washington in 1932. Although more or less systematic observations are now made at a number of places on the earth, furnishing, to a limited extent, a world-wide picture of the changes in the ionosphere, the need remains for field equipment which can be used for special experiments requiring the selection of time and position of the observations.

Several examples of such special experiments may be cited to demonstrate the usefulness of transportable and self-contained recording equipment. Observations may be made in the paths of solar eclipses. These are of special interest in ionosphere studies, since they give, in a unique manner, an indication of the structure and mechanism of formation of the various strata. The extent of clouds of ions responsible for sporadic reflections may readily be investigated. The variation of the effects of ionosphere storms and sudden ionosphere disturbances, as well as the variation of the regular ionosphere characteristics with latitude and longitude, may be studied in detail. Measurements at high latitudes are of particular interest in the study of the relation of the earth's magnetic field to the ionosphere, as well as in the study of anomalies in transmission over paths that pass through high lati-

tudes. Also, the calculations now used to extend vertical-incidence data to transmission over a distance may be checked by direct observation.

Compactness and minimum weight are important characteristics which the equipment should have. It also should be arranged for ease of installation and be self-contained, including shelter, primary source of power, and means of transportation. The equipment should be capable of recording automatically for several days without attention.

Past experience has indicated the desirability of a system which would record more quickly and more frequently than any heretofore developed. Frequent operation is especially desirable for observations during such rapid ionosphere changes as solar eclipses, ionosphere storms, sudden ionosphere disturbances, and sunrise periods. Fast recording also offers a saving in power consumption and reduces the effect of interference with outside radio services caused by the recording. Furthermore, if the records are made frequently enough, and if they are properly registered on motion-picture film, it should be possible to project them as a motion picture. Such projection would be of value for demonstration purposes and would probably show in a unique manner the progress of changes in the condition of the ionosphere. Although the present recorder was not designed for this type of registration, its performance has demonstrated the feasibility of the method. The recording system described in this paper requires only 1 minute to make a complete record, and with some modification could be adapted for ½-minute operation.

Before setting down the details of the component parts of the apparatus, a brief general description of the experiment and quantities measured may be of value. The method of measuring the heights and ionization densities of the various layers is fundamentally that developed by Breit and Tuve [1][1], with numerous modifications which allow for automatic registration and for variation of the radio frequency over an extensive band [2, 3, 4]. The apparatus consists of a radio transmitter, receiving set, and recording oscillograph. The transmitter and receiving set are always in tune with each other, and their frequency is changed continuously over the band. Instead of having the transmitter emit a continuous wave, the emission is broken up into a series of short pulses of about 10^{-4} second duration. For each pulse transmitted the receiving set receives one pulse directly and, at short intervals of time later, others which have been reflected from the ionosphere layers. These time intervals give a measure of the heights reached in the ionosphere. The function of the recorder is to register these time intervals automatically so that a continuous record of heights of the ionosphere layers may be obtained. The low-frequency waves are in general returned from a lower layer where the density of ionization is low. As the frequency is increased, the waves penetrate farther into the lower layer until a certain critical frequency is reached. As the frequency is further increased, the waves pass through the lower layer and are reflected from the next higher and more intensely ionized layer, and so on. Every layer has a characteristic critical frequency from which its maximum density of ionization may be computed [5]. If the frequency is increased to a high enough value, the waves will pass through the highest and most intensely

[1] Figures in brackets indicate the literature references at the end of this paper.

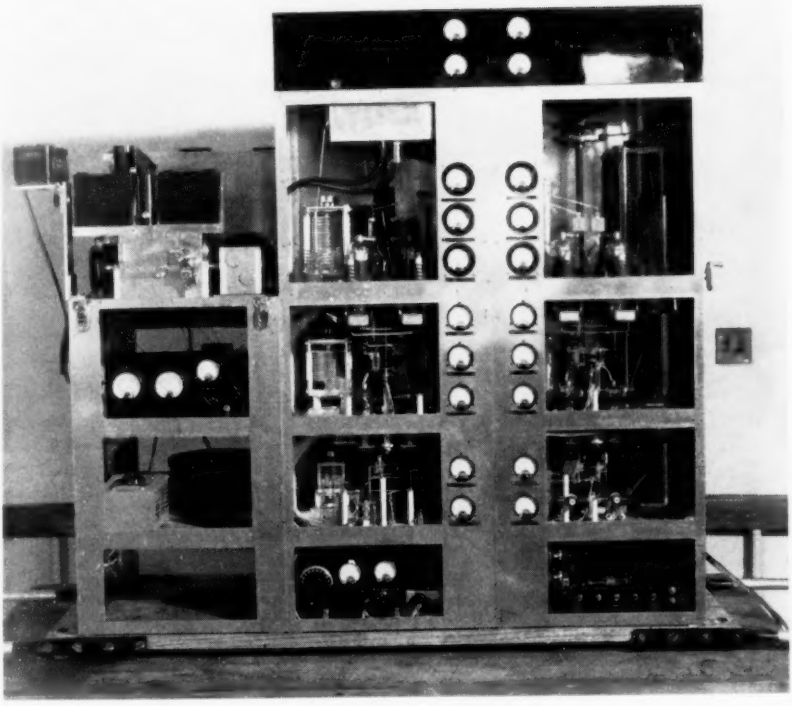

FIGURE 1.—*Front view of transmitter and recorder.*

The left-hand unit contains the recorder; the central unit contains equipment for frequency bands 3 and 4; and the right-hand unit, for bands 1 and 2.

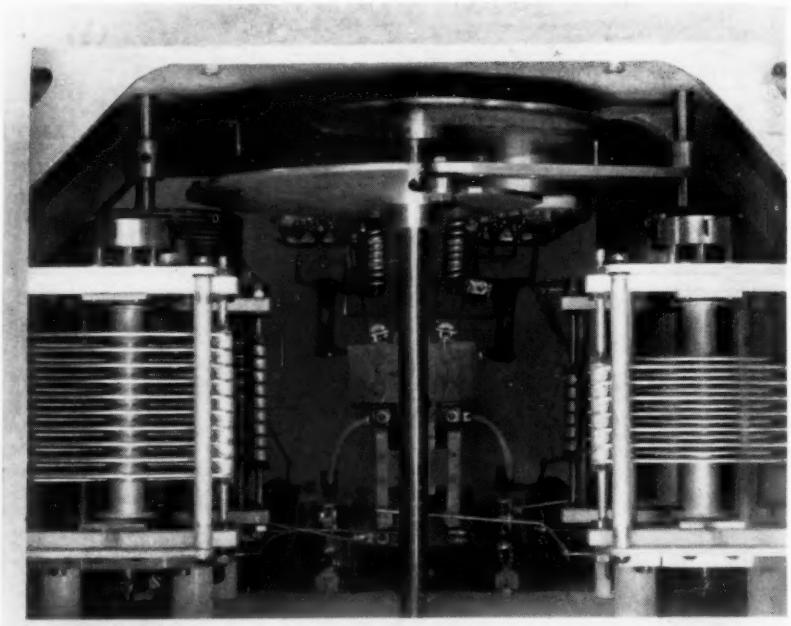

FIGURE 2.—*Rear view of one section of transmitter, showing the pair of cams used for tuning the condensers in the next section above the one shown.*

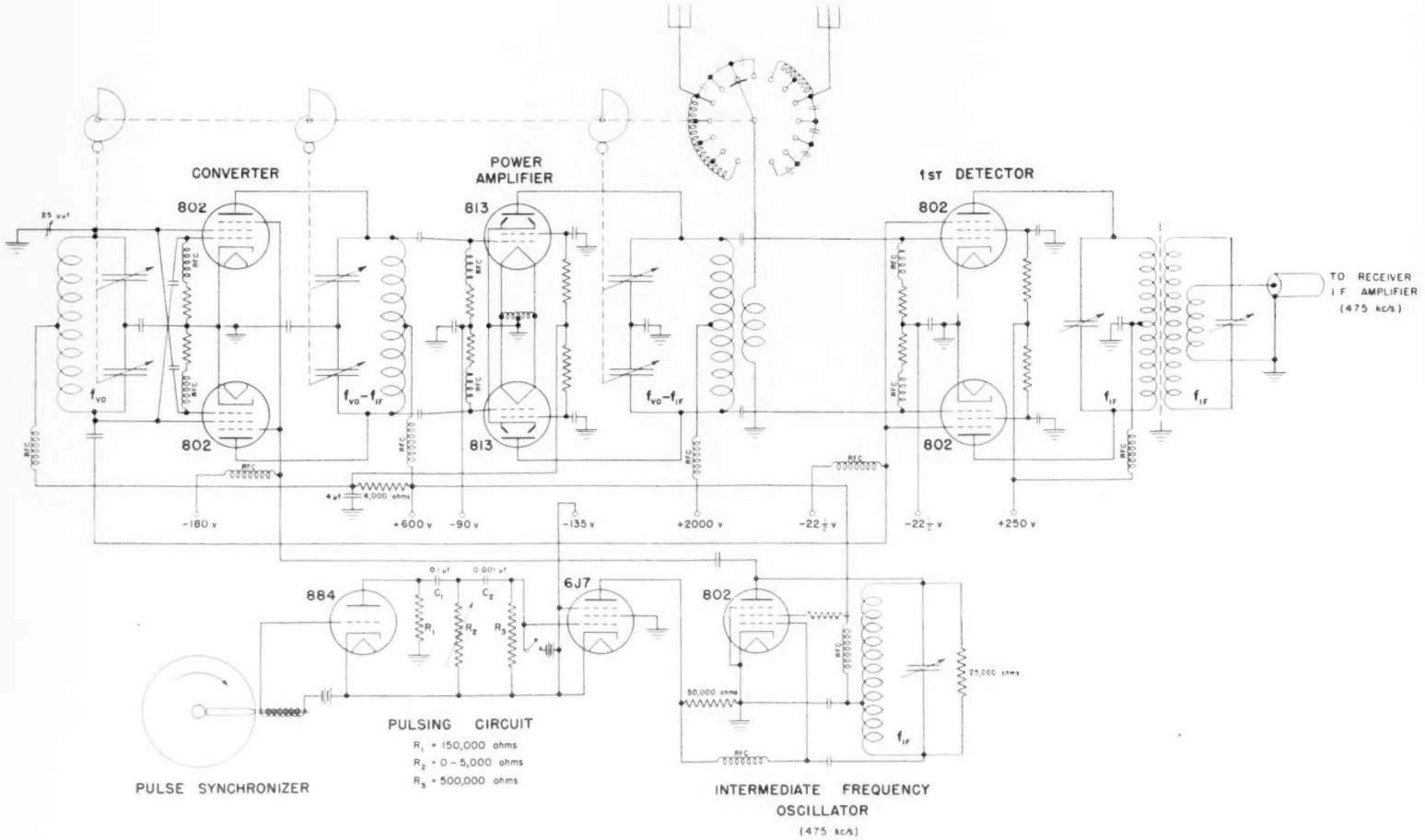

FIGURE 3.—*Simplified circuit diagram of one frequency band of the portable transmitter.*

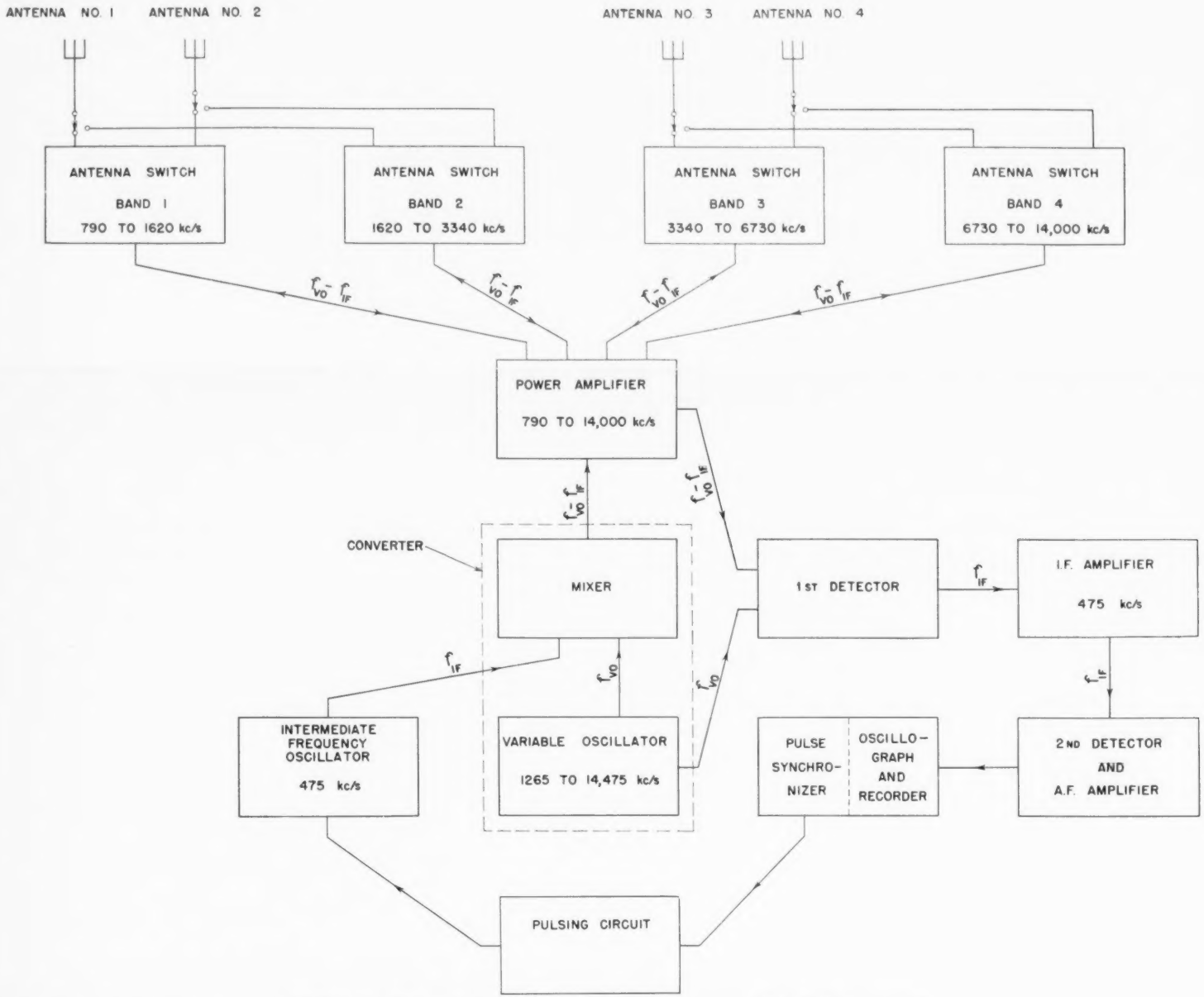

FIGURE 4.—*Block diagram, showing the method of operation of the entire apparatus.*

ionized layer and will not return to earth. With a sufficient knowledge of critical frequencies and virtual heights of the various layers, it is possible to interpret and predict certain characteristics of long-distance radio transmission. The large changes in these quantities with time of day, with season, and with phases of the sunspot cycle have already been studied in considerable detail [6]. With the field apparatus it is possible to study one more variable, that of geographical position, in more detail.

II. TRANSMITTER

The transmitter is composed of two units, each complete with a set of tubes and arranged for sweeping through two frequency bands. The limits of the four frequency bands are as follows: Band 1, 790 to 1,620 kc/s; band 2, 1,620 to 3,340 kc/s; band 3, 3,340, to 6,730 kc/s; band 4, 6,730 to 14,000 kc/s. Switching from one band to another is accomplished by relays. Each band requires three cams for operating the tuning condensers. Cams for the power amplifiers of bands 1 and 2 are shown in figure 2. The two transmitter units are contained in the central and right-hand sections shown in figure 1. The left-hand section contains the recorder.

Figure 3 is a simplified circuit diagram of one of the four bands of the transmitter with switching relays omitted. It will be noted in this figure, as well as in the complete block diagram of the system shown in figure 4, that the output frequency of the transmitter is always the difference between a fixed frequency, f_{IF}, and a variable frequency, f_{VO}. This circuit arrangement was devised [7] in order to maintain the receiving set always accurately in tune with the transmitter. The fixed, or *IF*, oscillator is set at a value equal to the intermediate frequency, f_{IF}, of the receiving set. This oscillator operates only during the time of each short pulse. During this time, its output is mixed with the variable oscillator frequency, f_{VO}, in the converter circuit shown at the left of figure 3. Thus, with the plate circuit of the converter tuned to $f_{VO}-f_{IF}$, the difference frequency will be impressed on the grids of the power amplifier tubes and will be amplified and emitted from the antennas. It will be noted that the variable oscillator utilizes the screens of the converter tubes while the fixed frequency, f_{IF}, is applied to the suppressors.

During the time of the pulse, $f_{VO}-f_{IF}$ will also be impressed on the grids of the first detector of the receiving set. After the end of the pulse, i. e., after the intermediate frequency oscillator stops, the tuned antenna and plate tank circuit of the transmitter power amplifier provide preselection tuning for the returning echoes. The signal voltage of the returning pulse energy is applied through the coupling condensers to the control grids of the first detector. Although the transmitter output is cut off with the stopping of the *IF* oscillator, the variable oscillator runs continuously, so that f_{VO} is always applied to the suppressor grids of the first detector. With the two frequencies, $f_{VO}-f_{IF}$ and f_{VO}, applied to the first detector and with the plate circuit tuned to f_{IF}, a voltage at this frequency will be applied through the transmission line to the *IF* amplifier. Thus, if the *IF* oscillator is always tuned to the same frequency as that of the *IF* amplifier, the receiving set is automatically locked in tune with the transmitter.

The rate of change of frequency is chosen so that the logarithm of

307823—41 (Page p. 379) No. 2

the frequency is proportional to time. With a pulse rate of 20 per second, the increment of frequency between pulses ranges from about 2 kc/s at the lower frequencies to 38 kc/s at the higher frequencies. Since the variable oscillator frequency is changing continously, the receiver will be slightly detuned at the time the signal returns from the ionosphere. However, even at high frequencies, where the rate of change is greatest, the receiver is detuned by only about 2 kc/s for signals returning from a virtual height of 400 km.

III. ANTENNA SYSTEM

Four L-type antennas are used, each antenna serving for two different frequency ranges. Each is used first in the ¼-wavelength range, and later in the ¾-wavelength range. Table 1 indicates the ranges for each antenna.

TABLE 1.—*Antenna frequency ranges*

Antenna number	¼ wavelength for—	¾ wavelength for—	Frequency ranges for which used
	kc/s	*kc/s*	*kc/s*
1	700	2, 100	790 to 1, 130 1, 620 to 2, 350
2	1, 000	3, 000	1, 130 to 1, 620 2, 360 to 3, 340
3	3, 000	9, 000	3, 340 to 4, 810 6, 730 to 9, 770
4	4, 300	12, 900	4, 810 to 6, 730 9, 770 to 14, 000

Tap switches attached to the camshaft are used to tune the antennas in the manner indicated at the top of figure 3. In the ¼-wavelength range condensers only are used, whereas in the ¾-wavelength range both inductances and condensers are used. The switch arms, contacts, and slip rings for bands 1 and 2 are shown at the top of figure 5.

The antennas are supported by guyed bamboo masts, each made up of three 12-foot sections. The arrangement as set up in the field is shown in figure 6.

IV. PULSING CIRCUIT

The pulsing voltage used to control the intermediate-frequency oscillator is generated by the discharge of a condenser through a grid-controlled Thyratron type 884 tube. Synchronization of the pulse with the rotation of the recorder mirror is obtained by means of a permanent magnet attached to the mirror shaft, with its magnetic axis perpendicular to the axis of rotation. An earphone with cover and diaphragm removed is supported near the rotating magnet, so that as the magnet passes the pole piece of the earphone, a voltage pulse is induced in the coil. The magnet is attached to the mirror shaft so that only one of its poles comes near enough to the earphone to induce an appreciable voltage. By shaping the pole of the rotating magnet and properly placing the earphone, a short pulse of about 100-volts amplitude can be produced for controlling the discharge of the 884 tube.

Figure 3 shows that condenser C_1 becomes charged through resistors R_1 and R_2. The bias voltage on the grid of the 884 tube is adjusted

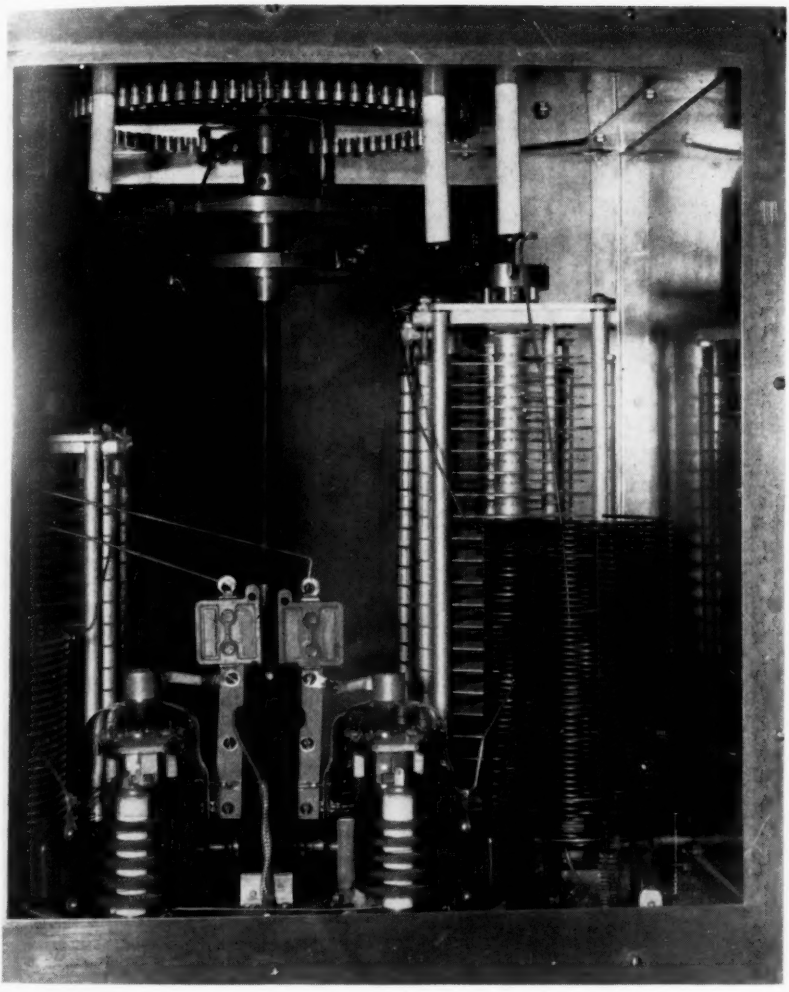

FIGURE 5.—*Power amplifier section of frequency bands 1 and 2.*
The slip rings, switch arms, and contacts for the antenna tuning switch are at the top.

FIGURE 6.—*Equipment as installed in the field, showing arrangement of bamboo masts and antennas.*

so that the condenser C_1 can discharge only when the synchronizing pulse is induced in the earphone. The network C_1R_2, C_2R_3 was suggested by N. Smith to aid in producing a pulse more nearly rectangular in shape than could be obtained with a simple resistance-capacitance circuit. The solid curve of figure 7 (A) represents the voltage applied to the grid of the 6J7 tube when condenser C_1 of figure 3 discharges. For comparison, the dashed curve represents the voltage applied to the grid of the 6J7 tube if C_2 and R_3 are eliminated. In figure 7 (B) the solid line indicates the shape of the pulse formed as the 6J7 plate current varies from saturation to cut-off. The dashed line shows the

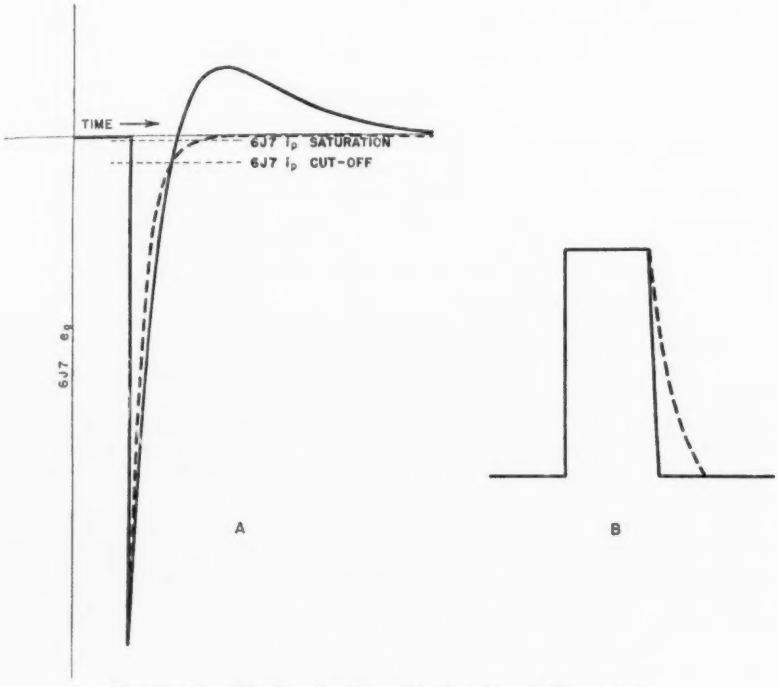

FIGURE 7.—*Graphs showing variations in pulsing circuit.*

A. The solid curve shows the voltage applied to the grid of the 6J7 tube when condenser C_1, figure 3, discharges.
The dashed curve shows the voltage which would be applied to the grid of the 6J7 if condenser C_2 and resistor R_3 were eliminated.
B. The solid line shows the shape of the pulse formed as 6J7 plate current varies from saturation to cut-off.
The dashed line shows the shape of pulse which would be formed if condenser C_2 and resister R_3 were eliminated.

shape of the pulse which would be formed if condenser C_2 and resistor R_3 were eliminated. It can be shown that the best shaped pulse is obtained if the time constant C_1R_2 is equal to C_2R_3 and if R_3 is large compared with R_2. In practice, however, either time constant may be as much as 10 times the other without seriously affecting the shape of the pulse. Therefore, only R_2 is varied when adjusting the duration of the pulse. Somewhat better control of the duration would be obtained by using ganged rheostats, or a step-by-step arrangement so that both R_2 and R_3 could be adjusted simultaneously with a single control.

The variations shown in figures 7 (A) and 7 (B) occur each time the magnetic synchronizer starts a discharge through the 884 tube. The voltages and load of the 6J7 are adjusted so that plate current saturation occurs with about minus 1 volt on the grid and cut-off with about minus 6 or 7 volts. When the 6J7 tube is drawing saturation current, the voltage across the 50,000-ohm resistor prevents operation of the *IF* oscillator. During the time of the pulse, the 6J7 tube draws no plate current, and the 50,000-ohm resistor then acts as the grid resistor of the *IF* oscillator. The tank circuit of the oscillator is loaded by means of a resistor, in order to damp out the oscillations more rapidly when the plate current of the 802 is cut off.

The key indicated with the pulsing circuit is used for transmitting identifying call letters and for testing purposes.

V. RECEIVER

Preselection tuning and operation of the first detector are described above. The *IF* portion of the receiver is a conventional transformer-coupled amplifier. The transformers are slightly overcoupled to produce a broad resonance peak. It has been found that a band width of about 10 kc is a satisfactory compromise between a wide band for faithful response to pulse signals and a narrow band for less interference from noise.

The audio portion must meet two rather rigid requirements: (1), a wide band (up to 10,000 cycles); and (2) quick recovery from signals other than pulse signals, as well as from exceedingly strong pulse signals. Resistance-capacitance coupled stages were used in preliminary tests but were found to block for a serious time interval when receiving a carrier. Replacement of the resistance-capacitance coupling by high-fidelity audio transformers was found to improve results considerably.

One of the desired chracteristics of the output circuit is that the output be limited so that all pulse signals above a certain level will be impressed on the oscillograph with the same amplitude. This is accomplished by applying the signal to the grid of the output tube in such a way that a predetermined signal level just cuts off the plate current. Therefore, no greater variation in plate current can be produced by any signal. The variations in plate current are transferred to the low impedance oscillograph through a high-fidelity matching transformer.

VI. RECORDER AND CONTROL EQUIPMENT

The recorder is identical in principle with the one previously described in detail [2]. A Duddell galvanometer-type oscillograph is used with a rotating mirror to record the time between the emission of the pulse and the reception of the echo. Through the use of proper lenses and masks, the direct pulse and each of the reflections produce traces on the photographic film or paper moving slowly parallel to the axis of the rotating mirror. Since the magnetic synchronizer described above is on the same shaft with the mirror, the direct pulse always occurs when the mirror is in the same position. Hence the direct trace is a straight line, whereas the traces for the echoes vary in position, depending on the virtual height of the reflection point. The recording film or paper is moved at a constant speed, and the

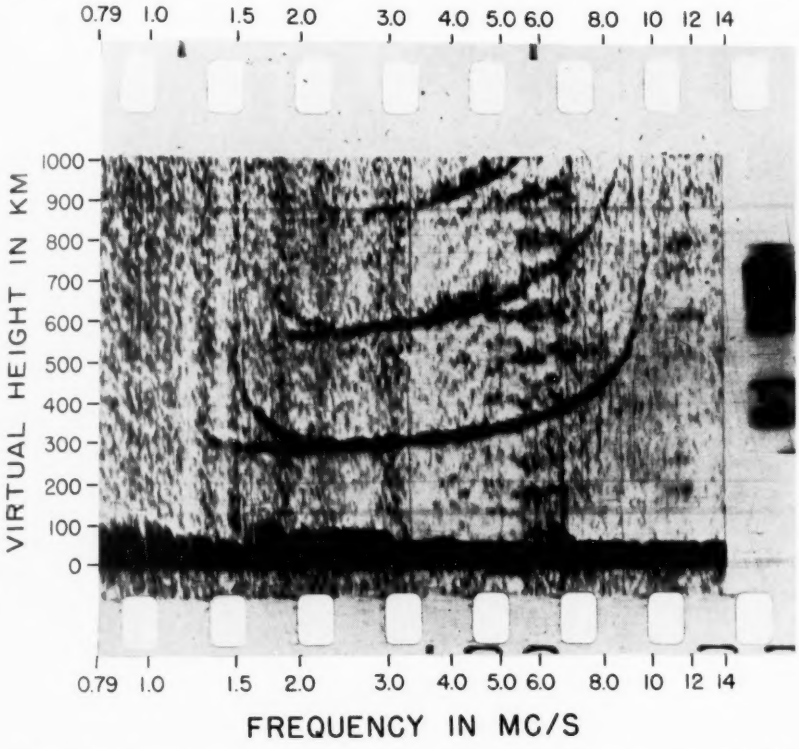

FIGURE 8.—*Sample record made with portable apparatus, September 27, 1940, 5:45 p. m., at Patos, Brazil, latitude 7°1′ S., longitude 37°17′ W.*

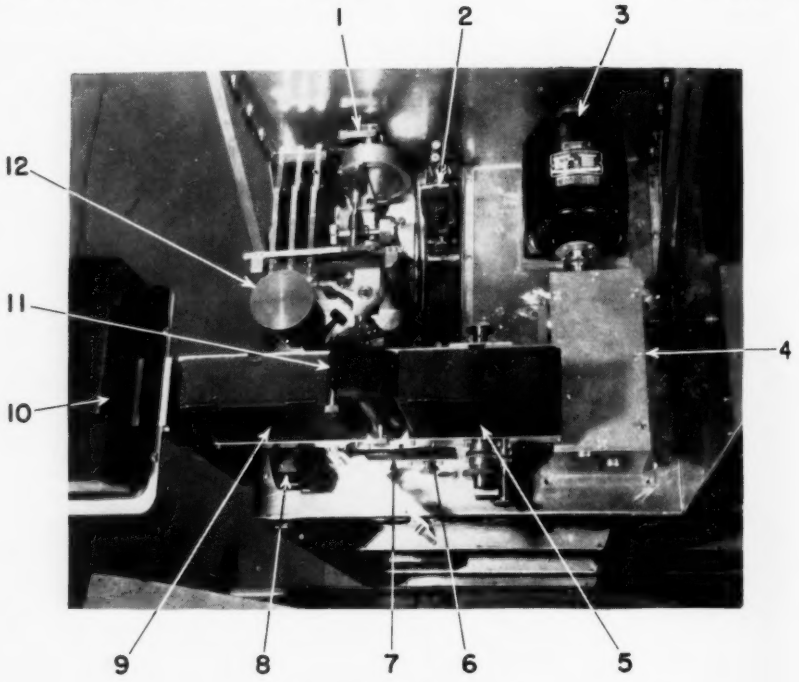

FIGURE 9.—*Recorder.*

1, control clock; 2, oscillograph element; 3, motor which drives recorder mirror, pulse synchronizer, film feed, and transmitter tuning cams; 4, gear box; 5, take-up magazine; 6, recording guide; 7, time-marking shutter (solenoid in rear); 8, pulse synchronizer (earphone magnet not shown); 9, supply magazine; 10, time-marking clock; 11, mirror to reflect image of clock onto film (the lens is supported in the tube below the mirror); and 12, lamp housing for time-marking lamp.

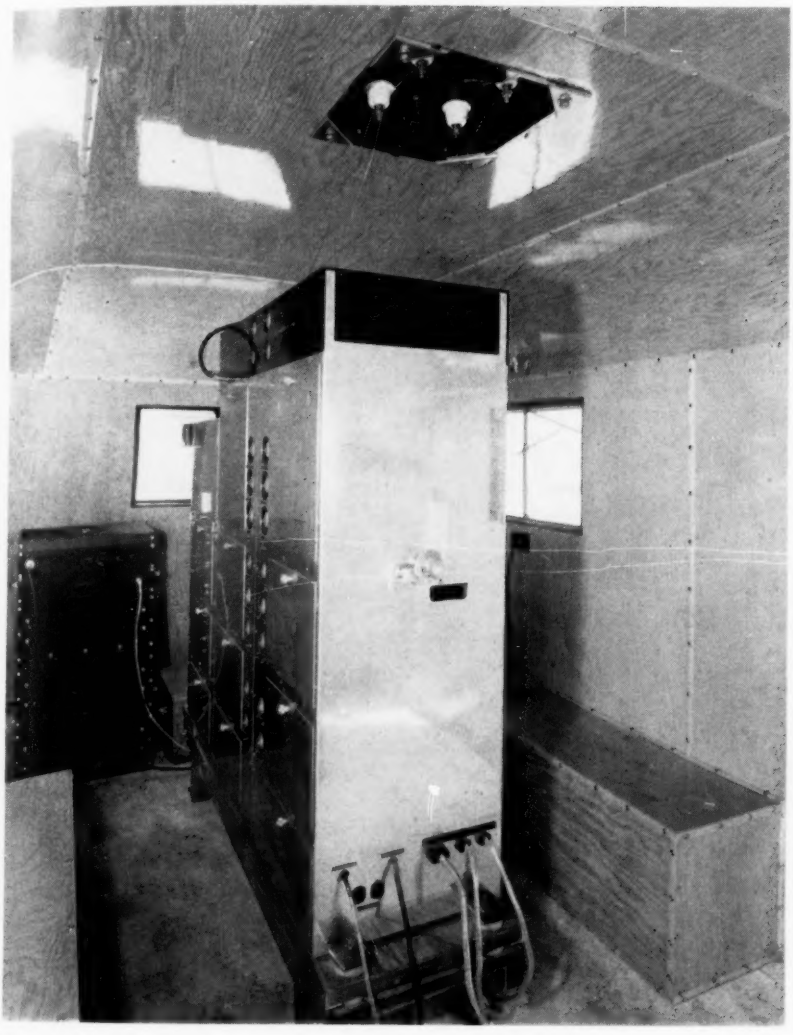

FIGURE 10.—*Interior of trailer, showing transmitter as installed for both transportation and operation.*

The receiver and power supplies are contained in the black box at left.

UNIV. OF MICH.

record can therefore be calibrated in terms of frequency versus virtual height.

In previous recorders, photographic paper has been used, permitting direct measurements without enlargement. For several reasons, however, it was decided to use 35-mm motion-picture film with the present equipment. In this manner the recorder itself was made smaller; less storage space, both for unexposed film and for completed records was required; developing and handling equipment was much more compact. Furthermore, it was found that positive film of the type used for sound recording could be used quite satisfactorily. Since this film actually costs less per foot than larger paper, and since many more records can be made satisfactorily per foot on 35-mm film than on large paper, the operating costs were greatly reduced. Another factor was the availability of standard parts for the construction of camera and recorder as well as equipment for development and handling. Finally, it was desired to make preliminary experiments on the idea of recording ionosphere phenomena for projection as a moving picture.

It is quite important to have the time at which each record was made marked on the film with the associated record. In the present equipment an image of a drum-dial synchronous clock is exposed on the film for each record by a solenoid-operated shutter.

The complete record with associated time mark occupies two standard motion-picture frames, i. e., 1 by 1½ inches. The frequency scale from 790 to 14,000 kc/s covers about 1⅝ inches and the time mark about ⅛ inch. Virtual heights of more than 1,000 km can be recorded across the width of the film. Figure 8 shows the arrangement of the record on the film. A small projector of the type used for projecting double-frame miniature camera transparencies is used for measuring and studying the records.

In previous recorders, separate motors have been used to drive the film, to rotate the mirror and synchronizing device, and to drive the transmitter tuning camshaft. This recorder uses only one motor, which performs all three functions through an appropriate gear box. This simplifies the control mechanism and helps to reduce the size, weight, and power consumption.

For the control of a self-contained system, an independent means of accurately timing the sequence of switching is required. For this purpose, a 60-cycle voltage is produced by a precision tuning fork. This voltage is amplified sufficiently to operate two synchronous clock motors. Both the tuning fork and the amplifier are designed to operate from the primary 32-volt d-c power source. One motor drives the time-marking clock mentioned above. The other drives a series of contactor cams, which provide for 2, 4, 20, or 60 complete records per hour. The accuracy of the frequency generated by the fork is such that during a week's operation in the field the clocks drifted less than 20 seconds from correct time. Figure 9 is a close-up view of the recorder unit showing the camera, contactors, time-marking clock, etc. Figure 1 shows the position of the recorder in relation to the transmitter.

In addition to the clock contactors, there are several contactor cams on the transmitter camshaft, which control the sequence of operations, such as turning on and off the high voltages, switching bands, marking the time on the record, etc.

VII. POWER

The primary source of power is a gasoline-engine driven generator producing 32 volts with a capacity of 28 amperes. This is used to charge two banks of automobile-type storage batteries. A small, high speed, 750-watt rotary converter is used to generate 115 volts at 60 cycles from the 32-volt supply. The converter is provided with a centrifugal governor controlling the field current to maintain the frequency constant to $\pm\frac{1}{2}$ cycle. Since speed is controlled by varying the field, the voltage regulation is poor. Hence it was found advisable to use a constant-voltage transformer.

The use of storage batteries has several advantages to compensate for the loss of efficiency and added weight. One important advantage is dependability. Failure of a mechanical source of power during an eclipse, for example, would be serious, if batteries were not floating on the line for standby. Constancy of voltage is another factor. Although the voltage drifts considerably during the discharge, it is a gradual change and is not subject to sudden periodic surges, as would be the case with a reciprocating engine.

It is expected that the equipment can be operated continuously, making a record every minute for about 4 hours without recharging the batteries. By running the gasoline-engine generator in parallel with the batteries, it should be possible to operate continuously for about 10 hours. By making only one record every 3 minutes, the time of operation on batteries alone may be greatly extended, and with the gasoline engine, the supply of fuel becomes the limitation.

The complete equipment is arranged for transport in a trailer and towing truck. The transmitter is mounted through rubber to the frame of the trailer and is both transported and operated in the position shown in figure 10. Auxiliary equipment is packed in boxes and may be transported completely in the truck and trailer. During operation the gasoline-engine generator, converter, batteries, and timing equipment are placed at a distance of about 200 feet from the trailer.

VIII. REFERENCES

[1] G. Breit and M. A. Tuve, *A test of the existence of the conducting layer*, Phys. Rev. **28,** 554–575 (Sept. 1926).

[2] T. R. Gilliland and G. W. Kenrick, *Preliminary note on an automatic recorder giving a continuous height record of the Kennelly-Heaviside layer*, BS J. Research **7,** 783–790 (1931) RP373. Proc. Inst. Radio Engrs. **20,** 540–547 (March 1932).

[3] T. R. Gilliland, *Note on a multifrequency automatic recorder of ionosphere heights*, BS J. Research **11,** 561–566 (1933) RP608. Proc. Inst. Radio Engrs. **22,** 236–246 (Feb. 1934).

[4] L. V. Berkner, H. W. Wells, and S. L. Seaton, *Automatic multifrequency technique for ionospheric measurements*, International Union of Geodesy and Geophysics, Assoc. of Terrestrial Magnetism and Electricity, Bulletin No. 10, p. 340–357, Trans. of Edinburgh Meeting, published Copenhagen, 1937.

[5] H. R. Mimno, *The physics of the ionosphere*, Rev. Mod. Physics **9,** 1–43 (January 1937). (This paper summarizes the theoretical analysis of the physical properties of the ionosphere and includes many references to other papers on the subject).

[6] J. H. Dellinger, *The role of the ionosphere in radio-wave propagation*, Trans. Am. Inst. Elec. Engrs. **58,** 803, (1939). (This paper gives a summary of the experimentally observed characteristics of the ionosphere and includes references to other papers on the subject.)

[7] T. R. Gilliland, *Ionospheric investigations*, Nature (London) **134,** 379, Sept. 8, (1934).

WASHINGTON, JANUARY 21, 1941.

U. S. DEPARTMENT OF COMMERCE NATIONAL BUREAU OF STANDARDS

RESEARCH PAPER RP1385

Part of Journal of Research of the National Bureau of Standards, Volume 26, May 1941

DEVELOPMENT OF TEXTURE IN COPPER BY COLD-ROLLING

By Herbert C. Vacher

ABSTRACT

The structural changes occurring in one polycrystalline and in five monocrystalline specimens as they were cold-rolled from 1- to 0.005-inch thickness were studied largely by X-ray diffraction methods. A pole-figure of the polycrystalline specimen after 99.5-percent reduction indicated twin 110–1$\bar{1}$2 and twin 112–$\bar{1}\bar{1}$1 orientations as the preferred orientations of severely cold-rolled copper. The macrostructure of cross sections of monocrystalline specimens, after increasing reductions, showed that in some specimens two or three distinct layers were developed whose boundaries were approximately parallel to the rolling plane. Changes in orientation showed that the lattices of adjacent layers of a monocrystalline specimen rotated in opposite directions around axes nearly parallel to the transverse direction to positions approximating two of five intermediate orientations. Orientations present after 99.5-percent reduction indicated that the five intermediate orientations were in the process of being changed to twin 110–1$\bar{1}$2 or twin 112–$\bar{1}\bar{1}$1 orientations.

CONTENTS

	Page
I. Introduction	385
II. Procedures	386
1. Preparation, cold-rolling, and metallographic examination of monocrystalline specimens	386
2. Determinations of average orientations after reductions of 90 percent and less	388
3. Construction of diagrams showing orientations present after 99.5-percent reduction	392
(a) Polycrystalline copper	392
(b) Monocrystalline copper	395
III. Results	395
IV. Discussion	399
1. Behavior of monocrystalline specimens during cold-rolling	399
2. Deformation bands	401
3. Development of texture in polycrystalline copper	402
V. Summary	403
VI. References	404

I. INTRODUCTION

Metallographic examination of polycrystalline copper that has been cold-rolled shows that, in general, the grains are elongated in the rolling direction, shortened in the normal direction, and almost unchanged in the transverse direction. Thus, the shape of a grain is oriented in respect to the principal directions of the strip. X-ray diffraction patterns of sections of rolled copper strip indicate that simultaneously with the change in shape of the grains there is a rotation of the crys-

tal lattices so that they approach or attain preferred orientations in respect to the principal directions of the strip. This oriented structure of the shape of grains and crystal lattices is called texture.

The preferred orientations are determined from stereographic diagrams called pole-figures, which show the prevailing arrangement of normals to a particular family of crystallographic planes, such as the cubic or octahedral planes. Schmid and Staffelbach [1][1] concluded from pole-figures of normals to the cubic and octahedral planes that there is only one preferred orientation in severely cold-rolled copper, this condition being defined when the [110] axis is parallel to the normal direction and the [1$\bar{1}$2] axis is parallel to the rolling direction.[2] A twin to this orientation, however, is indicated by the pole-figures of Schmid and Staffelbach. They undoubtedly considered the twin orientation in making their conclusion. It appears then that cold-rolling causes the lattice to rotate toward one of two preferred orientations having a twin relationship.

The texture of severely cold-rolled copper is similar to the texture of other face-centered cubic metals and alloys, such as aluminum, nickel and alpha brass. This similarity of textures has led to the belief that during cold-rolling the lattices of all face-centered cubic metals approach the same preferred orientations. Investigations [2, 3, 4] contributing information on the development of textures have indicated that preferred orientations not included in the texture of all face-centered cubic metals are sometimes attained. The purpose of the present investigation was to determine whether or not these orientations can be considered as transient or intermediate in the development of a severely cold-rolled texture in copper. This was done by cold-rolling relatively large monocrystalline specimens of copper and determining the structure after different degrees of cold work with the usual metallographic and X-ray methods.

II. PROCEDURES

1. PREPARATION, COLD-ROLLING, AND METALLOGRAPHIC EXAMINATION OF MONOCRYSTALLINE SPECIMENS

A charge of 4½ to 5 lb of tough-pitch electrolytic copper was melted in a graphite crucible to produce an ingot 1⅜ in. in diameter and 6 in. in length with the lower end tapered to a point. The melting was done in an Arsem vacuum furnace and the molten metal allowed to freeze slowly. This procedure [5] results in a monocrystalline ingot when the crucible is placed in the furnace so that the freezing begins at the pointed end and proceeds toward the top end. Ten monocrystalline ingots were made, and a typical monocrystalline ingot is shown in figure 1 (*A*).

The initial orientation of each of the 10 monocrystalline ingots was determined, using Greninger's back-reflection method [6], and, on the basis of these results, five different orientations were selected. A specimen was prepared from each of the five monocrystalline ingots by machining off its sides so as to produce two parallel surfaces, 1 in. apart, as is shown in figure 1 (*B*). The orientation of each of the five

[1] Figures in brackets indicate the literature references at the end of this paper.

[2] Throughout this paper, orientations in respect to the rolling plane and direction are defined by stating first the crystallographic axis which is parallel to the normal direction and then the crystallographic axis which is parallel to the rolling direction; thus the above orientation would be written as 110–1$\bar{1}$2.

monocrystalline specimens was determined accurately, and these orientations are shown on a stereographic diagram, figure 2, by the locations of the principal directions of each specimen in respect to the octahedral, dodecahedral, cubic, and icositetrahedral axes of a cubic crystal. The angular values for the initial orientations with respect to the [010] axis and (010) plane are given in table 1. The principal directions, X, Y, and Z, of the monocrystalline specimen coincide with the normal, rolling, and transverse directions, respectively, of the same after rolling—all rolling being done in one direction.

The monocrystalline specimens were cold-rolled to a final thickness of 0.005 in., care being taken always to keep the same side up and to

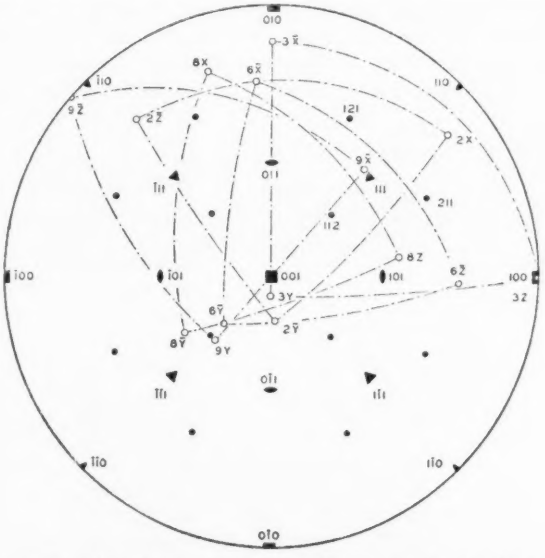

FIGURE 2.—*Stereographic diagram showing locations of principal directions of monocrystalline specimens in respect to crystallographic axes.*

enter the same end between the rolls during the entire reduction. The rolling was accomplished with a 16-in. diameter, two-high rolling mill operating at a speed of 50 to 80 rpm. This corresponds to a linear rolling speed of 3.5 to 5.6 fps. The reduction in thickness during each pass was from 0.03 to 0.05 in. Samples were cut from the end, first to enter the rolls, after each reduction of 0.15 in. until the thickness was 0.10 in. The specimens, after reduction to 0.10-in. thickness, were cold-rolled to thickness of 0.005 in. with a 5-in. diameter, two-high rolling mill operating at a speed of 50 rpm, corresponding to a linear travel of 1.1 fps. Similar samples of the strip of this thickness were cut from the end first to enter the rolls.

Metallographic examinations were made of polished and etched surfaces to show the structure of cross sections of the specimens at ¼ in. or more from the end first to enter the rolls. Samples representing 15-, 30-, and 45-percent reduction in thickness were photographed at a magnification of approximately 1½ diameters under oblique lighting. The source of light was an open window, the sample

being tilted at the angle that revealed the structure best. These photographs are shown in figures 3, 4, and 5. They are arranged in order of increasing reduction, and the upper edge in each case corresponds to the top rolling plane.

2. DETERMINATIONS OF AVERAGE ORIENTATIONS AFTER REDUCTIONS OF 90 PERCENT AND LESS

Diffraction patterns of a monocrystalline specimen after different degrees of cold-rolling show a gradual transition from a Laue pattern to a pattern consisting of arcs, characteristic of a severely cold-rolled polycrystalline specimen. The patterns indicate that the original crystal has broken into small fragments, known as crystallites. In small portions of the deformed specimen, the orientations of the crystallites diverge from a single "average" orientation that may differ from the specimen's initial orientation. The divergence in orientations of the crystallites increases as the degree of cold-rolling increases, and different portions of the specimen may show different average orientations. The determination of average orientation at different locations therefore can be used as a means of surveying the continuity and changes in position of lattice structure, assuming that agreement means continuity, although actually the lattice is badly distorted by the irregular alinement of crystallites. A survey of this kind was made of the five monocrystalline specimens of copper after 15-, 30-, 45-, and 90-percent reductions.

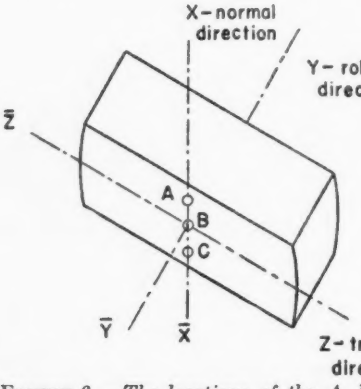

FIGURE 6.—*The locations of the A, B, and C areas on the polished surface of a typical sample used for metallographic examination.*

The method of surveying the cold-rolled specimens after reductions of 45 percent or less was as follows: in the section XX'—ZZ', back-reflection X-ray patterns were made using molybdenum radiation of three locations, A, B, and C, in the line X—X', as shown in figure 6. The average orientations indicated by these patterns, as well as the orientations of the undeformed specimens, then were plotted, by the location of octahedral poles, on stereographic diagrams, figures 7 and 8, using the XX'—ZZ' planes as projection planes. Thus the position of the lattice at the C location, on specimen 3, after 30-percent reduction is designated as the "3–30C position." The procedure used for determining the average orientations has been described and photographs of similar patterns have been shown in a previous publication [7].

The method, described above, of surveying the continuity of lattice structure was modified slightly so as to apply to specimens after 90-percent reduction. After 90-percent reduction, average orientations could be determined better from diffraction patterns of small

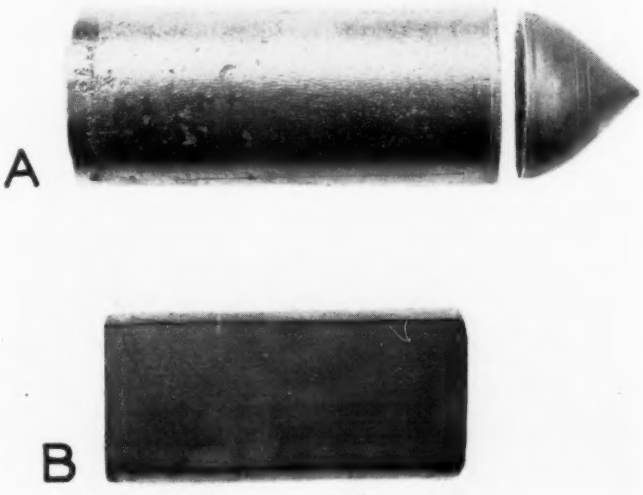

FIGURE 1.—*Monocrystalline copper.*

A, ingot, one-half actual size; surface view, with tapered end separated from body of ingot. *B*, specimen, one-half actual size; top view, showing machined surface.

FIGURE 3.—*Macrostructure of monocrystalline copper after 15-, 30-, and 45-percent reduction by cold-rolling.*

Approximately ×1½. Cross sections: *A*, specimen 9; *B*, specimen 2. Etched with 10-percent ammonium persulfate.

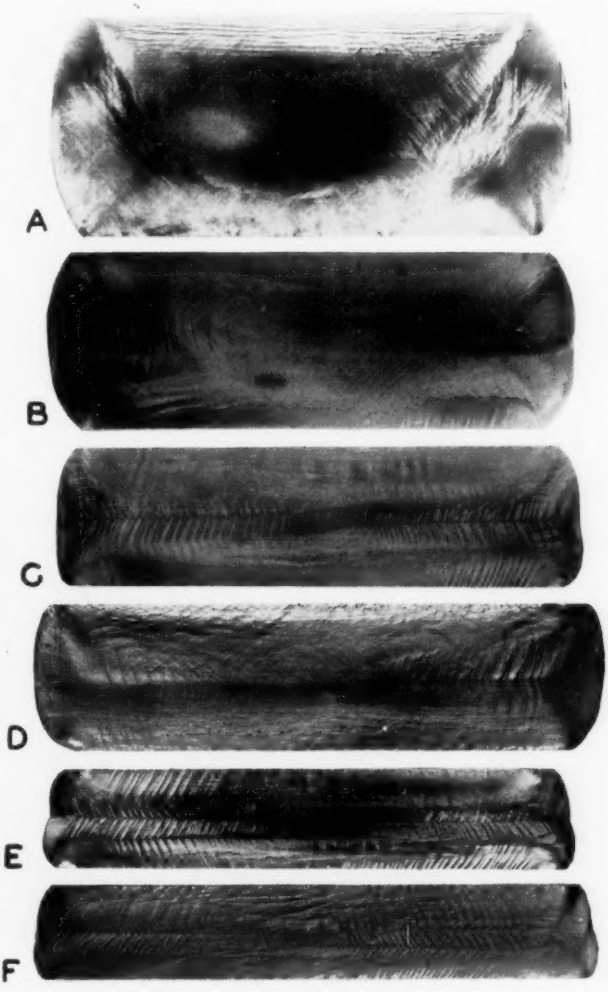

FIGURE 4.—*Macrostructure and end of monocrystalline copper, specimen 3.*

Approximately ×1½. *A*, *B*, *C*, and *E*, cross sections after 15-, 30-, 45-, and 69-percent reductions, respectively. Etched with 10-percent ammonium persulfate. *D* and *F*, photographs of the end first to enter the rolls, after 45 and 64 percent, respectively.

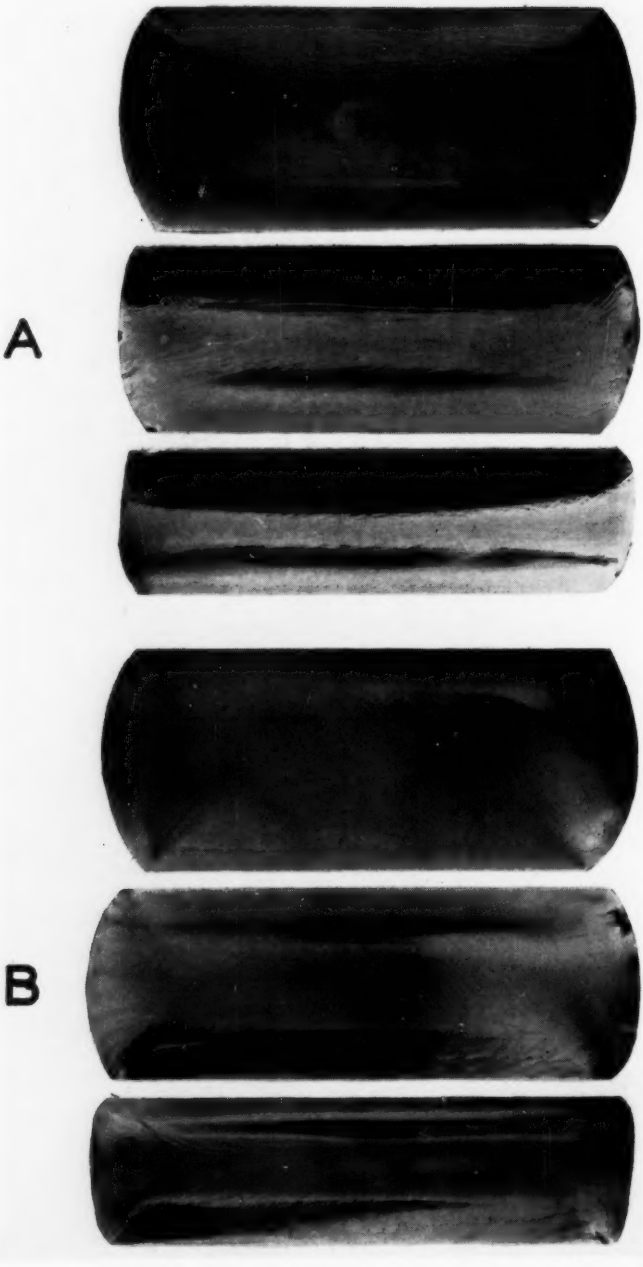

FIGURE 5.—*Macrostructure of monocrystalline copper after 15-, 30-, and 45-percent reductions.*

Approximately ×1½. Cross sections: *A*, specimen 8; *B*, specimen 6. Etched with 10-percent ammonium persulfate.

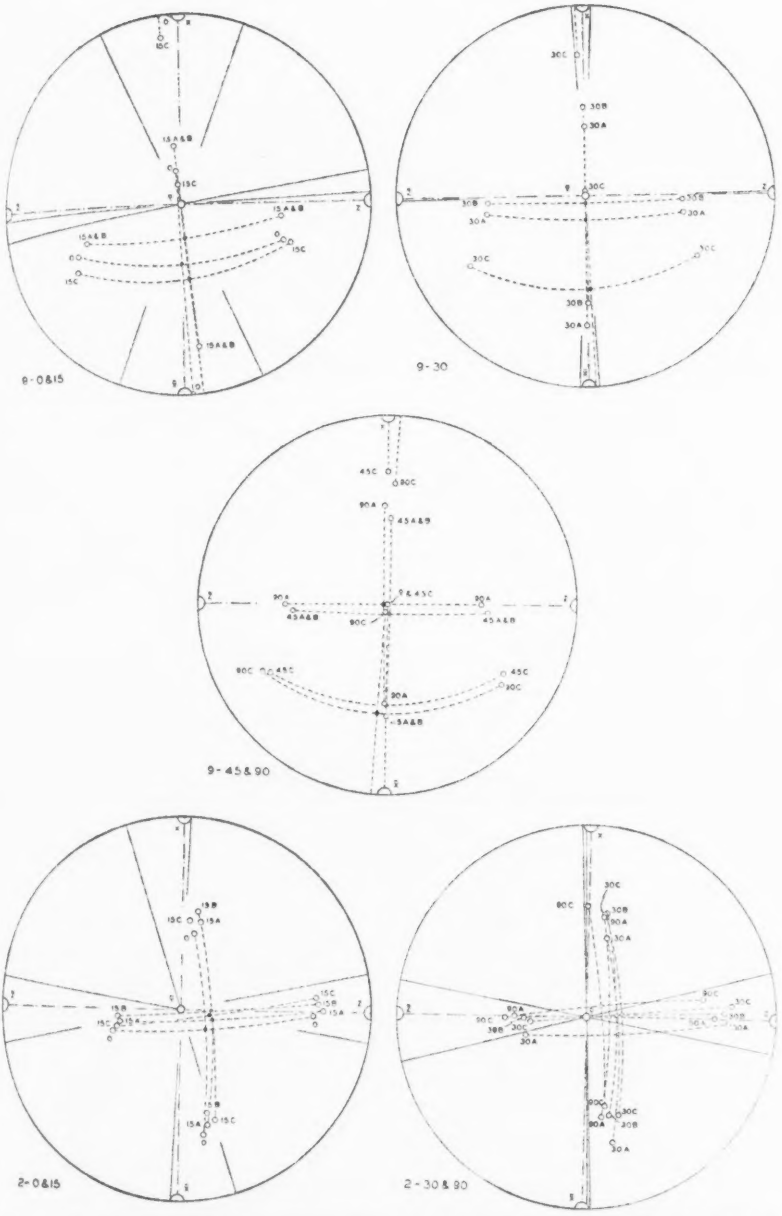

FIGURE 7.—*Stereographic diagrams showing initial orientations and positions of the lattice after 15-, 30-, 45-, and 90-percent reductions of specimens 9 and 2.*

areas located on the top and bottom rolling planes rather than on the line X—X', as shown in figure 6. The locations on the top and bottom rolling planes are referred to as A and C, respectively, because of their

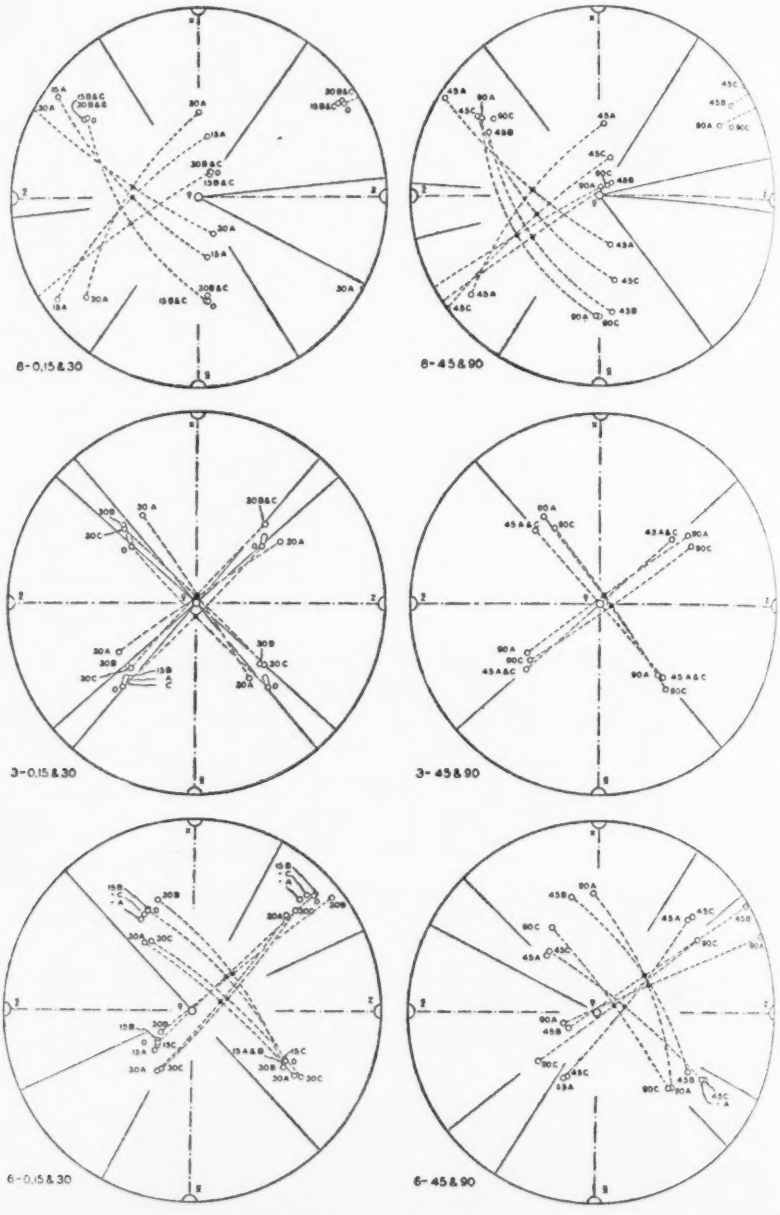

FIGURE 8.—*Stereographic diagrams showing initial orientations and positions of the lattice after 15-, 30-, 45-, and 90-percent reductions of specimens 8, 3, and 6.*

proximity to corresponding A and C locations on the *XX'—ZZ'* sections. Diffraction patterns of the A and C locations after 90-percent reduction consisted of long diffuse arcs, thereby making it

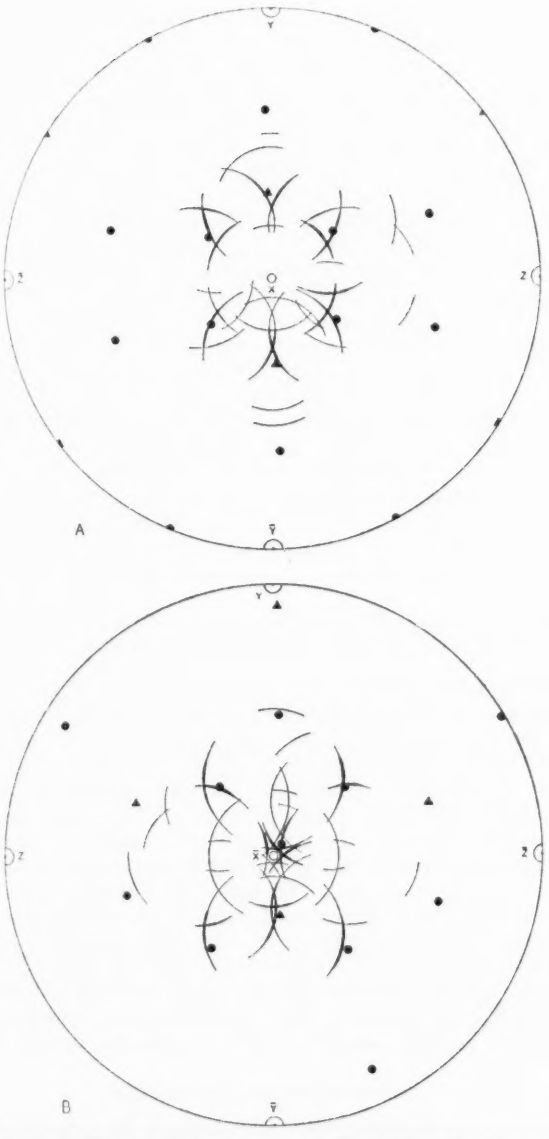

FIGURE 9.—*Stereographic diagrams A and B, illustrating the determination of the 9–90A and 9–90C positions, respectively.*

The arcs of large and small circles represent the arcs of intensity maxima in the 311 and 222 rings, respectively, from iron radiation. The solid circles and triangles are 311 and 111 poles, respectively.

impossible to determine the average orientation from a single pattern as was done for reductions of 45 percent and less.

The procedure used for determining the average orientations at different locations on specimens after 90-percent reduction is given

by describing the determination of the 9–90A and 9–90C positions. The arcs shown on the stereographic diagram of figure 9 (*A*) represent the intensity maxima in the 222 and 311 rings of a set of nine back-reflection patterns obtained with iron radiation. A similar set is represented in figure 9 (*B*). Each set included one made with the X-ray beam normal to the rolling plane and eight with the beam inclined at 30 degrees to the rolling plane, the sample being rotated through 45 degrees for each successive pattern. Before making the patterns, a layer about 0.001 in. in thickness was dissolved from the rolled surfaces of the sample. The purpose of this treatment was to remove the disturbed layer produced by the rough finish on the rolls, which shows itself in diffraction patterns as diffuse rings of uniform density. It can be seen from these diagrams that the area corresponding to diffractions from a particular (111) or (311) plane is large and equivalent to lattice rotations of 10 to 15 degrees from selected positions. The 111 and 311 poles of the selected positions are shown as solid triangles and circles, respectively. These selected positions (9–90A and 9–90C) are considered as being the average orientation of the crystallites and approximate the 110–001 and 112–$\bar{1}\bar{1}$1 orientations, respectively. In a similar manner the average orientations were determined for other cold-rolled specimens and are plotted by location of 111 poles, on the diagrams showing the average orientations after reductions of 45 percent and less, figures 7 and 8.

3. CONSTRUCTION OF DIAGRAMS SHOWING ORIENTATIONS PRESENT AFTER 99.5-PERCENT REDUCTION

Diagrams similar to those of figure 9 indicated that the divergence of the orientations of crystallites after 99.5-percent reduction was too great to permit separation of diffractions representing different octahedral planes. This made it impossible to determine the average orientation at different locations on the deformed specimen. It is very probable, however, that diagrams of this kind may indicate a transitory stage between the average orientations determined after 90-percent reduction and the preferred orientations of severely cold-rolled polycrystalline copper. In order to determine if this is true, stereographic diagrams, shown in figure 10, were constructed to show the following: (1) the 111 poles of the 90A and 90C positions; (2) maximum divergence of 111 poles of crystallites in cold-rolled copper after 99.5-percent reduction; (3) arcs representing intensity maxima in 111 and 222 rings obtained from molybdenum and iron radiations, respectively, of initially monocrystalline specimens after 99.5-percent reduction.

(a) POLYCRYSTALLINE COPPER

Pole-figures representing the orientations of crystallites in polycrystalline metals after different degrees of rolling show that the divergence of orientations is less when the degree of rolling is more. A pole-figure of polycrystalline copper that had been subjected to the same degree of cold-rolling as the initially monocrystalline specimens therefore is necessary in order that the maximum divergence of 111 poles of crystallites may be located accurately on the diagrams shown in figure 10.

A piece of oxygen-free hot-rolled copper,[3] 1 by 4 by 8 in., served as a

[3] The oxygen free copper was "Oxygen-Free-High-Conductivity" copper obtained from Revere Copper & Brass, Inc.

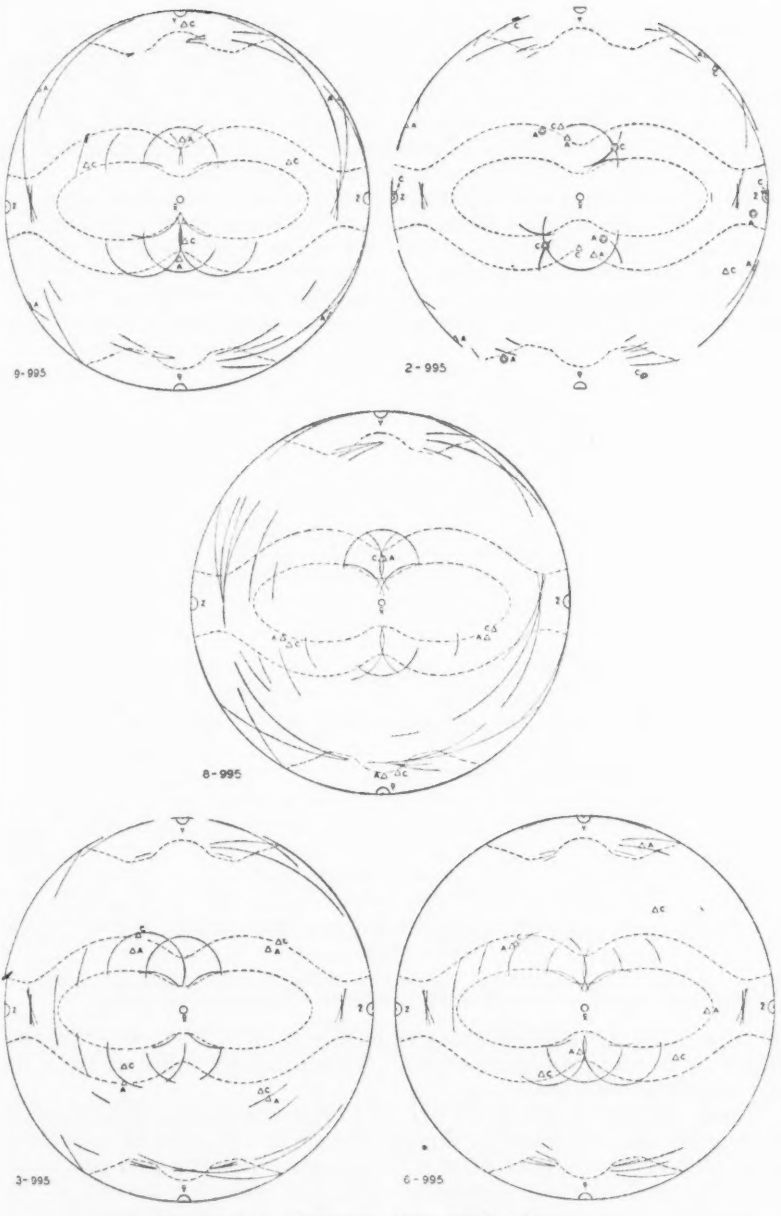

FIGURE 10.—*Summary stereographic diagrams.*

These diagrams show the 111 poles (open triangles) of the 90A and 90C positions, maximum divergence (dashed lines) of 111 poles of crystallites in cold-rolled copper after 99.5-percent reduction, arcs representing intensity maxima in 111 and 222 rings obtained from molybdenum and iron radiations, respectively, of initially monocrystalline specimens after 99.5-percent reduction.

polycrystalline specimen. This was cold-rolled in the same manner as the monocrystalline specimens to a thickness of 0.005 in. (99.5-percent reduction). Samples of this material were then treated with diluted nitric acid to remove the outer layers and to reduce the thickness to 0.002 to 0.003 in. These samples were used to obtain diffraction patterns representing different positions of the sample in respect to the X-ray beam. Molybdenum radiation was used.

The pole-figure shown in figure 11 was constructed from intensity maxima which appeared in the 111 ring as short arcs. No attempt was made to indicate areas corresponding to the less intense diffractions which connected the short arcs on some patterns. The shaded areas on the pole-figure, figure 11, are the areas which include normals corresponding to the short arcs. Since it is difficult to determine

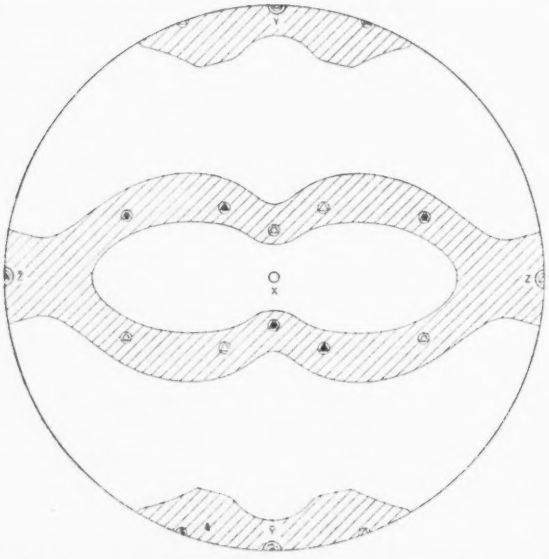

FIGURE 11.—*Pole-figure of polycrystalline copper after 99.5-percent reduction by cold-rolling.*

Shaded areas show divergence of 111 poles of crystallites. Triangles containing circles and triangles not containing circles are 111 poles of the twin 112–$\bar{1}\bar{1}1$ and twin 110–$1\bar{1}2$ orientations, respectively.

the extent of the shaded areas near the X pole when molybdenum radiation is used, this portion was determined by diffractions in the 222 ring from iron radiation.

The octahedral poles of the 110–$1\bar{1}2$ orientation were plotted on the pole-figure (fig. 11) showing the divergence of 111 poles of crystallites in polycrystalline copper after 99.5-percent reduction and are shown as circumscribed open triangles. The 111 poles of a twin of this orientation were plotted also and are shown as circumscribed filled triangles. The twin orientation is equivalent to a rotation of 60 degrees around the transverse direction. In addition to the 111 poles of these orientations, the 111 poles of the 112–$\bar{1}\bar{1}1$ orientation and of a twin were plotted, and are shown as triangles enclosing a circle. The twin orientation is equivalent to a rotation of 60 degrees around the rolling direction. From the evidence summarized in this

diagram, it was concluded that the preferred orientations of severely cold-rolled polycrystalline copper are twin 110–1$\bar{1}$2 and twin 112–$\bar{1}$11 orientations.

(b) MONOCRYSTALLINE COPPER

Transmission and back-reflection diffraction patterns from molybdenum and iron radiation, respectively, were obtained from small areas on samples of the initially monocrystalline specimens. The samples were initially etched slightly with diluted nitric acid to remove the surface layers, whose structure is not always representative of the rolling process. Each pattern represented a different position of the sample in respect to the X-ray beam. Arcs representing intensity maxima in the 111 ring from molybdenum radiation and in the 222 ring from iron radiation are shown in the stereographic diagrams of figure 10. The back-reflection patterns from iron radiation are caused by crystallites near the surface, whereas the transmission patterns from molybdenum radiation are caused by crystallites making up the body of the sample. Therefore, the patterns from iron radiation indicate changes in the 90A or 90C positions and the patterns from molybdenum radiation indicate changes in the 90A and 90C positions. The triangles in the diagrams of figure 10 are 111 poles corresponding to the 90A and 90C positions, and the dashed lines correspond to the shaded areas in figure 11.

III. RESULTS

Specimen 9.—The initial orientation of this specimen was such that the angle between an octahedral plane and the rolling plane was about 3 degrees and between an octahedral axis and the rolling direction about 20 degrees.

The macrostructure of cross sections of specimen 9, figure 3 (*A*), shows that rolling caused bands to develop within the metal. These bands were easily identified and occupied nearly the same relative cross-sectional areas after 60- and 75-percent reduction. After 90-percent reduction, the macrostructure was similar to that after smaller reductions, but the bands could not be identified with certainty. Therefore it can be concluded that these bands represent layers with the boundary between them nearly parallel to the rolling plane, during moderate reductions (75 percent).

After 15-percent reduction (9–15A and 9–15B positions, fig. 7) the lattice of the upper layer had rotated anticlockwise [4] about 15 degrees around an axis approximately parallel to the transverse direction, whereas the lattice of the bottom layer (9–15C position) had rotated clockwise about 8 degrees around the same axis. It is evident, therefore, that the initial 15-percent reduction by cold-working caused specimen 9 to divide into two layers differing in orientation by a rotation of 23 degrees about an axis approximately parallel to the transverse direction.

Further reductions, 30, 45, and 90 percent, by cold-rolling continued the rotation of the lattice of the upper layer until the cubic axis, whose locations are shown in figure 7 as filled circles, was approximately parallel to the rolling direction. Likewise, the lattice of the bottom layer continued to rotate until an octahedral axis was approximately

[4] The position of an axis of rotation for a clockwise (positive) rotation and anticlockwise (negative) rotation is with the negative pole toward the eye of the observer.

parallel to the rolling direction. Therefore, after 90-percent reduction by cold rolling, specimen 9 consisted of two layers, the orientation of one of which corresponded closely to the 110–001 orientation and of the other to the 112–$\bar{1}\bar{1}$1 orientation.

Orientations of the crystallites, as indicated by diffractions from octahedral planes (diagram 9–995, fig. 10), in specimen 9 after 99.5-percent reduction included the twin 110–1$\bar{1}$2 orientations as well as those represented by the 9–90A and 9–90C positions. The long arcs near the circumference of the diagram indicated intermediate orientations. It appears, therefore, that further cold-rolling after 90-percent reduction caused specimen 9 to attain orientations similar to those present in severely cold-rolled polycrystalline copper. If rolling could be continued indefinitely, all orientations not included in the cold-rolled texture would presumably disappear.

Specimen 2.—The initial orientation of this specimen was such that the angle between a cubic plane and the rolling plane was about 40 degrees and between a cubic axis and the rolling direction about 20 degrees.

The macrostructure of specimen 2 after 15-, 30-, and 45-percent reductions, figure 3 (*B*), was similar to the top layer of specimen 9 after corresponding reductions. The initial orientation of specimen 2, figure 2, corresponded approximately to the 110–001 orientation. This orientation has a $\bar{1}$10 axis parallel to the $\bar{Z}$ direction. It is noteworthy that the traces of two octahedral planes which make acute angles with the transverse direction (Z–$\bar{Z}$) correspond approximately to the slopes of the wavy lines seen in the macrostructure of specimen 2 and in the top layer of specimen 9.

Cold-rolling, producing an initial reduction of 15 percent (2–15A, 2–15B, and 2–15C positions, fig. 7), caused the lattice of the specimen as a whole to rotate around an axis nearly parallel to the transverse direction. After 30-percent reduction the condition was approximately the same as in the top layer of specimen 9. An increase in reduction to 90 percent caused little change from the lattice positions after 30-percent reduction. During the 90-percent reduction the changes in the position of the lattice did not proceed along great circles to a closer approximation of the 110-001 orientation as expected. The changes brought the lattice to a closer approximation of the 110–001 orientation only insofar as it could be accomplished by a rotation about an axis approximately parallel to the transverse direction.

Diffraction data representing the metal after 99.5-percent reduction, obtained from small areas in the top and bottom rolling planes, respectively, could be represented by two average orientations in the top plane and by one in the bottom plane, the latter one being the same as one of the average orientations in the top plane. An inspection of the summarizing diagram (diagram 2–995, fig. 10) shows that the 111 poles of these orientations (circumscribed triangles) nearly correspond to the twin 110–1$\bar{1}$2 orientations. The diagram as a whole indicates that further cold-rolling after 90-percent reduction caused the lattice of certain layers (2–90A position) to rotate anticlockwise while the lattice of other layers (2–90C position) rotated clockwise around axes nearly parallel to the normal direction. It is important to note that no orientations corresponding to the twin 112–$\bar{1}\bar{1}$1 orientations were present. This has been interpreted as

indicating that further cold-rolling after the 110-001 orientation has been approximated will not produce the complete cold-rolled texture of polycrystalline copper.

Specimen 8.—The initial orientation of this specimen was such that the angle between a cubic plane and the rolling plane was about 22 degrees and between an octahedral axis and the rolling direction about 15 degrees.

Cross sections of specimen 8, figure 5 (*A*), after 30-percent reduction showed bands in the macrostructure approximately parallel to the rolling plane. Their boundaries, however, were too irregular to suggest traces of crystallographic planes. As in specimen 9, these bands could be identified after larger reductions and therefore can be considered as cross sections of layers whose boundaries were approximately parallel to the rolling plane.

During the initial 15-percent reduction (8–15A position, fig. 8) the lattice of the top layer of specimen 8 rotated anticlockwise about 20 degrees around an axis nearly parallel to the transverse direction. This position corresponds approximately to the 100–011 orientation. The lattices of the central and bottom layers (8–15B and 8–15C positions) did not change their positions. Additional cold-rolling to 30-percent reduction caused the lattice of the top layer to rotate about 12 degrees more, but after 45-percent reduction, it has apparently rotated back about 7 degrees. The 8–30B and 8–30C positions were nearly the same as the 8–15B and 8–15C positions. These lattice positions represent the white areas shown in the macrostructure, figure 5 (*A*), which are considered as constituting the bottom layer. The dark area within the white area had approximately the same lattice position as the top layer. Cold-rolling to 45-percent reduction caused the lattice of the portion of the bottom layer represented by the 8–45B position to rotate clockwise about 5 degrees around an axis nearly parallel to the transverse direction (fig. 8), whereas the lattice of the portion represented by the 8–45C position rotated anticlockwise about 7 degrees. It cannot be stated with certainty, however, that the 8–45C position represents the bottom layer. Probably it represents the dark area within the bottom layer and thus indicates a possible lattice position of the top layer. The 8–90A and 8–90C positions (fig. 8) approximate the 112–$\bar{1}$11 orientation and are nearly twins of the 9–30C position, figure 7. It appears that cold-rolling to a reduction of 90 percent caused specimen 8 to develop layers having different lattice rotations. The lattice of the top layer rotated to a position approximating the 100–011 orientation, then rotated in the opposite direction along with the lattice of the bottom layer, each to a position approximating the 112–$\bar{1}\bar{1}$1 orientation.

Orientations of crystallites in specimen 8 after 99.5-percent reduction indicated (diagram 8–995, fig. 10) that orientations represented by the 8–90A and 8–90C positions persisted, but during the reduction from 90 to 99.5 percent some of the crystallites attained orientations characteristic of severely cold-rolled polycrystalline copper.

Specimen 3.—The initial orientation of this specimen was such that the angle between a cubic plane and the rolling plane was about 9 degrees and between a cubic axis and the rolling direction about 9 degrees.

Cross sections of specimen 3 (fig. 4) showed in the macrostructure a "herringbone" condition, largely confined to the sides, one side of the cross section being nearly a mirror image of the other side. The herringbone structure when fully developed (micrograph *E*) consisted of parallel bands projecting from the top and bottom rolling planes toward intermediate layers and from these toward the top and bottom rolling planes, respectively. In the fully developed stage the bands projecting from the top and bottom rolling planes met the bands projecting from the intermediate layer and the parallel bands made an angle of approximately 60 degrees with the rolling plane. The herringbone structure was very evident after 75- and 90-percent reductions. It appears that the herringbone structure represents sections of small parallel layers, whose sides increased progressively during reduction by rolling, from the top and bottom rolling planes and from the central layer of the specimen. Initially, the small parallel layers were nearly perpendicular to the rolling plane and parallel to the rolling direction, but in later stages they were inclined to the rolling plane but still parallel to the rolling direction.

The bands in the macrostructure had their counterpart in the wrinkled surface of the ends of the rolled specimens. Figure 4 (*D*) shows a wrinkled end of the specimen after 45-percent reduction. This is the reverse side of the sample whose macrostructure is shown by figure 4 (*C*), the two surfaces being approximately ½ inch apart. After 30-percent reduction the end was flat and perpendicular to the direction of rolling. Figure 4 (*F*) shows the end wrinkling that occurred between reductions of 60 and 64 percent. Examination of the wrinkled surface at higher magnification (fig. 12) after 45-percent reduction showed, near the lower ends of the ridges, slip lines in two directions; but on opposite slopes of the ridges the slip lines had only one direction. The two directions of the slip lines at the end of a ridge corresponded approximately to the directions on the two slopes of the ridge. These slip lines on the end surface of the specimen indicated that adjacent layers, shown as parallel bands in the macrostructure, and the portion near the sides which increased progressively during reduction by rolling, distorted by three different combinations of slip systems and therefore would approach three different orientations.

Specimen 3 initially approximated the 100–001 orientation, figure 2. Cold-rolling to a reduction of 90 percent produced little change in lattice position in the central portion of the specimen (fig. 8). The fine lines seen in the macrostructure were parallel to the traces of the octahedral planes, which indicated that they were formed as slip lines. After 99.5-percent reduction, orientations of crystallites (diagram 3–995, fig. 10) indicated that the twin 112–$\bar{1}\bar{1}$1, the twin 110–1$\bar{1}$2, and the 100–001 orientations were present. As in specimens 9, 2, and 8, the orientations present in the metal after rolling beyond 90-percent reduction proceeded to change to orientations identified with the texture of cold-rolled polycrystalline copper.

Specimen 6.—The initial orientation of this specimen was such that the angle between a cubic plane and the rolling plane was about 20 degrees and between a cubic axis and the rolling direction about 30 degrees.

The macrostructure of specimen 6, figure 5 (*B*), was unlike the structure of the preceding specimens. After 15-, 30-, and 45-percent

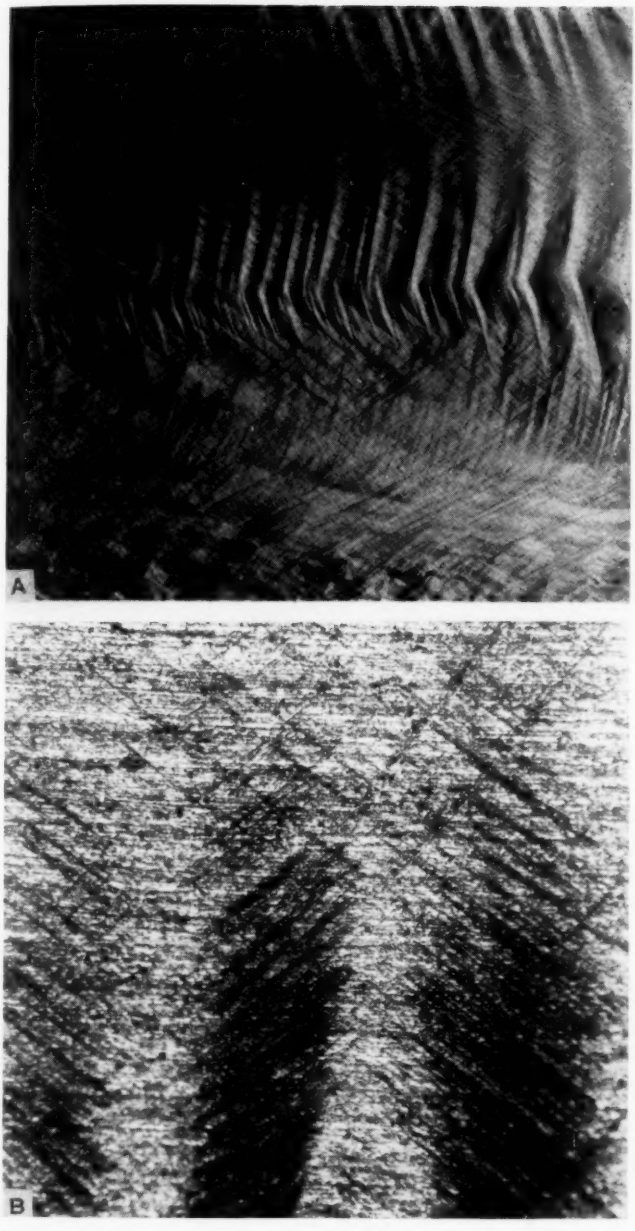

FIGURE 12.—*Appearance of the end first to enter the rolls, of specimen 3 after cold-rolling from 30- to 45-percent reduction.*

A, ×5; *B*, ×50.

UNIV. OF MICH.

reduction the specimen showed three bands in the structure, which persisted after larger reductions by cold-rolling. These bands were cross sections of layers approximately parallel to the rolling plane.

Cold-rolling to 15-percent reduction changes the initial orientation very little (fig. 8). However, further rolling to 30-percent reduction caused the lattice of the top and bottom layers (6–30A and 6–30C positions) to rotate clockwise about 15 degrees around an axis nearly parallel to the transverse direction. This rotation brought a cubic axis nearly into the rolling plane. The lattice of the center layer (6–30B position) rotated clockwise about 6 degrees around the octahedral axis in the lower right quadrant of the diagram. Further rolling to 45-percent reduction changed the top and bottom layers very little. However, the lattice of the center layer rotated 5 degrees more around the octahedral axis, which brought an octahedral axis nearly perpendicular to the rolling direction and an icositetrahedral axis [112] nearly parallel to the rolling direction. After 90-percent reduction the lattice of the bottom layer (6–90C position) approximated the 100–001 orientation. Inasmuch as changes in lattice position usually show a rotation to a preferred orientation, it is probable that the 6–90A position did not represent a lattice position of the top layer but one of the center layer and should be written as 6–90B. On this assumption, then, the lattice of the center layer after 90-percent reduction had rotated clockwise 11 degrees around an axis nearly parallel to the rolling direction. Continued rotation around the rolling direction to a position where the octahedral axis, which is nearly perpendicular to the rolling direction, became nearly parallel to the transverse direction, would approximate the 110–1$\bar{1}$2 orientation. The macrostructure and changes in lattice positions of specimen 6 indicate that cold-rolling to 90-percent reduction produced layers, in some of which the lattices rotated to a 100–001 orientation and in others to a 110–1$\bar{1}$2 orientation.

Orientations of crystallites in specimen 6 after 99.5-percent reduction by rolling (diagram 6–995, fig. 10) included the twin 110–1$\bar{1}$2 orientations. There appeared to be very few, if any, crystallites having the 100–001 orientation. A small number of crystallites having the twin 112–$\bar{1}\bar{1}$1 orientations was indicated by faint diffractions on the patterns obtained with molybdenum radiation. The diffraction patterns obtained after 99.5-percent reduction from specimen 8, as well as specimen 3, indicated that if the average orientation approximated the 100–001 orientation, additional rolling would cause a small number of crystallites to attain the twin 112–$\bar{1}\bar{1}$1 orientations and a much larger number to attain the twin 110–1$\bar{1}$2 orientations.

IV. DISCUSSION

1. BEHAVIOR OF MONOCRYSTALLINE SPECIMENS DURING COLD-ROLLING

It has been shown that the preferred orientations best representing the texture of cold-rolled polycrystalline copper after 99.5-percent reduction are the twin 110–1$\bar{1}$2 and twin 112–$\bar{1}\bar{1}$1 orientations. No attempt has been made to estimate the relative amounts of fragmented metal having the twin orientations. The presence of the twin 112–$\bar{1}\bar{1}$1 orientations is in disagreement with the conclusion of Schmid and

Staffelbach [1], who concluded that the texture of severely cold-rolled copper was represented only by twin 110–1$\bar{1}$2 orientations. Their published pole-figures indicate the presence of small amounts of crystallites having the twin 112–$\bar{1}\bar{1}$1 orientations. This is particularly true of their pole-figure of normals to octahedral planes, which definitely indicates that a large number of crystallites have octahedral axes nearly parallel to the rolling direction. Crystallites having the twin 112–$\bar{1}\bar{1}$1 orientations have octahedral axes parallel to the rolling direction.

In initially monocrystalline specimens after 99.5-percent reduction, the relative number of crystallites having the twin 110–1$\bar{1}$2 and twin 112–$\bar{1}\bar{1}$1 orientations appeared to vary depending upon the initial orientation. The results indicated that a large number of crystallites had attained the twin 110–1$\bar{1}$2 orientations in all specimens. No crystallites in specimen 2 had attained the twin 112–$\bar{1}\bar{1}$1 orientations, a small number in specimens 6 and 3, and a slightly larger number in specimens 8 and 9. The results obtained after increasing degrees of cold-rolling indicated that these final orientations are attained in two stages, the first being usually complete after reduction of approximately 90 percent, and the second nearly complete after 99.5-percent reduction.

During the first stage, the lattices of adjacent layers tend to rotate in opposite directions around axes nearly parallel to the transverse direction. Sections of these layers were observed in specimens 9, 8, and 6. The lattice rotations around the transverse direction resulted in what might be termed intermediate orientations. The intermediate orientations approximated were 110–001, 112–$\bar{1}\bar{1}$1, 100–011, 100–001.

The intermediate 110–1$\bar{1}$2 orientation was not attained in the monocrystalline specimens described in this paper by a rotation about an axis nearly parallel to the transverse direction. However, it was attained in this manner by Pickus and Mathewson [7] under conditions of deformation simulating the rolling process. Their method consisted in compressing monocrystalline specimens of alpha brass between two parallel surfaces and restricting the flow to a direction perpendicular to the axis of compression.

The second stage, which occurs only during extremely severe deformation, consists in rotations of lattices from intermediate orientations to the final twin 110–1$\bar{1}$2 and twin 112–$\bar{1}\bar{1}$1 orientations. It was not possible to determine directly if a portion of the specimen which had attained an intermediate orientation developed new layers whose lattices had rotated to one of the two pairs of final orientations. This manner of attaining the final orientations, however, appears the most probable, as any alternative would necesssitate rotation by means other than those resulting from slip on crystallographic planes.

The results described in this paper show that during rolling the lattices of different layers of specimen 2 rotated in opposite directions around the normal direction, from a position approximating the 110–001 intermediate orientation to the twin 110–1$\bar{1}$2 orientations. It appears then that the resistance to slip on the combination of slip systems necessary to maintain the 110–001 intermediate orientation had become sufficient to require other combinations of slip systems to operate. The new combinations were those which resulted in rotations around axes nearly parallel to the normal direction. The

results also show that during the later stages of the rolling, most of the rotation of the lattice of the central layer in specimen 6 took place around an axis nearly parallel to the rolling direction. This has been interpreted as indicating that when certain initial orientations are unfavorable to rotations around an axis nearly parallel to the transverse direction, the distortion proceeds by combinations of slip systems which result in a rotation around an axis nearly parallel to the rolling direction. A possible conclusion from these results is that during cold-rolling the lattice in portions of a monocrystalline specimen always tends to rotate around the principal directions, that is, the transverse, normal, and rolling directions. The primary tendency, which usually occurs during the first stage, is rotation around an axis nearly parallel to the transverse direction. The secondary tendency, usually occurring in the second stage, is rotation around an axis nearly parallel to the normal direction or to the rolling direction.

On the basis of this conclusion, it is possible to designate those rotations which are necessary to convert the five intermediate orientations into the final twin 110–1$\bar{1}$2 and twin 112–$\bar{1}\bar{1}$1 orientations. These rotations are shown in table 1.

TABLE 1.—*Orientations produced in monocrystalline specimens of copper by cold-rolling*

[The angular values for the initial orientations were obtained from the stereographic diagram of figure 2 (*A*). The angle θ is the angle between the 010 pole and principal direction; the angle ϕ is the azimuth on the (010) plane measured from the $\bar{1}$00 pole. The intermediate and final orientations show the locations of normal and rolling directions, respectively, after cold-rolling when referred to the crystallographic poles on the diagram of figure 2.]

Specimen	Initial orientation of specimen with respect to the [010] axis and (010) plane (degrees)						Intermediate orientations approximated	Possible rotations around principal directions from intermediate orientations (degrees)			Final orientations
	X-$\bar{X}$		*Y*-$\bar{Y}$		*Z*-$\bar{Z}$			*X*	*Y*	*Z*	
	θ	ϕ	θ	ϕ	θ	ϕ					
9	42	134	116	65	49	0	110–001 112–$\bar{1}\bar{1}$1	±35 -----	----- 60	----- -----	110–1$\bar{1}$2, 110–$\bar{1}$12 2$\bar{1}$1–$\bar{1}\bar{1}$1 112–$\bar{1}\bar{1}$1
2	52	167	109	92	44	23	110–001	±35	-----	-----	110–1$\bar{1}$2, 110–$\bar{1}$12
8	22	44	112	53	84	141	010–$\bar{1}$01 $\bar{1}$21–$\bar{1}\bar{1}$1	----- ----- ----- 20 ----- −20	60 ----- 30 ----- −30 45	----- ----- ----- ----- ----- -----	112–$\bar{1}\bar{1}$1 $\bar{1}$21–$\bar{1}\bar{1}$1 011–$\bar{2}$11 $\bar{1}$10–$\bar{1}$12
3	9	90	99	90	90	180	010–001	±35 45 -----	----- ----- -----	----- ----- ±35	110–1$\bar{1}$2, 110–$\bar{1}$12 $\bar{1}$21–$\bar{1}\bar{1}$1, $\bar{1}$21–$\bar{1}$11
6	19	76	110	70	92	160	$\bar{1}$10–$\bar{1}$12 010–001	----- −45 -----	----- ----- -----	60 ----- ±35	$\bar{1}$01–1$\bar{2}$1 $\bar{1}$10–$\bar{1}$12 $\bar{1}$21–$\bar{1}\bar{1}$1, $\bar{1}$21–$\bar{1}$11

2. DEFORMATION BANDS

The bands observed in the macrostructure of cross sections of specimens 9, 8, and 6 after rolling are similar to the deformation bands frequently observed within crystals of polycrystalline metal after deformation. Adjacent bands observed in these specimens were

shown to be layers whose lattices had rotated in different directions, and thus permitted the deformation of a single crystal to result in more than one orientation. The origin and behavior of deformation bands with respect to deformation of the parent crystal therefore become important in the study of the development of texture by cold-working.

The results obtained with specimens 9, 8, and 6 showed that the boundaries between bands were not initially straight and did not correspond to any particular plane. The lattices of layers corresponding to adjacent bands in these specimens rotated around an axis in the boundary plane. Recent researches by Barrett and Levenson have shown that the boundaries between deformation bands are straight in the early stages of deformation and correspond to traces of cubic or octahedral planes in iron crystals after deformation by drawing [9] and to traces of cubic planes in aluminum crystals after deformation by compression [10]. According to Barrett, the lattices of layers corresponding to adjacent deformation bands rotated around an axis perpendicular to the boundary plane. This was shown to be the case when a monocrystalline specimen of aluminum was deformed plastically by compression. It is reasonable to conclude that the position of the axes of rotation in layers shown as adjacent bands determines the kind of boundary between bands and that during deformation by drawing or compression, these axes tend to be perpendicular to the boundary plane, whereas in cold-rolling the axes of rotation tend to be in the boundary plane.

Deformation bands similar to those found in cross sections of specimen 3 have been observed by Samans [11] on a plane, parallel to the rolling plane, in his study on cold-rolling of a monocrystalline specimen of alpha brass. His specimen, as well as specimen 3 in this work, initially had 100–001 orientation. Samans showed that the orientations of adjacent bands differed by a rotation of 60 degrees around an octahedral axis and concluded that the bands had been produced by mechanical twinning. The results obtained with specimen 3 in this investigation suggest that the bands observed by Samans were sections of layers that were parallel to the rolling direction and grew in width during rolling. Slip lines observed on the end of specimen 3 indicated that adjacent layers approach different orientations during reduction by rolling. The explanation is offered that the bands observed by Samans were not sections of mechanical twins but that the 60 degrees' difference in rotation around an octahedral axis was attained by progressive rotation.

3. DEVELOPMENT OF TEXTURE IN POLYCRYSTALLINE COPPER

If the shape of individual crystals in a polycrystalline specimen during a reduction by cold-rolling changes exactly in accordance with dimensional changes of the specimen, then the results obtained with monocrystalline specimens could be used, without question, to describe the development of texture. The nonconformity of changes in shape of crystals with external changes of a specimen was demonstrated by Barrett [10]. In his experiments the inner faces of two compression blocks of polycrystalline aluminum became roughened by the deformation resulting from 22-percent reduction. The roughened surface can be explained by the initial orientations of some crystals being

able to conform more easily to dimensional changes of the specimen than others. In a previous investigation [7] it was shown that the crystal in a bicrystalline copper rod having a cubic axis nearly parallel to the rod axis conformed more nearly to dimensional changes resulting from swaging than the other crystal having an octahedral axis nearly parallel to the rod axis. In this case the crystal having the cubic orientation tended to flow around the crystal having the octahedral orientation. The nonconformity of changes in shape of crystals with dimensional changes of the specimen probably diminishes as the deformation proceeds and becomes negligible after severe reductions. This contention assumes that the resistance of an individual crystal to further deformation increases as the deformation proceeds, so that in time the crystals undergoing the most deformation will offer the same resistance as those that initially offered more resistance. When this condition is realized, the dimensional changes of all crystals should conform to the external changes of the specimen. Evidence that such a conformity is approached is given by metallographic examinations of severely cold-rolled specimens of polycrystalline copper. These examinations showed that in general all grains are elongated in the direction of rolling, shortened in the normal direction, and almost unchanged in the transverse direction. From the above consideration it is concluded that the interactions of neighboring crystals in polycrystalline specimens may result, during early stages of deformation by rolling, in lattice rotations which are not consistent with the behavior of monocrystalline specimens, but these inconsistencies are greatly reduced in later stages.

The development of texture in polycrystalline copper by cold-rolling, based on the behavior of monocrystalline specimens during cold-rolling, appears to be as follows: During moderate reductions, a crystal may develop layers by the rotation of the lattice in different directions. The lattice rotation of a crystal or of a layer within a crystal, during moderate reductions, tends to be around an axis nearly parallel to the transverse direction and ends at a position approximating one of five intermediate orientations, as follows: 110–1$\bar{1}$2, 112–$\bar{1}\bar{1}$1, 110–001, 100–001, and 100–011. Additional rolling causes the crystals or layers within crystals that approximate the 110–001 intermediate orientation to develop new layers. The lattices of some of the newly developed layers rotate to one of the twin 110–1$\bar{1}$2 orientations, and the lattices of the remaining layers rotate to the other. Crystals or layers within crystals approximating other intermediate orientations develop new layers whose lattices rotate in a similar manner to the twin 110–1$\bar{1}$2 and twin 112–$\bar{1}\bar{1}$1 orientations. The rotations required to attain one of the final orientations from an intermediate orientation appear to be only around axes that are nearly parallel to the normal or rolling directions.

V. SUMMARY

Five monocrystalline specimens differing in their initial orientation and one polycrystalline specimen were cold-rolled without intermediate annealing from 1-in. to 0.005-in. thickness. Care was taken to keep the same rolling surface up and to enter the same end between the rolls during the entire reduction. After 15-, 30-, 45-, 90-, and 99.5-percent reductions, samples were cut from the ends of the monocrystalline specimens first to enter the rolls. These samples were

used for metallographic examinations of the cross sections and the determination of lattice orientations. Samples from the polycrystalline specimen after 99.5-percent reduction were used to obtain data for constructing a pole-figure of normals to the octahedral planes.

The pole-figure of a polycrystalline specimen of severely cold-rolled copper indicated that the preferred orientations were twin 110–$1\bar{1}2$ and twin 112–$\bar{1}\bar{1}1$ orientations. The behavior of five monocrystalline specimens during cold-rolling showed that three specimens developed layers whose lattices rotated to positions approximating two of five orientations. These five orientations have been called intermediate because they are approached during moderate reductions and appear to be the starting positions for the development of the texture characteristic of severely cold-rolled polycrystalline copper. The five intermediate orientations are 110–$1\bar{1}2$, 112–$\bar{1}\bar{1}1$, 110–001, 100–001, and 100–011. The lattice of the other two monocrystalline specimens as a whole rotated to a position approximating one of the five intermediate orientations. After additional rolling all specimens showed more than one orientation. The final orientations approached were twin 110–$1\bar{1}2$ or twin 110–$1\bar{1}2$ and twin 112–$\bar{1}\bar{1}1$ orientations, which are characteristic of cold-rolled polycrystalline copper.

The lattice rotations resulting in positions approximating the intermediate orientations tend to be around axes nearly parallel to the transverse direction. Other rotations tend to be around axes nearly parallel to the normal or rolling directions.

An explanation of the development of texture in severely cold-rolled polycrystalline copper, based on the behavior of monocrystalline specimens, is given.

VI. REFERENCES

[1] E. Schmid and F. Staffelbach, *The texture of rolled copper and nickel*, Schweizer. Arch. angew. Wiss. Tech. **1,** 221–224 (1935).
[2] S. Tanaka, *The effect of rolling on single crystals of aluminum*, Mem. Coll. Sci., Kyoto Imp. Univ. **10,** [A] 303–309 (1927).
[3] C. H. Samans, *An X-ray study of orientation changes in cold-rolled single crystals of alpha brass*, Trans. Am. Inst. Mining Met. Engrs. **111,** 119–135 (1934).
[4] M. R. Pickus and C. H. Mathewson, *On the theory of the origin of rolling textures in face-centered cubic metals*, J. Inst. Metals **64,** 555–576 (1939).
[5] J. G. Thompson, *Large single crystals of copper, simplified method for their preparation*, Metals & Alloys **7,** 19–21 (1936).
[6] Alden B. Greninger, *A back-reflection Laue method for determining crystal orientation*, Z. Krist. [A] **90,** 424–432 (1935); Trans. Am. Inst. Mining Met. Engrs. **117,** 61–74 (1935).
[7] H. C. Vacher, *Development of a fibrous texture in cold-worked rods of copper*, J. Research NBS **22,** 651–668 (1939) R. P. 1210.
[8] M. R. Pickus and C. H. Mathewson, *Plastic deformation and subsequent recrystallization of single crystals of alpha brass*, Trans. Am. Inst. Mining Met. Engrs. **133,** 161–186 (1939).
[9] C. S. Barrett and L. H. Levenson, *Structure of iron after drawing, swaging, and elongation in tension*, Trans. Am. Ins. Mining Met. Engrs. **135,** 327–352 (1939).
[10] C. S. Barrett and L. H. Levenson, *Structure of aluminum after compression*, Trans. Am. Inst. Mining Met. Eng. **137,** 112–127 (1940).
[11] C. H. Samans, *The deformation lines in alpha brass*, J. Inst. Metals (London) **55,** 209–213 (1934).

WASHINGTON, January 17, 1941.

U. S. Department of Commerce National Bureau of Standards

RESEARCH PAPER RP1386

Part of Journal of Research of the National Bureau of Standards, Volume 26, May 1941

COLORIMETRIC DETERMINATION OF PHOSPHORUS IN STEEL AND CAST IRON

By John L. Hague and Harry A. Bright

ABSTRACT

A colorimetric method is described for the determination of phosphorus in steels and irons. The phosphomolybdenum blue reaction is utilized, and the transmittancy of the colored solution is measured with a photoelectric colorimeter and a Corning Lantern Shade Yellow filter, No. 349. Provision is made for the effects of arsenic and silicon, and a method of compensating for the color of alloying constituents is given. An accuracy of ± 0.003 percent was indicated for steels whose phosphorus content ranged from 0.01 to 0.11 percent. With cast irons containing 0.25 to 0.80 percent of phosphorus, values accurate to ± 0.02 percent were obtained. A single determination of phosphorus in steel can be made in about 20 minutes, and a set of eight determinations can be completed in approximately 45 minutes.

CONTENTS

	Page
I. Introduction	405
II. Apparatus and reagents	406
1. Apparatus	406
2. Reagents	407
III. Procedure	407
IV. Results	408
V. Discussion	411

I. INTRODUCTION

The most widely used method for the determination of phosphorus in steels and irons involves its precipitation as the yellow ammonium phosphomolybdate, and subsequent titration of the phosphomolybdate with a standard alkali solution. The development of improved filter photometers has directed attention to the possibility of using rapid colorimetric or turbidimetric methods for the determination of phosphorus in ferrous materials, and a number of photometric procedures for this determination have been published. Koch [1] described a turbidimetric method based on the reaction of the phosphomolybdate ion with strychnine. Murray and Ashley [2] used the yellow phosphovanadomolybdate complex, and measured the extinction coefficient of the solution with a Pulfrich step-photometer and a suitable filter. Bursuk [3] employed the phosphomolybdenum blue complex for

[1] Arch. Eisenhüttenw. **12**, 69 (1938).
[2] Ind. Eng. Chem., Anal. Ed. **10**, 5 (1938).
[3] Zavodskaya Lab. **8**, 12 (1939).

the determination of phosphorus in carbon steels, and measured the color intensity of the solution with a photoelectric colorimeter.

The phosphomolybdenum blue reaction has been used for many years in biochemical work for the determination of phosphorus. A summary of the different reducing agents employed, and the methods used to obtain the "blue compound" is given by Snell and Snell [4] and by Yoe.[5] The sensitivity of the reaction is of particular value for steels of low phosphorus content (P $<$0.03 percent). The intensity of the blue color can be measured with simple apparatus, and relatively high percentages of alloying elements wnich give colored ions can be tolerated, because the corrections are small and conveniently made.

This paper reports an application of the phosphomolybdenum blue reaction to the determination of phosphorus in steels and irons. A procedure has been developed in which a reagent containing hydrazine sulfate and ammonium molybdate is used to form the blue compound. This type of reagent, used by Morris and Calvery [6] for the colorimetric determination of arsenic, gives with the phosphate ion a stable phosphomolybdenum blue complex with but little background color. The sample is dissolved in diluted nitric acid (sp gr 1.20), a definite amount of perchloric acid is added, and the solution is then evaporated to fumes of perchloric acid. Perchloric acid is used to remove the nitric acid, and to insure the oxidation of all phosphorus to the ortho acid; the use of a definite amount provides for the proper adjustment of the initial acidity. Water and a solution of sodium sulfite are added to the cooled residue, and the solution is heated to boiling to reduce the iron. Phosphorus is then converted to the blue compound by adding a solution containing hydrazine sulfate and ammonium molybdate and heating at 90° for about 5 minutes. The transmittancy of the colored solution is measured with a photoelectric colorimeter (comparator). The quantity of phosphorus is read from a standard curve or table prepared from data obtained by treating steels containing known amounts of phosphorus in the same manner as was used for the unknown. A single determination can be made in about 20 minutes, and a set of eight determinations can be completed in approximately 45 minutes.

II. APPARATUS AND REAGENTS

1. APPARATUS

A photoelectric colorimeter of the Evelyn [7] type was used in most of the work. The light-sensitive cell is an Electrocell, and the current-measuring instrument is a low-resistance (50-ohm) microammeter (0 to 100 microamperes). A Pyrex test tube (16 by 150 mm) is used as an absorption cell.[8] The filter is a Corning Lantern Shade Yellow, No. 349.

[4] F. D. Snell and C. T. Snell, Colorimetric Methods of Analysis, vol. 1 (D. Van Nostrand Co., Inc., New York, N. Y., 1936).
[5] J. H. Yoe, Photometric Chemical Analysis, vol. 1 (J. Wiley & Sons, New York, N. Y., 1928).
[6] Ind. Eng. Chem., Anal. Ed. 9, 448 (1937).
[7] J. Biol. Chem. 115, 63 (1936).
[8] The effective thickness of a column of liquid in a tube of this diameter is equivalent to approximately 13 mm. Transmittancy measurements were made on a number of tubes when filled with water and when filled with a solution containing the color developed by approximately 30 μg of phosphorus in a volume of 50 ml. The tubes which gave transmittancy readings identical with those of the tube used to prepare a calibration curve were kept as a reserve supply of matched tubes.

2. REAGENTS

Diluted nitric acid (sp gr 1.20).—Add 380 ml of nitric acid (sp gr 1.42) to 620 ml of water.

Perchloric acid (60 percent).

Diluted hydrobromic acid (1+4).—Dilute 20 ml of hydrobromic acid (48 percent) with 80 ml of water.

Sodium sulfite solution (10 percent).—Dissolve 100 g of anhydrous sodium sulfite in 500 ml of water, dilute to 1,000 ml, and filter.

Hydrazine sulfate solution (0.15 percent).—Dissolve 1.5 g of hydrazine sulfate in 1,000 ml of water.

Ammonium molybdate solution (2 percent in 11 N H_2SO_4).—Add 300 ml of sulfuric acid (sp gr 1.84) to 500 ml of water and cool. Dissolve 20 g of ammonium molybdate in the solution and dilute to 1,000 ml with water.

Ammonium molybdate-hydrazine sulfate reagent.—Dilute 25 ml of the ammonium molybdate solution to 80 ml with water, add 10 ml of the hydrazine sulfate solution, and dilute to 100 ml with water. This solution is not stable and should be prepared as needed.

III. PROCEDURE

Carbon steel.—Transfer 50 mg of the sample to a 125-ml Erlenmeyer flask and add 5 ml of diluted nitric acid (sp gr 1.20). Heat until the sample is in solution. Add 3 ml of perchloric acid (60 percent) from a transfer pipette. Evaporate the solution to fuming, and fume gently until all of the nitric acid is removed, usually 3 to 4 minutes.[9] Cool somewhat [10] and add 10 ml of water and 15 ml of the sodium sulfite solution. Heat the solution to boiling and boil gently for 20 to 30 seconds.[11] Add 20 ml of the ammonium molybdate-hydrazine sulfate reagent, heat to about 90° C, and allow to digest at that temperature for 4 to 5 minutes. Then heat the solution just to boiling temperature, but do not boil.[12] Cool rapidly to room temperature, transfer the solution to a 50-ml volumetric flask, and dilute to the mark with a diluted solution (1+4) of the ammonium molybdate-hydrazine sulfate reagent. Mix thoroughly, transfer a portion of the solution to the cell (a matched test tube), and measure the percentage transmittancy of the solution, the indicator of the microammeter having been previously adjusted to 100-percent transmittancy for a cell filled with water. The percentage of phosphorus is obtained from a calibration curve or table prepared from data obtained by carrying steels containing known amounts of phosphorus through all the steps of the method.

Alloy steels.—For steels containing less than 2 percent of chromium, 5 percent of vanadium, or 35 percent of nickel, proceed as with carbon steels. If the sample is insoluble in diluted nitric acid (high-chromium steels), add 3 ml of diluted hydrochloric acid (1+1) to the nitric acid solution. If the steel contains more than 2 percent of chromium, 5 percent of vanadium, or 35 percent of nickel, a separate

[9] At this stage the neck of the flask becomes dry, and the perchloric acid refluxes on the walls of the flask.

[10] When the arsenic content of the sample exceeds 0.05 percent, this element should be eliminated as follows: Add 5 ml of diluted hydrobromic acid (1+4) to the cool perchloric acid solution of the sample, evaporate to fuming and fume gently to remove the hydrobromic acid. The interference of as much as 0.25 percent of arsenic can be avoided by this treatment.

[11] The brown coloration which appears when the sulfite is first added should disappear completely.

[12] Alternatively, the blue coloration may be developed with less attention by digesting for 15 to 20 minutes on the steam bath (85° to 90° C).

50-mg portion is taken to obtain the correction for the absorption due to the solution of the sample. This sample is carried through all the steps of the method, except that 20 ml of diluted sulfuric acid (8+92) is substituted for the 20 ml of ammonium molybdate-hydrazine sulfate reagent specified in the procedure, and the final dilution to 50 ml is made with water. The correction for the transmittancy of the unreduced solution is made as described in section IV.

Cast iron.—Transfer a 100-mg sample to a 125-ml Erlenmeyer flask, and dissolve the sample in 25 ml of diluted nitric acid (sp gr 1.20). Boil until nitrous fumes are expelled, cool, and dilute the solution to exactly 100 ml. Allow the graphite to settle, and pipette a 5-ml aliquot portion into a 125-ml Erlenmeyer flask. Add 3 ml of perchloric acid (60 percent) and proceed as with carbon steels, eliminating arsenic by treatment with hydrobromic acid.

IV. RESULTS

The results obtained with a series of carbon steels are shown graphically in figure 1. It will be seen that Beer's law holds up to

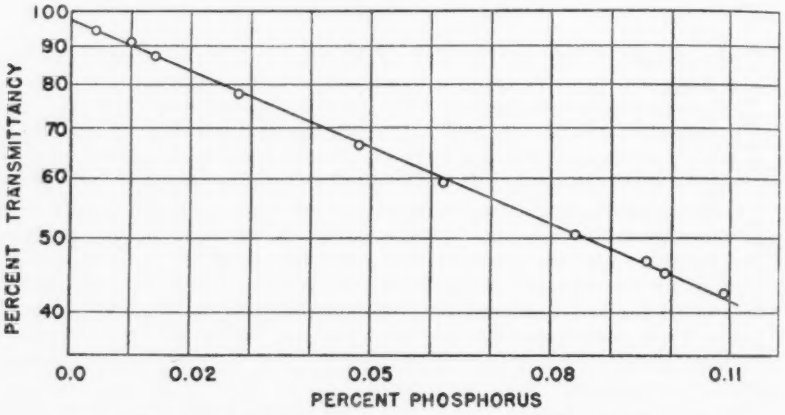

FIGURE 1.—*Curve showing conformance to Beer's law.*

0.11 percent of phosphorus, within an experimental error of about 0.003 percent of phosphorus. The curve does not pass through the 100-percent transmittancy point, because no attempt was made to correct the measurements for the small amount of absorption due to iron, to phosphate in the reagents, to the small amount of arsenic (approximately 0.01 percent) generally present in steels, and to other blank effects. Each new lot of reagents, therefore, must be carefully tested by carrying standards through all the steps of the method in order to check the calibration curve.

The values for individual determinations of phosphorus may be read from a graph of the type illustrated in figure 1, or from a table in which the percentage of phosphorus corresponding to various percentage transmittancy values has been calculated from the equation $\log T_2 - \log T_1 = k(C_2 - C_1)$. Using the percentage transmittancy obtained on NBS Standard Samples 8e and 55a as standards, a table

of phosphorus-transmittancy values was calculated.[13] Individual values for the carbon steel samples were read from this table, and the results obtained are shown in table 1. The maximum error is 0.007 percent of phosphorus, and the average error is about 0.002 percent.

TABLE 1.—*Results obtained by the procedure recommended for carbon steels*

NBS Standard Sample	Phosphorus		Difference	Type of steel
	Certificate value	Found		
	Percent	*Percent*		
55a [1]	0.004	0.004	0.000	Open-hearth iron.
		.005	+.001	
		.005	+.001	
		.004	.000	
		.003	−.001	
51a	.010	.009	−.001	Electric, 1.2 percent of carbon.
		.010	.000	
		.007	−.003	
15c	.014	.015	+.001	B. O. H., 0.1 percent of carbon.
		.014	.000	
34a	.028	.029	+.001	A. O. H., 0.8 percent of carbon.
		.029	+.001	
20d	.048	.050	+.002	A. O. H., 0.4 percent of carbon
		.048	.000	
21c	.062	.064	+.002	A. O. H., 0.6 percent of carbon.
		.062	.000	
22b	.084	.084	.000	Bessemer, 0.6 percent of carbon.
		.084	.000	
9c	.096	.096	.000	Bessemer, 0.2 percent of carbon.
		.094	−.002	
		.092	−.004	
8e [1]	.099	.099	.000	Bessemer, 0.1 percent of carbon.
		.098	−.001	
		.102	+.003	
		.099	.000	
		.098	−.001	
129	.109	.113	+.004	High sulfur.
		.102	−.007	
		.105	−.004	
		.108	−.001	

[1] Used as a standard, but data given to show the precision of single determinations.

The results obtained on alloy steels with phosphorus contents ranging from 0.01 to 0.03 percent are shown in table 2. The maximum error is 0.003 percent, and the average error is about 0.001$_2$

[13] *Example:*
A transmittancy value (T_1) of 94.5 percent was observed for NBS Standard Sample 55a, which contains 0.004 percent (C_1) of phosphorus. A transmittancy value (T_2) of 45.0 percent was observed for NBS Standard Sample 8e, which contains 0.099 percent (C_2) of phosphorus. Substituting in the above equation, solve for k:

$$\log T_1 = 1.9754 \qquad C_1 = 0.004$$
$$\log T_2 = 1.6532 \qquad C_2 = 0.099$$

$$k = \frac{\log T_2 - \log T_1}{C_2 - C_1} = \frac{1.6532 - 1.9754}{0.099 - 0.004} = -3.39.$$

Calculate the intercept T_0 (where $C_0 = 0.000$ percent):

$$\log T_2 = 1.6532 \qquad C_2 = 0.099$$
$$\log T_0 = \log T_2 - k(C_2 - C_0)$$
$$\log T_0 = 1.6532 - (-3.39 \times 0.099) = 1.9888$$
$$T_0 = 97.5$$

To calculate the percentage of phosphorus (C_x) equivalent to an observed percent transmittancy (T_x) value:

$T_0 = 97.5$; $\log T_0 = 1.9888$ $\qquad C_0 = 0.000$
T_x = transmittancy for which a phosphorus equivalent is wanted.

$$\text{percentage of phosphorus} = C_x - C_0 = \frac{\log T_x - \log T_0}{k} = \frac{\log T_0 - \log T_x}{-k}$$
$$= C_x = \frac{1.9888 - \log T_x}{3.39}$$

These data apply only to the Evelyn-type colorimeter and tubes used in this work, but are given to show the method of calculation employed.

percent of phosphorus. The percentage of phosphorus was read from the phosphorus-transmittancy table calculated for carbon steels. The percentage transmittancy observed for NBS Standard Samples 73, 101, 101a, and 121 (high-chromium steels) was corrected for the absorption due to the solution of the sample in which the phosphomolybdenum blue color was not developed. For example, the transmittancy observed for NBS Standard Sample 101a (P=0.017 percent), when the phosphomolybdenum blue color was developed, was 74.5 percent. The transmittancy of another sample in which the phosphomolybdenum blue color was not developed was 87.0 percent. The corrected transmittancy value, 74.5 divided by 87.0, is 85.6 percent, and from the phosphorus-transmittancy table calculated for carbon steels is found to equal 0.017 percent of phosphorus.

TABLE 2.—*Results obtained by the procedure recommended for alloy steels*

NBS Standard Sample	Phosphorus		Difference	Type of steel
	Certificate value	Found		
	Percent	*Percent*	*Percent*	
125	0.008	0.007	−0.001	Silicon (4.97 Si).
		[a].009	+.001	
72a	.016	.016	.000	Chromium-molybdenum (0.66 Cr, 0.20 Mo).
		.015	−.001	
32b	.016	.015	−.001	Chromium-nickel (1.21 Ni, 0.64 Cr).
		.013	−.003	
30c	.019	.018	−.001	Chromium-vanadium (0.98 Cr, 0.24 V).
		.016	−.003	
111	.023	.024	+.001	Nickel-molybdenum (1.75 Ni, 0.22 Mo).
		.021	−.002	
100	.023	.025	+.002	Manganese-rail (1.38 Mn).
		.022	−.001	
30b	.024	.025	+.001	Chromium-vanadium (1.03 Cr, 0.21 V).
		.025	+.001	
130	.025	.025	.000	Lead-bearing (0.20 Pb).
		.025	−.000	
33b	.037	.035	−.002	Nickel (3.48 Ni).
		.035	−.002	
101	.010	[b].012	+.002	Chromium-nickel (17.6 Cr, 8.4 Ni).
		[b].012	+.002	
121	.016	[b].018	+.002	Chromium-nickel, titanium-bearing (17.8 Cr, 9.0 Ni, 0.39 Ti).
		[b].018	+.002	
101a	.017	[b].017	.000	Chromium-nickel (18.3 Cr, 9.0 Ni).
		[b].017	.000	
73	.023	[b].021	−.002	Chromium (13.9 Cr).
		[b].021	−.002	

[a] Two drops (0.05 ml) HF present during solution of sample.
[b] Result obtained by correcting for absorption due to the sample. See section IV.

The results obtained by the procedure for cast irons are shown in table 3. A table of phosphorus-transmittancy values was calculated, using 4e and 7c as standards, and the values given were read from this table. The maximum error is 0.02 percent, and the average error is less than 0.01 percent of phosphorus. A few experiments indicated that the color obtained from a given amount of phosphorus was constant when the amount of iron present was varied from 5 to 50 mg. For cast irons, values read from the table prepared for carbon steels, multiplied by 10 to compensate for the difference in weight of sample, were almost as accurate as those shown in table 3.

TABLE 3.—*Results obtained by the procedure recommended for cast irons*

NBS Standard Sample	Phosphorus		Difference
	Certificate value	Found	
	Percent	*Percent*	*Percent*
4c [1]	0.109	0.11	0.00
		.11	.00
		.12	+.01
5g	.261	.26	.00
		.26	.00
		.24	−.02
6d	.486	.51	+.02
		.50	+.01
		.49	.00
7c [1]	.778	.78	.00
		.78	.00
		.78	.00

[1] Used as a standard.

V. DISCUSSION

The spectral transmittancies of the phosphomolybdenum blue compound, of iron, and iron plus chromium, and the spectral transmission of the Corning filter (No. 349), were obtained with a Coleman

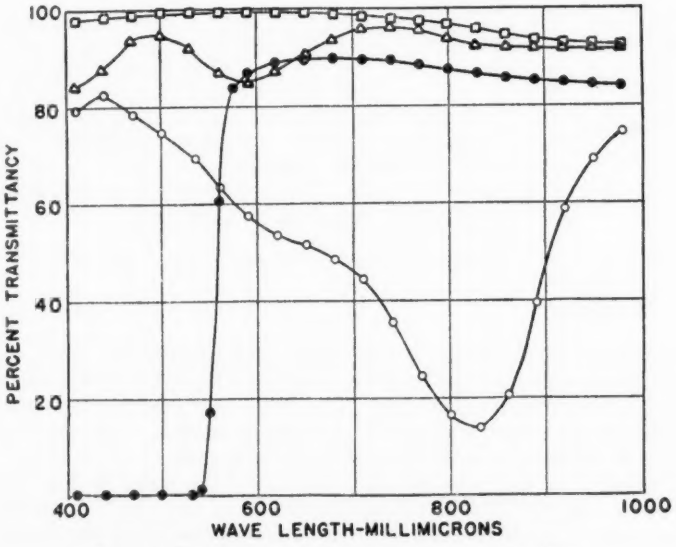

FIGURE 2.—*Curves showing regions of absorption.*

● Filter.
○ Phosphomolybdenum blue complex.
△ 50-mg NBS Standard Sample 73 (14 percent of Cr).
□ 50-mg NBS Standard Sample 55a (ingot iron).

DM spectrophotometer (model 10S). The data are shown in figure 2. It will be noted that the maximum absorption due to the phosphomolybdenum blue compound occurs at approximately 830 mμ. A few measurements made at this wavelength and at 650 mμ indicate that the solutions follow Beer's law at both wavelengths. Measure-

ments made on the Evelyn-type colorimeter were limited to the region from 550 mμ to approximately 700 mμ by the filter and by the spectral sensitivity of the photocell.

Roe, Irish, and Boyd [14] have studied the phosphomolybdenum blue reaction and have summarized the conditions which must be controlled: (1) the concentration of molybdic acid, (2) the concentration of the reducing agent, (3) the time allowed for completion of the reaction, (4) the hydrogen ion concentration, (5) the presence of salts, and (6) the amount of phosphorus in the sample being analyzed.

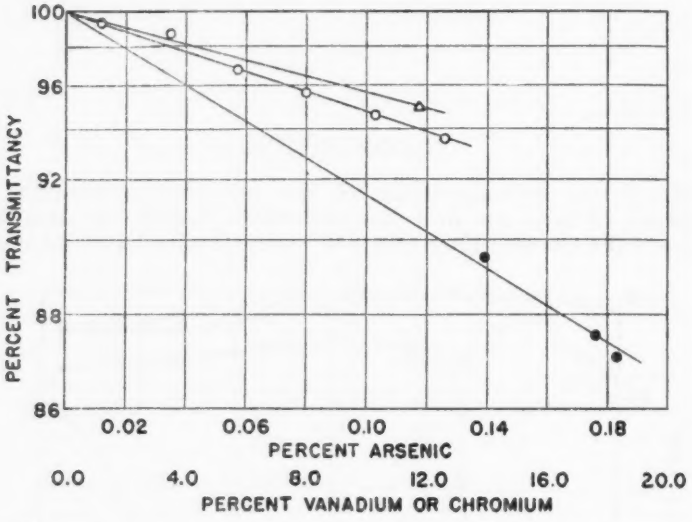

FIGURE 3.—*Curves showing extent of interference by certain elements.*
△ Vanadium.
○ Arsenic
● Chromium.

The concentration of molybdic acid and hydrazine sulfate under the conditions specified in the procedure is sufficient to cover the range of phosphorus from 0 to 60 μg. The time required for the complete development of color depends on the temperature. The color, once properly developed, is stable for at least 24 hours.

The acidity of the solution in which the blue color is developed is important, and the limiting range depends in part on the amount of salts present. With the salt concentration specified in the method of Roe, Irish, and Boyd, the permissible range of acidity is given as 0.9 *N* to 1.9 *N* sulfuric acid. Tests of the effect of acidity in the procedure given in this paper were subject to the uncertainty of the amount of residual sulfurous acid. However, experiments in which the acidity of the ammonium molybdate solution was varied from 5 *N* to 16 *N* sulfuric acid (corresponding to an acidity of 0.5 *N* to 1.6 *N* sulfuric acid in the final solution) indicated that (1) some bleaching of the color occurs in solutions approximating 1.6 *N* in sulfuric acid,

[14] J. Biol. Chem. **67**, 580 (1926).

and (2) erratic results are obtained when the acidity is less than 0.8 *N* sulfuric acid.

Arsenate gives a molybdenum-blue reaction similar to that of phosphate, and the extent of this interference is shown in figure 3. Experiments indicate that 0.05 percent of arsenic may be present without leading to an error greater than 0.003 percent of phosphorus.

It has been stated that silicon gives a molybdenum-blue compound. This reaction, however, does not occur under the conditions given in the recommended procedure. Large amounts of silicon give rise to an objectionable turbidity, and a few experiments made with a high-silicon steel, NBS Standard Sample 125, indicate that this difficulty can be overcome by adding 2 drops (about 0.05 ml) of hydrofluoric acid to the original nitric–perchloric acid solution of the sample, and evaporating to fumes as directed in the procedure.

Copper, nickel, chromium, and vanadium do not interfere with the development of the phosphomolybdenum blue color, but give colored ions which may interfere unless proper compensation is made. Experiments indicate that as much as 35 percent of nickel, 15 percent of copper, 5 percent of vanadium, or 2 percent of chromium may be present without leading to an error greater than 0.002 percent of phosphorus, when the calibration curve is prepared from carbon steels. The extent of the interference of chromium and vanadium is shown in figure 3. When the above-mentioned elements are present in amounts greater than those indicated, correct results can be obtained by preparing a calibration curve with the same type of material being tested, or alternatively, a correction can be applied by measuring the transmittancy of a solution of the sample in which the phosphomolybdenum blue color is not developed.

WASHINGTON, January 8, 1941.

U. S. DEPARTMENT OF COMMERCE NATIONAL BUREAU OF STANDARDS

RESEARCH PAPER RP1387

Part of Journal of Research of the National Bureau of Standards, Volume 26, May 1941

METHOD FOR DETERMINING THE COMPONENTS OF ASPHALTS AND CRUDE OILS

By O. G. Strieter [1]

ABSTRACT

The ordinary procedure for the analysis of asphalts, which uses petroleum naphtha and carbon bisulfide as solvents, does not yield satisfactory results. Recently it has been found that by substituting pentane for the petroleum naphtha and ether for the carbon bisulfide, accurately reproducible results can be obtained for the content of asphaltenes, resins, and the oily constituents.

CONTENTS

	Page
I. Introduction	415
II. Revised procedure	416
1. Asphaltenes	416
2. Oily constituents	416
3. Asphaltic resins	417
III. Analytical data	417

I. INTRODUCTION

The components of asphalt, according to Marcusson,[2] are the asphaltic acids and their anhydrides, oily constituents, resins, and asphaltenes. The asphaltic acids and their anhydrides are determined by saponifying with cold and hot alcoholic potash, respectively, but owing to the formation of troublesome emulsions and to the fact that they are present in the asphalt only in small amounts, their determination is usually omitted, so the ordinary procedure is:

1. The asphaltenes are precipitated with 88° Bé petroleum naphtha.
2. The petroleum naphtha filtrate, which contains the oily constituents and the resins, is reduced in volume by evaporation and then is completely absorbed by fuller's earth.
3. The oily constituents are extracted from the fuller's earth with petroleum naphtha.
4. After the oily constituents are removed from the fuller's earth, the resins are extracted with carbon bisulfide or benzol.

Petroleum naphtha is not a definite compound, but a mixture of hydrocarbons that varies with the nature of the crude petroleum from which it is obtained. A naphtha that consists chiefly of hydrocarbons of the paraffin series will precipitate the asphaltenes more

[1] Research Associate at the National Bureau of Standards, representing the Asphalt Roofing Industry Bureau.

[2] Herbert Abraham, Asphalt and Allied Substances, 4th ed., p. 1007. (D. Van Nostrand Co., Inc., New York, N. Y.) 1938.

completely than will a naphtha of the same boiling range but composed of naphthenes and aromatics. The revised method substitutes *n*-pentane for the petroleum naphtha. Because *n*-pentane is of nearly constant composition, it has the advantage over petroleum naphtha that different lots of it will precipitate the same percentage of asphaltenes from a given sample of asphalt or of crude oil. In addition, because it is a paraffin hydrocarbon, it will precipitate the asphaltenes almost completely, and will give more accurate results than are possible to get with petroleum naphtha.

For the extraction of the resins from the fuller's earth, the revised method substitutes ethyl ether for the carbon bisulfide or benzol ordinarily used. On a given sample, it was found that extraction of the resins with carbon bisulfide yielded 8.3 percent and with benzol 13.2 percent, but extraction with ethyl ether according to the revised procedure yielded 22.7 percent. In these cases, the sums of the components of the asphalt when using carbon bisulfide, benzol, and ether, were 88.1, 94.7, and 99.4 percent, respectively.

II. REVISED PROCEDURE

Weigh 5.000 g of asphalt in small pieces on a tared watchglass and transfer to a 400-ml wide-mouthed Erlenmeyer flask. Add 100 ml of normal pentane, and rotate the Erlenmeyer flask until the asphalt is partially disintegrated. Add an additional 75 ml of pentane, and again rotate until the asphalt is completely disintegrated. Then add 50 ml of pentane, lightly cork the flask, and allow to settle overnight.

1. ASPHALTENES

Filter the pentane solution through a tared Gooch crucible, with slight suction. Catch the filtrate, without attempting to transfer all the asphaltenes to the Gooch crucible, in a 600-ml beaker under a bell jar. Wash the residue in the flask and on the crucible with successive small portions of pentane until the filtrate is colorless. Dry the Gooch crucible in an oven at 105° C, cool in a desiccator, and weigh. Dissolve in carbon tetrachloride the residue adhering to the walls of the Erlenmeyer flask, and transfer the solution to a 250-ml beaker. Evaporate to dryness by allowing the beaker to stand in a warm place, dry at 105° C, and weigh. The combined weights of the residue divided by 5 and multiplied by 100 gives the percentage of asphaltenes.

2. OILY CONSTITUENTS

Allow the filtrate containing the oily constituents and the resins (600-ml beaker) to evaporate slowly to dryness at room temperature under the hood. Wash the sides of the beaker with pentane, and dissolve the residue in a total volume of 25 ml of pentane.

To the 25-ml pentane solution in the 600-ml beaker add 20 g of fuller's earth which passes a 100-mesh screen, and thoroughly mix with a steel spatula. Add 15 g of 30- to 60-mesh fuller's earth, and mix with the finer fuller's earth to make the latter more porous.

Transfer the fuller's earth mixture, not too wet but before it becomes dusty, to a Soxhlet extraction thimble (43 mm in diameter and 123

mm high). Plug the top of the thimble with cotton to prevent washing the fuller's earth out of the thimble during the subsequent extraction. Let the thimble with its contents stand for 4 hours, then place it in a Soxhlet extraction apparatus, cover with pentane, and allow to soak overnight. Extract with pentane for 6 hours, and again allow the thimble to soak overnight. Then extract for an additional 6 hours. (Place glass beads in the distilling flask to prevent bumping). Transfer the pentane solution, a little at a time, to a 250-ml beaker and evaporate at room temperature under the hood. The beaker must never be more than half-filled, otherwise the evaporation of the pentane will cause the oily constituents to creep over its rim. Place the beaker on the steambath and then in an oven at 105° C to drive off the last traces of pentane, cool in a desiccator, and weigh. The weight of the oily constituents divided by 5 and multiplied by 100 gives the percentage of them in the sample. The oily constituents should be amber colored. If darker they must be treated again with fuller's earth and reextracted.

3. ASPHALTIC RESINS

After the removal of the oily constituents, extract the fuller's earth in the thimble with ethyl ether in the manner described for the oily constituents. Evaporate the ether solution to dryness, heat in an oven at 105° C, cool, and weigh. The weight of the residue divided by 5 and multiplied by 100 gives the percentage of asphaltic resins.

III. ANALYTICAL DATA

Table 1 illustrates the type of analytical results obtained with the revised method, using pentane and ether as solvents.

The results given in table 1 are the average of two determinations. The duplicate asphaltene determinations varied by less than 0.3 percent. The maximum difference between determinations of the oily constituents was 1.5 percent and of the resins 1.0 percent.

TABLE 1.—*Composition of four asphalts determined by the revised method*

Components	A	B	C	D
	%	%	%	%
Asphaltenes	40.1	48.3	36.7	44.9
Oily constituents	41.0	33.2	40.0	39.0
Resins	18.2	17.8	22.7	15.5
Total	99.3	99.3	99.4	99.4

The revised method is applicable not only to asphalts but to crude oils as well. Hence, every crude oil can be classified with respect to the proportion of asphaltenes, resins, and oily constituents that it contains. This is illustrated by the analysis of various crude oils as shown in table 2. In this table the percentages of the oily constitu-

ents were obtained by difference. The oily constituents of the crude oils are volatile and so can not be determined directly without a slight change in technic.

TABLE 2.—*Analysis of crude oils by the revised method*

Specimen	Source	Asphaltenes	Oily constituents	Resins
		%	%	%
1	Arkansas	4.3	79.9	15.8
2	Texas	7.2	76.6	16.2
3	do	5.5	80.7	13.8
4	do	7.7	77.9	14.4
5	California	6.7	74.7	18.6
6	do	17.5	63.7	18.8
7	do	9.8	75.4	14.8
8	Kentucky	0.1	95.8	4.1

WASHINGTON, February 25, 1941.

U. S. DEPARTMENT OF COMMERCE NATIONAL BUREAU OF STANDARDS

RESEARCH PAPER RP1388

Part of Journal of Research of the National Bureau of Standards, Volume 26, May 1941

METHODS FOR DETERMINING SOUND TRANSMISSION LOSS IN THE FIELD [1]

By Albert London

ABSTRACT

In the customary method of determining the transmission loss of a wall or floor partition, it is necessary to measure the difference in sound levels existing in two rooms which have the partition as a separating wall or floor. Also the ratio A_2/S, where A_2 is the total sound absorption of the receiving room and S the transmitting area of the partition, must be known. Difficulties are experienced in field measurements because of the nonuniformity of sound levels in the test rooms and an uncertain knowledge of A_2. Two new methods which eliminate these difficulties are described. In both of these methods the sound level on the quiet side is measured at the panel face, in the one method with a pressure microphone and in the other with a pressure gradient (ribbon) microphone. In the latter method, the transmission loss is independent of the value of A_2/S if the panel face has little sound-absorptive value, while in the former it is possible, in most cases, to eliminate the necessity of measuring A_2 by determining in addition the average sound level in the receiving room.

Also, the possibility of using the ribbon microphone as a radiation pickup is indicated.

CONTENTS

	Page
I. Introduction	419
II. Description of methods	420
1. Usual method	420
2. Alternate methods	422
(a) Pressure-microphone alternate method	422
(b) Ribbon-microphone alternate method	422
III. Experimental results	422
1. Pressure-microphone alternate method	422
2. Ribbon-microphone alternate method	436
IV. Interpretation of results	440
1. Pressure-microphone alternate method	440
2. Ribbon-microphone alternate method	449
V. Further applications of the ribbon-microphone alternate method	451

I. INTRODUCTION

This work was initiated with the purpose of developing a method of determining the sound-insulating efficiency of wall and floor partitions which would give results for field measurements comparable to those obtained in the laboratory. The method in most general use for laboratory determinations is one which consists in inserting the panel in an opening between two rooms in one of which a source of sound is located. The difference in sound level in the source and receiving room

[1] Presented in part at the twenty-third meeting of the Acoustical Society of America, April 29 and 30, 1940, under the title, *The Dependence of Sound Transmission Measurements on Microphone Position.*

may be related to give the efficiency of the construction in terms of the transmission loss, which is defined by the equation:

$$\text{Transmission loss} = L_1 - L_2 + 10 \log_{10} (S/A_2), \quad (1)$$

where L_1 = average sound level in decibels in room 1, the source room,
L_2 = average sound level in decibels in room 2, the receiving room,
S = total area of sound transmitting surface,
A_2 = total absorption in room 2, A_2 measured in same units as S.

If it is attempted to use eq 1 in field determinations of the transmission loss, one may meet with several difficulties of a more or less serious nature. The sound level in the rooms under question may vary considerably from point to point, so that just what the average sound level is may be highly indefinite. Means for determining A_2 may not be available, or even if available, a satisfactory field determination of the absorption in the receiving room may be difficult to make. To eliminate these and similar possibilities of error, two alternate methods have been developed, which, it is believed, are more suitable for field measurements.

II. DESCRIPTION OF METHODS

1. USUAL METHOD

The term "usual method" refers to the procedure which is ordinarily used in our laboratory for the determination of the transmission loss. Since the results obtained by the alternate methods are to be compared with those obtained in the usual method, it will be of some interest to describe the latter also.

A description of the sound-transmission rooms has been given previously by V. L. Chrisler and W. F. Snyder.[2] It will suffice to say here that the receiving room (for wall panels) is about 9 ft. high, 12 ft. wide, and 16 ft. long. The opening between the two rooms will accommodate panels 7 ft. 4 in. high and 5 ft. 10 in. wide, while the dimensions of the sound-transmitting area of the panel are 6½ by 5 ft. There is no sound-absorption treatment in either of the rooms, the concrete walls being left bare.

In this same paper there are described some experimental devices which were used in the source room to obtain a diffuse sound field, that is, one in which the energy density is uniform at different regions in the room and the energy flow takes place equally in all directions. The necessity for doing this will be apparent from a perusal of a paper by Buckingham,[3] who gives the theoretical basis upon which eq 1 is founded. In this article a fundamental assumption is the uniformity of sound-energy densities in both the source and receiving room. To approach this ideal condition the following means are used:

1. As a source of sound, a warble note instead of a pure tone is used. The measurements are taken at nine different frequencies: 128, 192, 256, 384, 512, 768, 1,024, 2,048, and 4,096 c/s, the listed frequency being the center of the band; the band width is 36 percent of the band center at 128 and 256 c/s, and 18 percent at the seven other frequen-

[2] J. Research NBS **14**, 749 (1935) RP800.
[3] Sci. Pap. BS **20**, 193 (1925) S506.

FIGURE 1.—*Multiple-loudspeaker unit.*

Only three of the loudspeakers are visible. Three others are located on the rear faces. Note that each speaker points in a different direction.

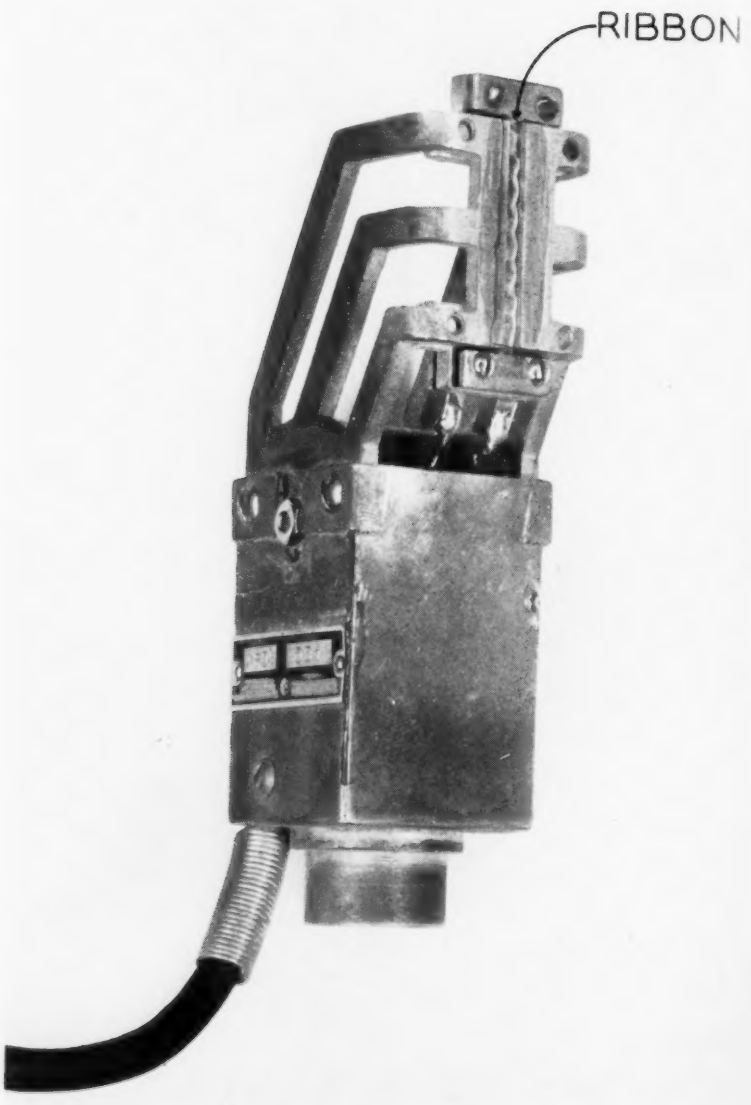

FIGURE 2.—*Microphone used in the ribbon-microphone alternate method.*

cies. Doubling the band width at the two lower frequencies reduces materially the scatter in the transmission-loss measurements while producing no significant change in the results.

2. The loudspeaker unit consists of a box (which rotates when in use) on which are mounted six loudspeakers. This device is pictured in figure 1. Three speakers each are mounted on opposite ends of the box, each one being directed into a different direction in the room. The net effect of the varied orientations of the speakers, in conjunction with the rotation of the box, is a considerable improvement in sound pattern. As compared with a rotating source consisting of one speaker, the spread in sound-pressure level over the panel face was reduced from 5 or 6 decibels to only 2 or 3 db (decibels). Also, the uniformity of sound-pressure distribution in both source and receiving room was considerably improved.

To minimize effects arising from fluctuations in the pressure level or from the sound pattern in the test rooms, the following devices are utilized:

1. The microphone signal is passed into an amplifier having at its output a thermoelement as a rectifier and a galvanometer as an indicator. The speed of response of this combination is somewhat sluggish, so that variations in signal level are effectively ironed out. Further details of this arrangement are given in Research Paper RP800 (see footnote 2).

2. Four nondirectional pressure microphones (Western Electric Type 633A, "salt shaker" type) are used in taking the measurements, two being used in the source room and two in the receiving room. The outputs of the two microphones are effectively averaged by a commutating device which switches rapidly from one microphone to the other. Thus the signal obtained at the amplifier output is a composite affair consisting of short samplings from the two microphones. This type of arrangement indicates a pressure level which is the average of two positions. The two microphones are arranged on a cross arm with a separation of about 2½ ft between them, and the latter is connected to a trolley which rides on a rail. Different microphone positions are obtained with the aid of a semiautomatic positioning device which is connected by a system of pulleys and cables to the trolley.

At the four lower frequencies at which measurements are taken, readings are made in both rooms at eight different positions 6 in. apart along a line perpendicular to the panel face. At the five upper frequencies, readings are taken only at four positions, at 1-ft intervals, because of the uniformity in sound level. In the noisy room all microphone positions were confined to distances greater than about 2 ft from the panel face, whereas in the quiet room all distances were greater than 3 ft. Reasons for these restrictions on the microphone positions will be evident when some of the experimental results are discussed.

After readings are taken on the one side with the two microphones, a similar set of readings is taken on the other side with the two other microphones. Another independent set of measurements is taken with the microphones interchanged so as to eliminate differences in response, although the four microphones have almost identical response curves.

2. ALTERNATE METHODS

A description of both alternate methods will be given here. However, a statement of the predisposing reasons favoring these methods for field measurements will be given in section III.

(a) PRESSURE-MICROPHONE ALTERNATE METHOD

The only detail in which this method differs from the usual method is the placement of the pressure microphones on the quiet side. In this case, the measurements in the receiving room are taken at the panel face. The two microphones are hung on a crossarm with a separation of about 2 ft between them. Eight readings are taken over the face of the partition at 6-in. intervals in a vertical direction (for wall panels) at the lower frequencies and four readings at 1-ft intervals for the higher frequencies. It is desirable that the microphones be placed as close as possible to the panel face without touching, although for the particular microphones which were used, no difficulties were encountered if the microphones were permitted to touch the panel loosely.

(b) RIBBON-MICROPHONE ALTERNATE METHOD

In this method the pressure microphones are entirely dispensed with and a single pressure gradient microphone is substituted. On the noisy side the microphone position is varied over exactly the same distance as in the usual method, while on the quiet side the measurements are taken at the panel face. As before, in the source room eight readings are taken at the lower frequencies and four at the upper frequencies. In the receiving room eight readings are taken over the panel face at all of the nine frequencies, the particle-velocity level indications at the higher frequencies varying somewhat more in this case than in the pressure-microphone alternate method. It is important that the microphone does not touch the panel, as "chattering" occurs and this results in an inordinate increase in level. The microphone used in these experiments is of the ribbon type and was built for us by Shure Bros. This is shown in figure 2. Its special design features will be indicated in section III–2. In use, the plane of the ribbon is placed parallel to the panel face, the face of the microphone being as close as possible without touching the panel.

III. EXPERIMENTAL RESULTS

1. PRESSURE-MICROPHONE ALTERNATE METHOD

One of the important experimental phenomena associated with our problem is pictured in figure 3 (A to I). There is shown in this series of curves the nature of the sound pattern in the receiving room and how it varies with distance from the face of the panel and with the amount of sound absorption in the receiving room. The curves, which are drawn through the experimental points, were obtained using four pressure microphones arranged to cover an area of about 2 sq ft, their outputs being commutated. The values of absorption range from that of the bare room (A'_1) to that when the room was as absorbent as it could be made conveniently (A'_5). The more promi-

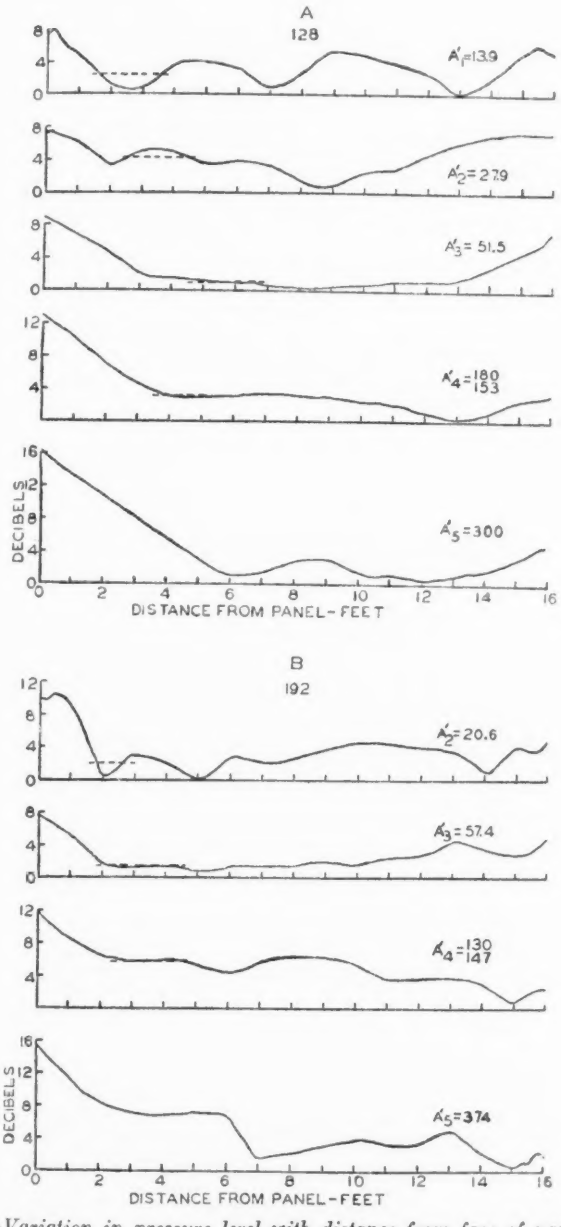

FIGURE 3.—*Variation in pressure level with distance from face of panel on quiet side.*

The total absorption of the receiving room is given in Sabins as A'_1, A'_2, A'_3, A'_4, and A'_5. Zero decibels for each curve is entirely arbitrary. Measurements were taken at nine different frequencies.
A, 128 c/s; *B*, 192 c/s.

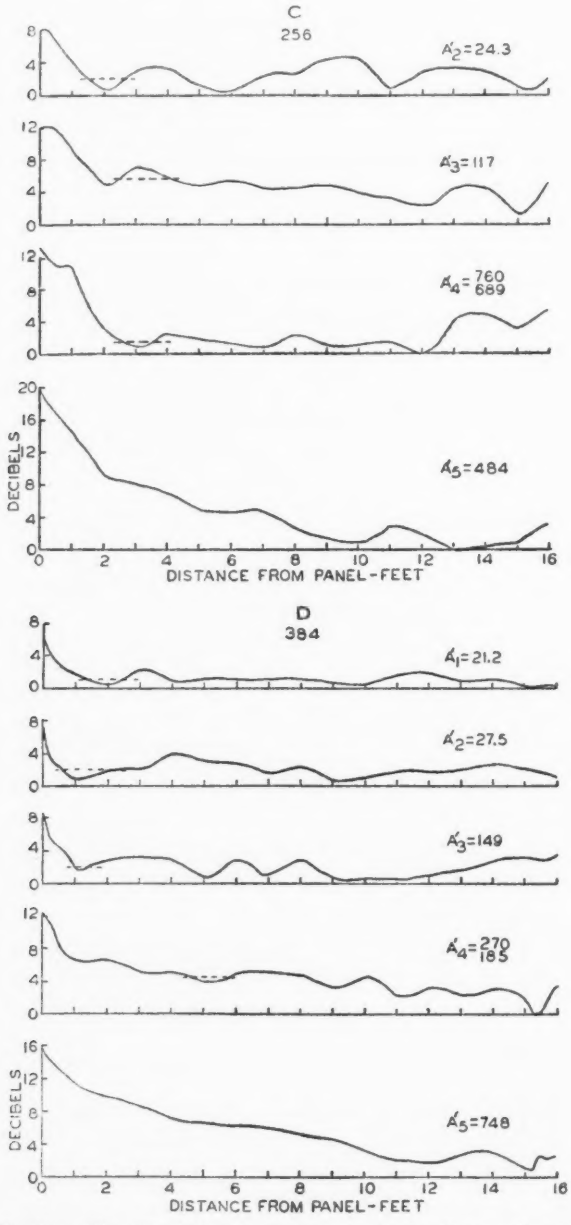

FIGURE 3 (Continued).—*Variation in pressure level with distance from face of panel on quiet side.*

C, 256 c/s; *D*, 384 c/s.

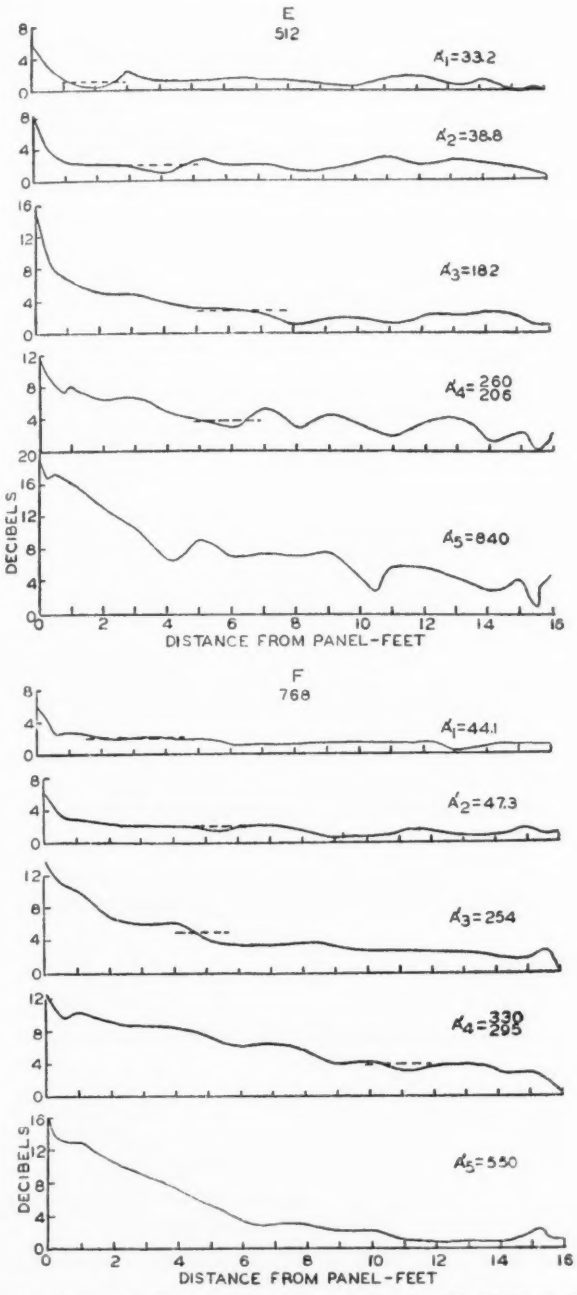

FIGURE 3 (Continued).—*Variation in pressure level with distance from face of panel on quiet side.*

E, 512 c/s; *F*, 768 c/s.

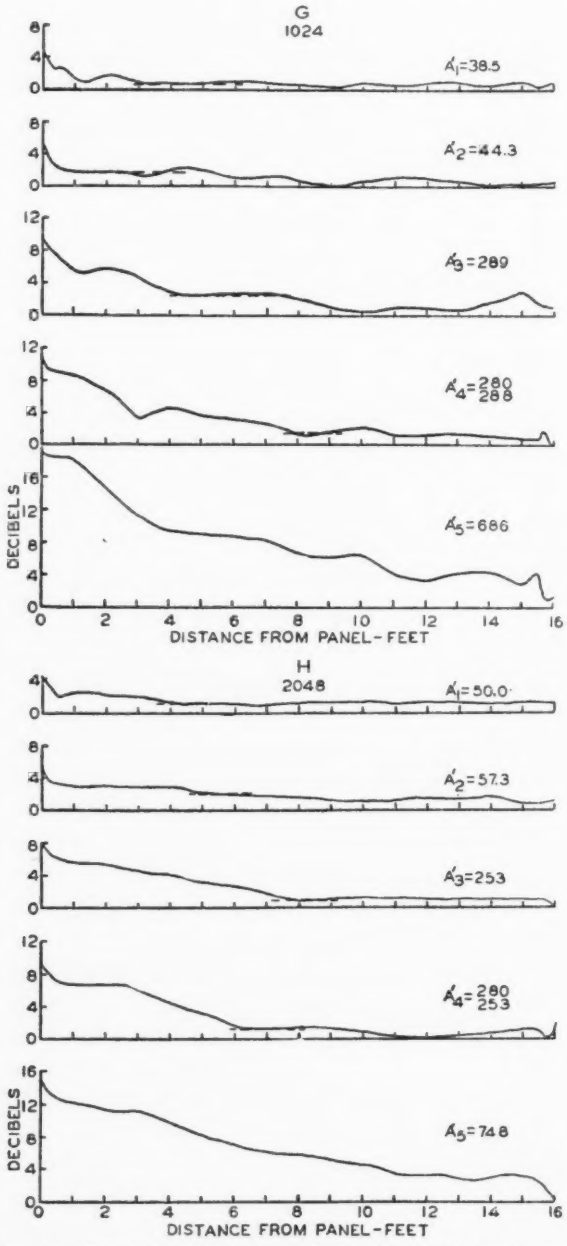

FIGURE 3 (Continued).—*Variation in pressure level with distance from face of panel on quiet side.*

G, 1,024 c/s; *H*, 2,048 c/s.

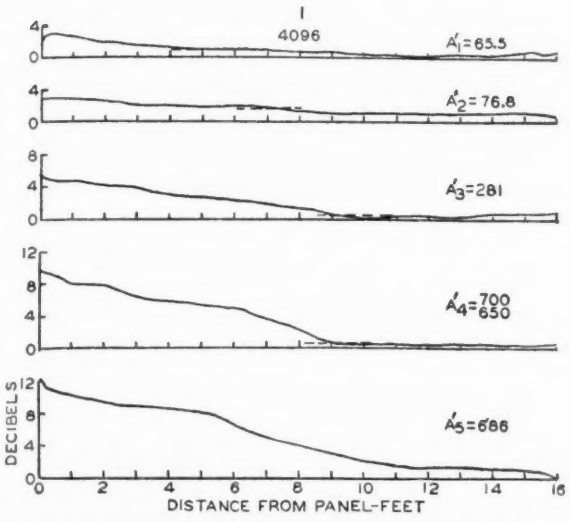

FIGURE 3 (Continued).—*Variation in pressure level with distance from face of panel on quiet side.*

I, 4,096 c/s.

nent features of the curves are the initial drop in sound-pressure level,[4] which occurs within a relatively short distance from the panel, and the flattening out of the curve to give a plateau with slight ridges and valleys. As the absorption increases, the initial drop becomes larger; further, the plateau is not quite established, the level dropping off slowly with increasing distance from the panel. For the highest values of absorption, that of A'_5 at the higher frequencies, there is really no leveling off of the curve anywhere in the room.

It is thus seen that considerable difficulty may be encountered in taking field measurements, since the amount of absorption in the receiving room may vary widely. In the first place, only in the case of rooms which are not too highly absorbent will a fairly uniform pressure level exist throughout most of the room. The position at which the pattern curve starts to flatten out and the average pressure level about which the level in the room fluctuates is indicated by the dotted line in figures 3 (*A* to *I*). The observer should keep away from positions very close to the panel if he wishes to use eq 1, as errors of 5 to 10 db, or even larger, may be involved. Furthermore, this requires an investigation of the variation of pressure level with distance from the panel face, so as to determine the positions in the room where the pattern has flattened out. In the case of highly absorbent rooms, such as a dead or moderately dead room, no uniform pressure level exists throughout any part of the room.

[4] The term "sound-pressure level" (abbreviated to pressure level) as used in this paper refers to the decibel reading of the thermoelement-galvanometer indicating system when a pressure microphone is used as a pickup. Similarly, if a velocity microphone is used, reference will be made to particle-velocity level, or velocity level. The reference level of zero decibels is entirely arbitrary, as of chief interest are differences of level.

It is evident that the pressure-microphone alternate method eliminates these obstacles, as in this test procedure the microphones are placed next to the panel on the quiet side. The question arises whether it is possible to correlate the alternate-method results with those obtained by the usual method. We have been able to derive equations which give good agreement between both test procedures. The actual development of these expressions will be given in section IV. However, the physical considerations involved will be briefly stated here.

The sound energy density at the panel face on the quiet side is considered to consist of contributions from two distinct components. First, part of this sound energy arises from sound energy radiated directly off the panel; second, the remainder is energy which arises from the diffuse or reverberant component existing throughout the room. That is, the energy which is radiated by the panel suffers a great number of reflections at the boundaries of the room, and the net effect is the establishment of a diffuse state throughout the whole room. In the vicinity of the panel, however, there is superimposed on this reverberant energy the energy radiated directly from the vibrating partition. This means that the level at the panel face will be greater than that existing in the part of the room where the diffuse sound field is present. The average pressure level caused by the latter is represented by the dotted lines of figure 3 (*A* to *I*).

As a consequence of these and other similar considerations, the following equations were derived for the pressure microphone alternate methods:

$$TL=(PL)_1-(PL)_{20}+10\log_{10}\left[\frac{1}{2}(1+2\sqrt{S/A_2})^2\right], \qquad \nu=128 \text{ c/s}, \quad (2)$$

$$TL=(PL)_1-(PL)_{20}+10\log_{10}(1/2+2S/A_2), \qquad \nu=192 \text{ to } 2{,}048 \text{ c/s}, \quad (3)$$

$$TL=(PL)_1-(PL)_{20}+10\log_{10}(3/8+S/A_2), \qquad \nu=4{,}096 \text{ c/s}, \quad (4)$$

where

TL = transmission loss in decibels.
$(PL)_1$ = average pressure level in the source room.
$(PL)_{20}$ = average pressure level at the panel face in the receiving room.
S = total area of sound-transmitting surface
A_2 = total absorption in receiving room, A_2, measured in same units as S.
ν = frequency in cycles per second.

Equation 2 is to be used for measurements taken at 128 c/s, eq 3 for those taken at frequencies ranging from 192 to 2,048 c/s, and eq 4 for those taken at 4,096 c/s. It is seen that the transmission loss is given in each case by the difference in level which is observed, plus a correction term. The correction terms are plotted in figure 4 for different values of the ratio A_2/S.

In table 1 are presented results on 16 different measurements of transmission loss made on 9 different panels. For reference purposes, the absorption (in square feet) of the receiving room and the corresponding correction as determined from figure 4 with $S=32.5$ sq. ft (the sound-transmitting area of our panels) head the series of observations which were made at this value of absorption. Under "*TL*, usual" there is given the transmission loss as measured at the

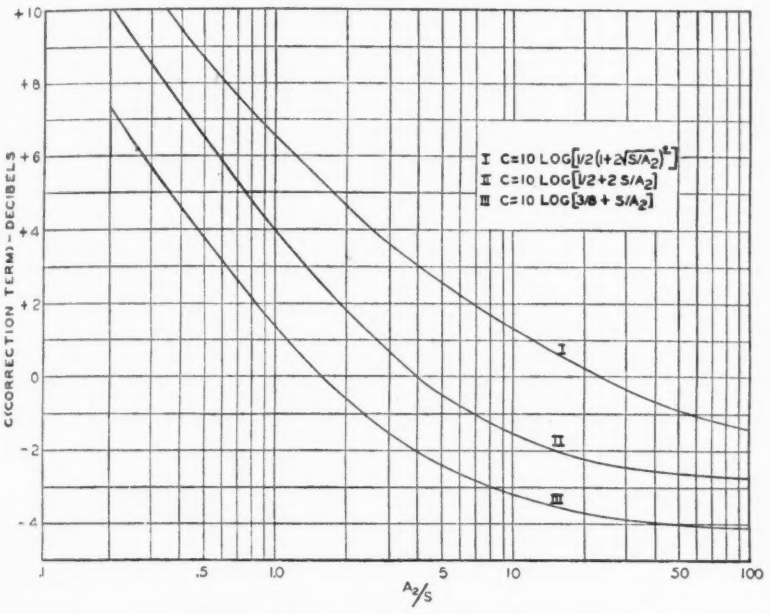

FIGURE 4.—*Dependence of the correction term, C, on the ratio A_2/S.*

Curve I is valid for a frequency of 128 c/s; curve II for 192 to 2,048 c/s; and curve III for 4,096 c/s.

different frequencies, 128 to 4,096 c/s, by the usual method, and "*TL*, alternate" gives the transmission loss determined by the alternate method. In the column captioned "average," the average transmission loss (average of the transmission loss measured at the nine different frequencies) is listed and opposite "correction," the average of the nine individual corrections. The panels measured had average transmission losses varying from about 10 to 50 db, and the types of construction represented include porous building block, porous building block with plastered surface, solid plaster on metal lath, and complex wood stud partition with very little tie between the two surfaces. There are thus included homogeneous, porous, and complex structures; thicknesses range from 2 to 12 in.

TABLE 1.—*Comparison between results obtained by usual and pressure-microphone alternate methods*

Frequency, c/s:	128	192	256	384	512	768	1,024	2,048	4,096	Average	Test No.	Panel No.
Units of absorption (A_1)	13.9	14.4	19.7	21.2	33.2	44.1	38.5	50.0	65.5			
Corrections	9.1	6.9	5.7	5.4	3.8	3.0	3.4	2.6	−0.6	4.4		
TL, usual	34.2	41.2	39.7	39.7	42.6	43.9	44.6	50.1	58.9	43.9	F4	Z2
TL, alternate	32.7	38.4	39.2	40.0	41.6	42.5	44.9	50.9	60.2	43.4		
TL, usual	32.3	32.4	33.5	34.0	36.2	36.2	39.0	41.6	51.8	37.4	F7	X2
TL, alternate	34.7	28.4	33.3	31.3	34.5	36.2	39.7	42.4	52.6	37.0		
Units of absorption (A_1)	27.9	20.6	24.3	27.5	38.8	47.3	44.3	57.3	76.8			
Corrections	7.0	5.5	4.9	4.5	3.2	2.8	2.9	2.2	−1.0	3.6		
TL, usual	34.2	41.2	39.7	39.7	42.6	43.9	44.6	50.1	58.9	43.9	F3	Z2
TL, alternate	33.8	38.1	39.5	39.2	41.9	42.6	44.5	51.6	59.4	43.4		
TL, usual	30.9	26.9	27.4	35.8	34.6	33.1	35.9	40.2	46.6	34.6	F5	X1
TL, alternate	33.2	27.9	30.4	37.6	35.9	32.4	37.1	42.9	48.7	36.2		
TL, usual	32.3	32.4	33.5	34.0	36.2	36.2	39.0	41.6	51.8	37.4	F6	X2
TL, alternate	32.1	29.9	35.8	32.2	35.1	35.4	40.6	42.9	52.2	37.4		
Units of absorption (A_1)	51.9	44.6	48.3	48.5	55.7	66.5	65.7	82.0	100			
Corrections	5.2	3.0	2.7	2.7	2.3	1.8	1.8	1.2	−1.5	2.1		
TL, usual	13.0	16.7	16.1	20.5	21.8	19.2	20.5	24.6	29.7	20.2	F2	Z1
TL, alternate	15.0	17.6	17.2	21.1	22.1	20.6	21.3	26.9	30.7	21.4		
Units of absorption (A_1)	51.5	57.4	117	149	182	254	289	274	281			
Corrections	5.1	2.2	0.2	−0.3	−0.6	−1.2	−1.4	−1.3	−3.1	0		
TL, usual	32.3	32.4	33.5	34.0	36.2	36.2	39.0	41.6	51.8	37.4	H1	X2
TL, alternate	32.5	32.9	33.3	31.5	35.2	36.0	40.4	41.3	50.8	37.1		
TL, usual	43.8	46.6	47.4	47.7	47.4	49.9	50.0	52.1	63.4	49.8	H2	X3
TL, alternate	44.1	45.3	42.5	45.4	43.2	46.0	46.2	51.1	62.5	47.4		
TL, usual	35.2	33.3	22.3	31.6	31.3	30.8	37.7	46.7	54.9	36.0	H3	X4
TL, alternate	32.3	33.3	25.7	32.5	30.2	29.0	36.8	47.0	53.1	35.5		
Units of absorption (A_2)	166	138	724	227	233	313	284	266	675			
Corrections	2.5	−0.1	−2.2	−1.0	−1.0	−1.5	−1.3	−1.2	−3.8	−1.1		
TL, usual	43.8	46.6	47.4	47.7	47.4	49.9	50.0	52.1	63.4	49.8	J1	X3
TL, alternate	42.6	47.3	43.3	47.2	45.7	46.3	47.7	52.6	65.5	48.7		
TL, usual	35.2	33.3	22.3	31.6	31.3	30.8	37.7	46.7	54.9	36.0	J2	X4
TL, alternate	26.9	31.5	20.4	32.2	29.8	27.4	37.3	49.2	54.4	34.3		
TL, usual	35.2	33.3	22.3	31.6	31.3	30.8	37.7	46.7	54.9	36.0	J3	X4
TL, alternate	29.8	30.9	27.5	32.6	30.2	29.3	37.5	48.2	52.8	35.4		
Units of absorption (A_1)	300	374	484	748	840	550	686	748	686			
Corrections	1.4	−1.7	−2.0	−2.3	−2.3	−2.1	−2.2	−2.3	−2.2	−1.7		
TL, usual	29.2	29.9	25.6	30.4	30.5	33.5	37.0	46.4	53.8	35.1	F1	Z5
TL, alternate	30.3	28.2	25.9	32.0	31.1	34.1	39.0	46.0	51.0	35.3		
TL, usual	7.9	7.5	5.2	7.3	8.6	12.2	14.1	18.5	17.4	11.0	F1	Z4
TL, alternate	5.3	6.3	5.2	5.4	7.3	13.4	12.0	16.2	17.0	9.8		
TL, usual	35.2	33.3	22.3	31.6	31.3	30.8	37.7	46.7	54.9	36.0	K1	X4
TL, alternate	30.1	30.5	23.0	31.7	30.6	28.0	36.2	47.1	54.0	34.6		
TL, usual	34.3	26.4	33.0	36.8	34.6	37.4	43.2	50.5	56.9	39.2	K2	X5
TL, alternate	32.1	28.1	27.6	37.0	33.9	36.3	44.3	51.2	58.5	38.8		

In table 2 the difference between the alternate *TL* and the usual *TL* is given. A minus sign indicates that the alternate *TL* was less than the usual *TL*.

The average deviation of the differences between the average *TL*'s as measured by the two methods is only 0.8 db, well within the experimental error. If these differences are averaged without disregarding their signs, the average difference of −0.4 db is obtained for the average *TL*'s. It should be pointed out that the possible error in determining the average transmission loss of a panel is about 1.5 db. Thus, tests J2 and J3 were made under identical conditions on the same panel, about 6 weeks apart. The two measurements differ by 1.1 db, perhaps owing to aging of the plaster. If two different panels nominally built in accordance with the same specifications are measured, the results may differ by as much as 2 db. In one extreme case at our laboratory there was a difference of 2.5 db.

TABLE 2.—*Figures give the difference between the transmission loss measured by the pressure-microphone alternate method and that measured by the usual method*

Panel No.	Test No.	128	192	256	384	512	768	1,024	2,048	4,096	Difference between Avg. *TL*'s
Z2	F4	−1.5	−2.8	−0.5	+0.3	−1.0	−1.4	+0.3	+0.8	+1.3	−0.5
X2	F7	+2.4	−4.0	−.2	−2.7	−1.7	0	+.7	+.8	+0.8	−.4
Z2	F3	−0.4	−3.1	−.2	−0.5	+0.7	−1.3	−.1	+1.5	+.5	−.5
X1	F5	+2.3	+1.0	+3.0	+1.8	+1.3	−0.7	+1.2	+2.7	+2.1	+1.6
X2	F6	−0.2	−2.5	+2.3	−1.8	−1.1	−.8	+1.6	+1.3	+0.4	0
Z1	F2	+2.0	+0.9	+1.1	+0.6	+0.3	+1.4	+0.8	+2.3	+1.0	+1.2
X2	H1	+0.2	+.5	−0.2	−2.5	−1.0	−0.2	+1.4	−0.3	−1.0	−0.3
X3	H2	+.3	−1.3	−4.9	−2.3	−4.2	−3.9	−3.8	−1.0	−0.9	−2.4
X4	H3	−2.9	0	+3.4	+0.9	−1.1	−1.8	−0.9	+0.3	−1.8	−0.5
X3	J1	−1.2	+.7	−4.1	−.5	−1.7	−3.6	−2.3	+.5	+2.1	−1.1
X4	J2	−8.3	−1.8	−1.9	+.6	−1.5	−3.4	−0.4	+2.5	−0.5	−1.7
X4	J3	−5.4	−2.4	+5.2	+1.0	−1.1	−1.5	−.2	+1.5	−2.1	−0.6
Z5	F1	+1.1	−1.7	+0.3	+1.6	+0.6	+0.6	+2.0	−0.4	−2.8	+.2
Z4	F1′	−2.6	−1.2	0	−1.9	−1.3	+1.2	−2.1	−2.3	−0.4	−1.2
X4	K1	−5.1	−2.8	+.7	+0.1	−0.7	−2.8	−1.5	+0.4	−.9	−0.4
X5	K2	−2.2	+1.7	−5.4	+.2	−.7	−1.1	+1.1	+.7	+1.6	−.4
Average deviation		2.4	1.8	2.1	1.2	1.2	1.6	1.3	1.2	1.3	0.8
Average difference		−1.3	−1.2	−0.1	−0.3	−0.9	−1.2	−0.1	+0.7	0	−0.4

It may therefore be said that all the deviations are within the error of measurement except for test H2, where the deviation is 2.4 db. This particular panel was constructed in two units with very little connection between the two. However, it is believed the difference is not due to this complexity of structure, since test J1 was made on the same panel and the deviation here was 1.1 db.

Resonance effects at the lower frequencies, 128, 192, 256 c/s, cause a greater scattering of the data, the average deviation being about 2 db. The value of the average difference indicates how well the individual differences scatter to either side of the usual value. The tendency to be a bit low is evident. On the average, however, eq 2, 3, and 4 may be said to give results in very good agreement with those obtained by the usual method.

Some important characteristics of the correction terms may now be considered. For example, for $A_2=233$ sabins and $S=32.5$ sq ft the correction is -1.0 db (from curve II, fig. 4). This is to be compared with the value of the correction one would need to use if the measurements were taken by the usual method. The correction from eq 1 has the value $-10\log_{10}(23.3/32.5)=-8.6$ db. It may be seen that the alternate-method correction in this case is much less than the usual-method correction. In fact, figure 4 shows that in the range of values 2 to 15 for A_2/S, the correction varies only between $+2$ and -2 db for curve II. For field measurements, where an accuracy of within 2 db is usually satisfactory, the correction term may be neglected. Furthermore, if one is interested chiefly in the average of the nine transmission losses and not in the individual values, it is possible to get good results by using correction curve II for all frequencies since curves I and III deviate in opposite directions relative to II.

When this is possible, a rough estimate of the ratio A_2/S will suffice, as the correction term is relatively insensitive to errors in A_2/S. Another way of determining this ratio, without recourse to a reverberation method of measuring A_2, is to investigate the variation in pressure level with distance from the face of the panel (as in fig. 3, *A* to *I*).

Equations (see section IV) may be derived which will give the difference in level between that at the face of the panel on the quiet side and the average level existing in the quiet room. These equations are:

$$(PL)_{20}-(PL)_2=10\log_{10}\left[\frac{1}{2}\frac{A_2}{S}\left(1+2\sqrt{\frac{S}{A_2}}\right)^2\right],\ \nu=128\text{ c/s},\qquad(5)$$

$$(PL)_{20}-(PL)_2=10\log_{10}\left(1/2\frac{A_2}{S}+2\right),\qquad \nu=192\text{ to }2{,}048\text{ c/s}\qquad(6)$$

$$(PL)_{20}-(PL)_2=10\log_{10}\left(3/8\frac{A_2}{S}+1\right),\qquad \nu=4{,}096\text{ c/s},\qquad(7)$$

where all symbols have been previously defined. To test the validity of eq 5, 6 and 7, a series of measurements were taken on a number of panels. In each case the pattern in the quiet room was observed, curves similar to figure 3 (*A* to *I*) being drawn. From these curves the differences in level between that at the panel face and the level about which the curves begin to flatten (indicated by the dotted lines of fig. 3, *A* to *I*) were obtained. These are indicated as the observed values of Δdb in table 3.

TABLE 3.—*Comparison between observed and calculated Δdb values*

[Δdb=difference in level between that at face of panel and the average level about which the pattern in the receiving room flattens out.]

Panel No.	Absorption (A_2)	Δdb		Absorption (A_2)	Δdb		Absorption (A_2)	Δdb	
		Observed	Calculated		Observed	Calculated		Observed	Calculated
		128			192			256	
X5	13.9	4.9	5.4						
X5	27.9	3.1	6.3	20.6	8.0	3.6	24.3	6.0	3.8
X5	51.5	8.0	7.3	57.4	5.3	4.6	117	6.3	5.8
Z2	27.9	7.6	6.3	20.6	4.1	3.6	24.3	5.4	3.8
X2				14.4	5.8	3.4	19.7	8.1	3.6
X2	51.5	4.9	7.3	57.4	4.8	4.6	117	6.4	5.8
X3	51.5	10.0	7.3				117	7.5	5.8
X4	51.5	7.0	7.3	57.4	4.0	4.6	117	9.0	5.8
		384			512			768	
X5	21.2	4.8	3.6	33.2	4.8	4.0	44.1	4.1	4.3
X5	27.5	6.0	3.9	38.8	4.3	4.2	47.3	4.2	4.4
X5	149	6.5	6.3	182	12.3	6.8	254	9.0	7.8
Z2	27.5	4.9	3.9	38.8	4.5	4.2	47.3	5.0	4.4
X2	21.2	3.2	3.6	33.2	5.8	4.0	44.1	4.2	4.3
X2	149	7.5	6.3	182	10.1	6.8	254	7.4	7.8
X3	149	6.9	6.3	182	11.0	6.8	254	10.7	7.8
X4	149	8.5	6.3	182	5.5	6.8	254	8.5	7.8
		1,024			2,048			4,096	
X5	38.5	4.5	4.2	50.0	3.3	4.5	65.5	1.0	2.4
X5	44.3	3.5	4.4	57.3	3.2	4.6	76.8	1.5	2.8
X5	289	6.7	8.1	253	7.0	7.7	281	5.2	6.2
Z2	44.3	3.5	4.4	57.3	1.2	4.6	76.8	1.0	2.8
X2	38.5	3.6	4.2	50.0	3.3	4.5	65.5	1.5	2.4
X2	289	9.5	8.1	274	5.3	7.7	281	5.3	6.2
X3	289	10.9	8.1	274	7.8	7.7	281	4.2	6.2
X4	289	9.5	8.1	274	5.5	7.7	281	3.5	6.2

The calculated values of Δdb were obtained by substituting $S=32.5$ sq ft and A_2 as determined from reverberation measurements in eq 5, 6, and 7; the three different room treatments represented in table 3 correspond to the values of absorption A'_1, A'_2, and A'_3 of figure 3 (A to I).

In table 4 there is listed for each frequency the average of the differences between the observed and calculated values of $(PL)_{20}-(PL)_2$ given in table 3. Under the column "average deviation" the absolute values of the differences have been averaged.

TABLE 4.—*Average deviation and difference for the data in table 3*

Frequency	Average deviation	Average difference
c/s		
128	1.6	+0.3
192	1.3	−1.1
256	2.0	−2.0
384	1.1	−1.0
512	2.0	−1.8
768	0.8	−0.6
1,024	1.1	−0.1
2,048	1.4	+1.4
4,096	1.4	+1.4

The similarity between the entries in table 2 and those in table 4 should be pointed out here. In table 2 there is listed the difference in transmission loss as obtained by the alternate method and that obtained by the usual method. Designate this quantity as $(TL)_A-(TL)_U$. For the middle range of frequencies one gets from eq 1 and 3

$$(TL)_A-(TL)_U=(PL)_2-(PL)_{20}+10\log_{10}\left(1/2+2\frac{S}{A_2}\right)-10\log_{10}\left(\frac{S}{A_2}\right)$$

$$=10\log_{10}\left(1/2\frac{A_2}{S}+2\right)-[(PL)_{20}-(PL)_2]$$

But $10\log_{10}\left(1/2\frac{A_2}{S}+2\right)$ is the calculated value of Δdb, while $(PL)_{20}-(PL)_2$ would be the observed value of Δdb were $(PL)_2$ obtained the same way in both sets of experiments. In the transmission measurements $(PL)_2$ is the average level existing between 3 and 6½ ft from the panel face on the quiet side, and it was observed only once under room treatment A'_1 and A'_2, while in the Δdb measurements, $(PL)_2$ is obtained from the pattern curves and was observed over a wider range of variation in A_2. The conclusion one may draw from table 4 is that the average level which is to be used in eq 1 is that about which the pattern curve begins to flatten out. To determine the region in the room where this happens, it is necessary to explore the sound field. It is then possible to determine the correction terms for eq 2, 3, and 4 by utilizing 5, 6, and 7 to determine A_2/S from a measurement of $(PL)_{20}-(PL)_2$. Thus, in figures 3 (A to I) the curves obtained for room treatment A'_4 were used to calculate the value of A'_4 and from this value of absorption the corrections to the alternate transmission measurements were obtained.

Two values of A'_4 are given, the upper one being obtained from the curves of figure 3 (A to I), the lower one from data taken on a different panel. The values check closely enough for the purpose desired, since the transmission loss corrections are relatively insensitive to small changes in absorption. Note, in particular, in figure 3 (B) the measurement of A'_4 at a frequency of 256 c/s. The absorption so determined seems considerably out of line with other values; however, as far as the transmission loss correction is concerned, the error made in it will be relatively small and unimportant.

In section IV–1, expressions are given, eq 42, 43, and 44, in which A_2/S already has been eliminated from the equation for the transmission loss, so that the latter is only a function of the readily observable quantities $(PL)_1-(PL)_{20}$ and $(PL)_{20}-(PL)_2$.

In table 1, the corrections as determined from the A'_4 curves were used in tests J1, J2, and J3. Also in table 1 the tests F1, F1′, K1, and K2 were made when the quiet side had the room treatment A'_5.

To get A'_5, the absorption when the room was as absorbent as it could be made, the Norris-Andree [5] method was used. The decay curves so obtained could not be taken over a range greater than about 30 db, the reverberation time being about 0.1 or 0.2 second. In most of the A'_5 curves, there is very little evidence of flattening out, indicating that a reverberant condition is not really formed. It was not possible to get agreement between the absorption as measured by the Norris-Andree method and from $(PL)_{20}-(PL)_2$ of the pattern for the few curves which did seem to level off. This disagreement is probably due to the insecure basis on which both types of measurement rest, in the case when the room is so absorbent.

So far there have been discussed only modifications in the usual method which are necessitated by the possibility of a nonuniform sound energy distribution on the quiet side. The noisy side has been neglected because it is usually possible to obtain a fairly diffuse sound field in the source room. However, under certain field conditions it may be somewhat difficult to do this. The pattern due to furniture or obstacles may be erratic, or absorption on the noisy side may perturb the uniformity of sound level in the room. It would then be of advantage to restrict measurements on the noisy side to positions at the panel face. The question arises as to what correction should be applied in this case.

Kellogg [6] has shown that a sound-level measuring arrangement—such as a pressure microphone, amplifier, and square-law rectifier (in which the deflection of the output meter is thus proportional to the square of the pressure amplitude of the sound wave)—would give, at a perfectly reflecting wall, a deflection twice as great as at a position away from the wall where a diffuse sound field exists. Thus a meter calibrated to read in decibels would read 3 db higher at the wall. To establish the validity of this conclusion, a series of measurements were taken on the noisy side in which the variation of pressure level with distance from the face of the panel was investigated.

Figure 5 shows the results of this set of experiments. Four pressure microphones arranged to cover an area of about 2 sq ft were used, their outputs being commutated. There is still in evidence in the

[5] J. Acous. Soc. Am., **3**, 361 (1932).
[6] J. Acous. Soc. Am., **4**, 61 (1932).

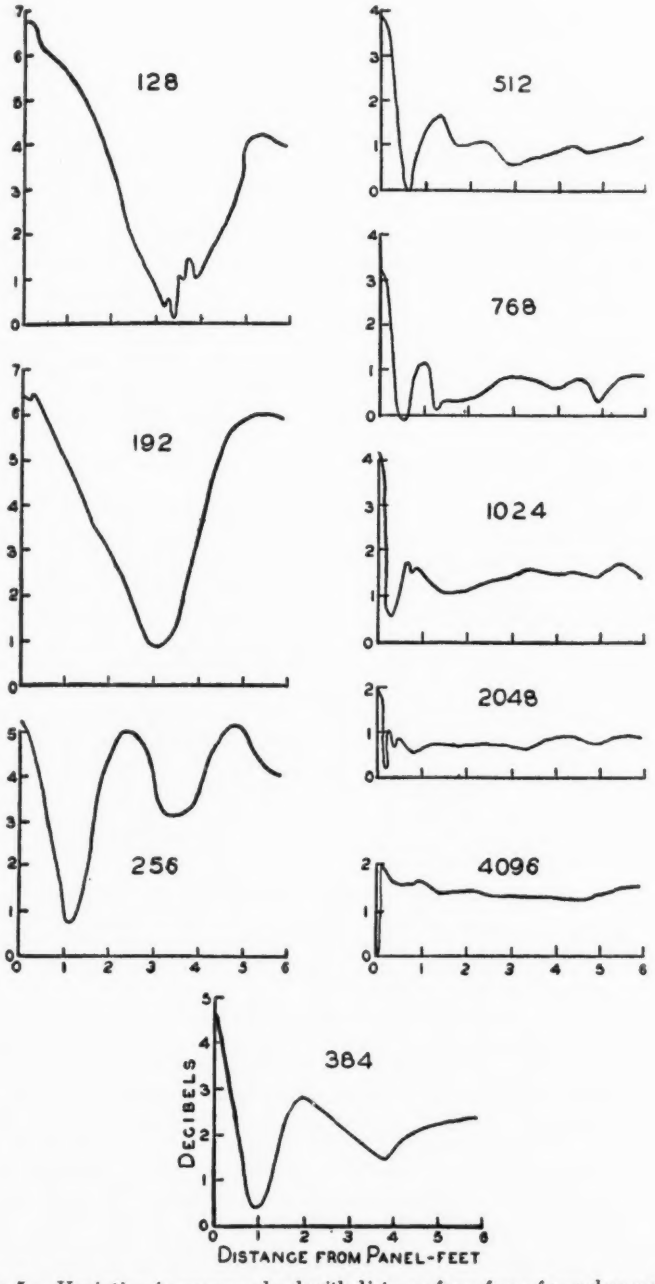

FIGURE 5.—*Variation in pressure level with distance from face of panel on noisy side*

Zero decibels for each individual curve is entirely arbitrary. Frequency concerned is given with each curve.

307823—41——6

vicinity of the panel face some kind of an interference pattern, even though a warble note and the rotating multiple speaker source of six loudspeakers were used. It is to be seen that if the average pressure level is taken as that existing between 2 and 6 ft away from the panel then there is, roughly, a 2.5 to 3 db increase for frequencies up to $\nu =$ 1,024 c/s. This increase is somewhat masked at the lower frequencies because of the nature of the pattern. At 2,048 c/s, the level increase deviates considerably from 3 db and at 4,096 c/s the level actually decreases, probably because of the fact that our microphone is not small enough. At the point of closest approach of the microphone to the wall, the diaphragm is actually centered over the minimum in the pattern, hence the drop in level.

As a consequence of this series of data, it is believed that in tests where it is desirable to keep the pressure microphone immediately next to the test wall on the noisy side, a flat correction of about 2.5 db should be subtracted from the average transmission loss.

To recapitulate: In this section (III–1) there have been considered some of the important experimental facts associated with the problem of measuring sound transmission losses by the pressure-microphone alternate method. It has been indicated how this type of measurement eliminates difficulties arising from the nonuniformity of pressure levels experienced in test rooms. Another type of advantage accrues to this method in the case in which the ambient noise level is rather high or the partition is a very good sound insulator. It is clear that in the latter circumstances it is best to work at the panel face on the quiet side, as the pressure level is greatest there and an additional 3 to 10 db, or even more, may be gained in this way. Under certain conditions the correction to be applied to the observed difference in level between the two rooms may be neglected, and for cases where the room is not too highly damped, the correction term may be determined without the necessity of any reverberation determination of A_2. Furthermore, for laboratory measurements of transmission loss, certain precautions to be observed relative to placement of microphones under varying room treatments have been indicated.

2. RIBBON-MICROPHONE ALTERNATE METHOD

The ribbon-microphone alternate method has the great advantage that the observed difference in velocity level between the two rooms is independent of the amount of sound absorption in the receiving room. In table 5 are presented results on a number of panels which were tested by the ribbon-microphone alternate method. The absorption on the quiet side was varied from the case where the room was completely bare to that in which the wall surfaces were completely covered with absorbents. The figures given in the table are the observed differences in level (where VL is a velocity level). It will be noticed that the spread in the figures in the average column was not as great as 1 db even though the absorption was varied through this wide range. To indicate the amount of absorption in the room, only the absorption at 512 c/s is listed. Under similar circumstances the observed level differences would have differed by 6 db in the case of the pressure-microphone alternate method. This is indicated in

the column labeled "average pressure-microphone alternate method correction". (Compare average correction in table 1.)

TABLE 5.—*Independence of* $(VL)_1 - (VL)_{20}$ *when measured by the ribbon-microphone alternate method of absorption in the receiving room*

Panel No.	Test No.	Absorption at 512 c/s in sabins	Average pressure-microphone alternate method correction (db)	Frequency (c/s)									
				128	192	256	384	512	768	1,024	2,048	4,096	Avg.
X9	S8	33.2	+4.4	26.1	30.6	29.9	32.6	31.8	33.0	34.8	41.6	44.3	33.9
	S9	233	−1.1	26.2	32.2	28.0	32.4	31.7	32.7	35.2	41.6	46.3	34.0
X10	S13	33.2	+4.4	19.4	20.0	23.2	26.4	29.4	34.0	38.1	42.6	.....	29.1
	S11	233	−1.1	19.9	21.2	23.4	27.9	30.4	34.8	38.8	43.6	.....	30.0
X11	S16	33.2	+4.4	21.2	18.3	20.2	31.4	27.4	34.6	37.4	37.6	50.1	30.9
	S17	182	0	18.9	17.1	19.9	31.0	27.4	33.5	37.0	40.0	52.4	30.8
	S19	840	−1.7	19.6	17.2	20.0	32.4	28.5	34.7	37.6	39.8	53.6	31.5
X12	S21	33.2	+4.4	13.3	19.3	23.2	28.0	30.4	36.2	41.6	45.6	61.2	33.2
	S20	840	−1.7	10.8	20.2	23.3	27.4	30.6	35.8	41.1	47.0	61.6	33.1

The results of the experiments listed in table 5 may be readily explained. As has been indicated before, the sound energy density at the face of the panel on the receiving side may be considered to consist of two components, the direct component arising from sound energy radiated directly off the panel, and the reverberant component due to the reverberant energy existing throughout the room. This latter component may be considered to consist of a great number of waves which strike the panel at random angles of incidence with random phases. For each wave which strikes a perfectly reflecting rigid wall, its component of particle velocity normal to the wall becomes zero at the surface of the wall. Hence when the ribbon (particle velocity) microphone is placed next to the panel face, the reverberant component will be attenuated, while the response to the direct component will not be affected. The diffuse component is discriminated against to such an extent that what the ribbon microphone measures is a function only of the sound radiated from the panel.

This discrimination is of the order of 18 to 20 db for most of the frequencies concerned, as a perusal of figure 6 shows. This series of curves was obtained by investigating the variation in velocity level with distance from the face of the panel on the noisy side, using the ribbon microphone of figure 2. It will be seen that at the panel face the response of the ribbon microphone to the reverberant sound field of the source room is greatly diminished. The noisy side is used in these experiments simply because in this case there is present only a diffuse component, so that this discriminatory effect may be investigated without the disturbing effect of the direct component.

It will be noticed that the attenuation at 2,048 and 4,096 c/s is somewhat less than that obtained at the other frequencies. This is because the plane of the ribbon of the microphone should be relatively closer to the wall for the high frequencies, in order to obtain the same attenuation as at the lower frequencies. For example, some measurements with and RCA 44–A ribbon microphone, in which the ribbon element is mounted 2 in. from the external protective screen,

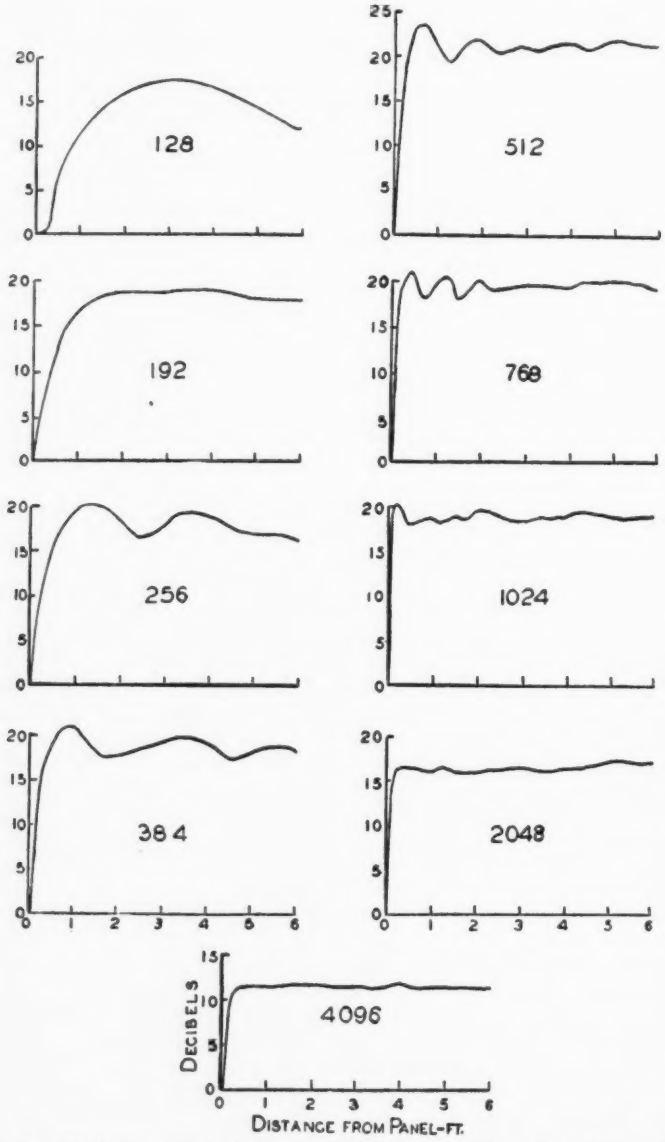

FIGURE 6.—*Variation in velocity level with distance from face of panel on noisy side.*
Zero decibels for each individual curve is entirely arbitrary. Frequency concerned is given with each curve.

showed that the reverberant component is only diminished to the extent of 10 db for the lower frequencies. It is also important that the sound waves have free access to both the front and back of the ribbon. Thus, in the RCA lapel microphone type MI–4001–A, in which the ribbon is mounted about one-fourth inch from its face,

partial screening of the ribbon occurs at the back of the ribbon by the permanent magnet of the microphone, so that only 2- to 4-db reductions are obtained at 2,048 and 4,096 c/s. The ribbon microphone used to obtain figure 6 was designed to overcome these objections. The ribbon is mounted about one-eighth inch from the face of the microphone and the back is entirely open, so that screening of the ribbon is reduced to a minimum. These features are readily apparent in figure 2.

The question next arises as to the relationship between the difference in level observed in the ribbon-microphone alternate method and the transmission loss of the panel. Table 6 furnishes experimentally determined corrections to be applied to the observed differences in level.

TABLE 6.—*Correction to be added to* $(VL)_1-(VL)_{30}$ *observed in the ribbon-microphone alternate method, to obtain transmission loss*

Frequency	Correction	Frequency	Correction
c/s	*db*	*c/s*	*db*
128	+8.2	768	+1.4
192	+6.7	1,024	+0.4
256	+6.6	2,048	−2.9
384	+4.4	4,096	−2.0
512	+3.6		
Correction for average transmission loss=+2.9			

If the corrections given in table 6 are used, the ribbon-microphone alternate method will give transmission losses which are in agreement with those obtained by the usual method. The number of ribbon-microphone transmission-loss measurements involved in the preparation of table 6 is 18, while the number of panels is 11. However, since three of the panels were similar to each other, the number of independent types of panels considered to be represented in the table is 9. These figures are given on a tentative basis, as it will be possible to obtain a more accurate set of corrections only after testing a larger number of panels.

In the nine panels so tested, the average transmission loss of these panels as determined by the ribbon microphone (using the corrections of table 6) exceeded the usual transmission-loss determinations by the following number of decibels: +3.4, +0.8, +0.1, +0.1, +0.1, −0.7, −1.4, −1.5, −1.8. The average deviation of these nine results is 1.2 db. The reason for the somewhat large deviation of 3.4 db is not clear.

Of course the corrections have been established only for the particular ribbon microphone used for these experiments, so that one may ask whether they will hold for any other ribbon microphone. It is believed that they are valid for any microphone in which the ribbon is mounted so that it may approach sufficiently close to the vibrating wall. The criterion for being "sufficiently close" is determined by the amount of attenuation the reverberant component will suffer (see fig. 6). For most rooms this discrimination should amount to no less than 10 db. To check this point, some *TL* measurements were taken with a quite different type of ribbon microphone, the RCA lapel microphone (type MI–4001–A). It is clear that from the objections,

described previously, to the use of this microphone in the alternate method, the *TL* measurements at 2,048 and 4,096 c/s would not be reliable. In table 7 the results obtained with the two ribbon microphones are compared.

TABLE 7.—*Comparison of results obtained with two different ribbon microphones*

Frequency	Shure Bros. ribbon	Lapel ribbon
c/s	*db*	*db*
128	5.2	5.5
192	17.0	14.4
256	19.9	21.6
384	26.7	28.0
512	27.8	27.4
768	36.4	35.4
1,024	38.1	37.4
2,048	46.6	49.0
4,096	47.2	40.8
Average...	29.4	28.8

Significant differences occur only at 2,048 and 4,096 c/s. The average transmission loss for the frequencies 128 to 1,024 c/s is for the Shure Bros. ribbon 24.4 db and for the lapel ribbon 24.2 db, which is excellent agreement.

The results of this section may be summarized thus: With the use of the ribbon-microphone alternate method it is possible to determine the transmission loss of partitions without a determination of the ratio A_2/S. Experimental evidence has been presented to show that the ribbon-microphone measurements are independent of A_2. Of course this holds only when the panel in question does not have a sound-absorbing treatment on its face, since in this case the amount of attenuation the reverberant component will suffer may be reduced considerably. The independence of the results of variations in the value of S follows from the fact that, because of the directional characteristics of the ribbon microphone and its proximity to the panel face, the response of the microphone arises from sound being radiated from a small area centered about the microphone. This point will be considered further in section V.

With the aid of table 6, the observed difference in level $VL_1 - VL_{20}$ may be corrected to give transmission losses in agreement with the usual method.

IV. INTERPRETATION OF RESULTS

1. PRESSURE-MICROPHONE ALTERNATE METHOD

In this section it is proposed to derive eq 1 to 7.

Let us consider the deduction of eq 1.

Assume a reverberant room in which there is a uniform energy density, E. At what rate will energy strike a unit area of the wall? The total amount of energy contained in dV (fig. 7) is EdV, and this amount of energy is radiated by dV in all directions. Hence the amount of energy which will ultimately reach dS is

$$\frac{d\Omega}{4\pi} EdV, \tag{8}$$

where $d\Omega$ is the solid angle subtended by dS at point P.

$$d\Omega=\frac{dS\cos\theta}{R^2} \tag{9}$$

$$dV=R\sin\theta\, d\phi\, Rd\theta dR \tag{10}$$

The rate at which energy strikes dS is given by

$$\frac{EdS}{4\pi dt}\int_0^{cdt}\int_0^{2\pi}\int_0^{\pi/2}\cos\theta\sin\theta d\theta d\phi\, dR, \tag{11}$$

since all the energy within a distance cdt, where c is the velocity of sound, will hit dS in time dt. Upon carrying out the integration of eq 11 and dividing by dS, one obtains the amount of energy, J, which hits a unit area of the wall in unit time

$$J=\frac{Ec}{4}. \tag{12}$$

Thus, if E_1 is the sound-energy density in the source room, then the rate at which energy is incident on the panel on the noisy side is $(E_1cS)/4$. The rate of energy transmission into the receiving room is $(\tau E_1cS)/4$, where $_1$ is the transmissivity—that is, the fraction of energy incident on S in the source room, which is transmitted into the receiving room.

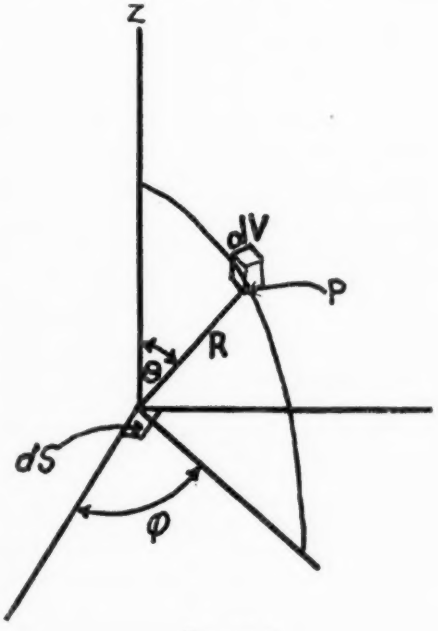

FIGURE 7

If a room has a source of power, P, present, then in the steady state the amount of sound energy absorbed by the walls per second must equal the rate at which sound energy is introduced into the room—that is, $JA=P$, where A is the total absorption of the room. Thus, from eq 12 the energy density in the steady state is

$$E=\frac{4P}{cA}. \tag{13}$$

The energy density in the receiving room, E_2, is then

$$E_2=\frac{4}{cA_2}\frac{\tau E_1cS}{4}=\frac{\tau E_1S}{A_2}. \tag{14}$$

The deduction of eq 14 is similar to one given by Buckingham.[7] Equation 14 may be put in the form

$$10\log_{10}\left(\frac{1}{\tau}\right)=10\log_{10}\left(\frac{E_1}{E_2}\right)+10\log_{10}\left(\frac{S}{A_2}\right). \tag{15}$$

[7] Sci. Pap. BS **20**, 193 (1925) S506.

The term $10 \log_{10} (1/\tau)$ is the transmission loss, and $10 \log_{10} (E_1/E_2)$ is equal to $L_1 - L_2$, the difference in sound level between the two rooms, so that eq 15 is just eq 1 written in a somewhat different fashion.

It is to be noted that in setting $L_1 - L_2 = 10 \log_{10} (E_1/E_2)$ we have assumed that the sound lever meter indications are proportional to the energy density in the sound field. Of course, what is really measured, if a pressure microphone is used, is the time average of the square of the excess pressure. However, if the sound field is truly diffuse—that is, uniform energy-density distribution exists—then the disturbance at any point may be considered to arise from the superposition of a large number of plane wave trains with random phases and with all directions of propagation equally probable. Rayleigh [8] has shown that for n vibrations of the same frequency, and with phases distributed at random, the mean value to be expected for the square of the resultant amplitude is the sum of the squares of the amplitudes for each individual vibration, so that the square of the resultant pressure amplitude indicated by the sound-level meter is equal to the sum of the squares of each individual pressure amplitude. The energy density in a plane wave is proportional to the square of the pressure amplitude of the wave. Since P^2 (pressure amplitude squared) of each wave is additive, the resultant P^2 is proportional to the sum of the energy density in each individual wave train. Hence, under the condition of a diffuse sound field, the sound-level meter indications are proportional to the energy density.

If, however, the distribution of sound energy is much different from the diffuse condition, the relationship between the P^2 which is measured and the energy density is somewhat difficult to state. To get a more accurate treatment of transmission problems, it would then be necessary to calculate the value of P^2 for each point in the room. It is clear that such a calculation is quite formidable, especially when it is considered how very different in physical properties the panels (which act as the source of sound for the quiet side) may be. The energy-flow treatment involving the measurement of the transmission loss with the aid of a pressure-actuated device is then to be considered as an approximate method of dealing with this problem. The beauty of the energy-flow treatment is that it gives an answer which is sufficiently accurate for most purposes, and eliminates the necessity of making a detailed calculation of the pressure wave in both the source and receiving rooms. In the development of equations 2 to 7 the energy-flow method will be used.

First, the energy density at the panel face due to the energy radiated from the panel will be calculated.

As the simplest assumption to make, it will be assumed that the panel radiates in such a fashion that the energy density is uniform over its face, except at the boundary edges of the panel. A more extreme case of this assumption is that of an infinite panel which may be assumed to radiate so that the whole (free) space which it bounds has a uniform energy-density distribution. Such a sound field, however, is not entirely diffuse, since only half the total possible directions of flow are permitted; that is, the energy can flow away from the panel only. This means that the total amount of energy which will strike unit area per second when placed in such a sound field will be $Ec/2$ as

[8] Theory of Sound, vol. 1, 2d ed., sec. 42a, p. 36–42 (Macmillan and Co., London, 1894).

compared to $Ec/4$ for a completely diffuse field; an element of volume such as dV can radiate into a solid angle of 2π for the former as compared to 4π for the latter.

Hence,

$$J'=\frac{E'c}{2}, \tag{16}$$

the primes referring to the state in which the energy flow is "half" diffuse. This immediately leads to the conclusion that if the panel radiates J' units of energy per unit area per second, the energy density will be $E'=2J'/c$.

For a panel of finite size, if E_0 is the energy density at the panel face, and J_0 is the rate of energy emission per unit area, then

$$E_0=\frac{2J_0}{c} \tag{17}$$

for positions not too close to the edges of the panel.

What has been assumed then is that the uniform and diffuse energy density on the noisy side, after being attenuated by the panel, reappears on the quiet side as a uniform and "half" diffuse energy density. That this is a plausible assumption is evident from a theorem first proved by Schoch,[9] which states that for sufficiently high frequencies above the fundamental frequency of a vibrating plate, the distribution of amplitude of vibration over the face of the plate is directly proportional to the distribution of driving pressure. Any diffuse distribution of energy incident on the panel face causes an exact image displacement of the panel so that a uniform energy density at the noisy face of the panel is duplicated at the quiet face. Of course, the use of this assumption at low frequencies and on complex partitions is justifiable only if the equations derived agree with the experimental results.

A modification of eq 11 gives as the rate at which energy is incident on dS from the solid angle included between θ and $\theta+d\theta$, in a uniform, "half" diffuse sound field

$$\frac{EcdS}{2\pi}\cos\theta 2\pi\sin\theta d\theta. \tag{18}$$

The solid angle included between θ and $\theta+d\theta$ has the value $2\pi\sin\theta d\theta$. Hence the total amount of energy reaching dS per second from the solid angle included between θ and $\theta+d\theta$ is proportional to $\cos\theta$. If one reverses the reasoning and thinks of the area dS as radiating to reproduce this uniform "half" diffuse sound field, then it follows that the amount of energy radiated between θ and $\theta+d\theta$ is proportional to $\cos\theta$. This is the analog of Lambert's law in optics, which states that a glowing plate must emit energy proportional to $\cos\theta$, at an angle θ, in order to look equally bright in all directions.

Using Lambert's law, eq 17 may be derived now in a more direct manner.

[9] Akustische Z. **2**, 113 (1937). See also English summary in J. Acous. Soc. Am. **9**, 168 (1937).

Consider the element of area dS radiating according to the $\cos\theta$ law (fig. 8).

Let $J_\Omega = \frac{dJ}{d\Omega}$ = energy radiated per second per unit area per unit solid angle between Ω and $\Omega + d\Omega$,

J_0 = total energy radiated per unit area per second,
B = a constant to be determined.

Then

$$J_\Omega d\Omega = B \cos\theta \, 2\pi \sin\theta d\theta, \tag{19}$$

$$J_0 = \int J_\Omega d_\Omega = B2\pi \int_0^{\pi/2} \cos\theta \sin\theta d\theta, \tag{20}$$

so that

$$B = \frac{J_0}{\pi} \tag{21}$$

Therefore,

$$J_\Omega d\Omega = 2J_0 \cos\theta \sin\theta d\theta \tag{22}$$

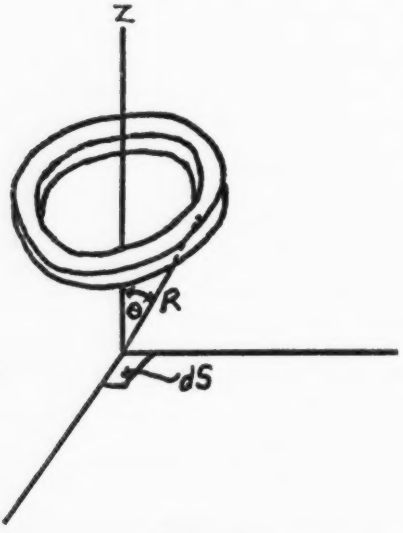

FIGURE 8

The contribution of dS to the energy density $E_{dS}(R, \theta)$ at point $P(R, \theta)$ is the total amount of energy which flows into the volume of the ring, $2\pi R^2 \sin\theta d\theta dR$ in the time dR/c, from the elementary area dS.

$$E_{dS}(R,\theta) = \frac{J_\Omega d\Omega}{2\pi R^2 \sin\theta d\theta dR} \frac{dR}{c} dS,$$

or

$$E_{dS}(R,\theta) = \frac{J_0 \cos\theta}{\pi c R^2} dS. \tag{23}$$

Consider a vibrating, circular plate (fig. 9) of radius a. The total energy density, at a point Q located on the polar axis of the disk, due to contributions from all elements is

$$E(Z)=\frac{J_0}{\pi c}\int_0^a \frac{\cos\theta}{R^2}\,2\pi r\,dr, \tag{24}$$

But

$$R^2=r^2+Z^2.$$

Whence,

$$2RdR=2rdr$$

$$E(Z)=\frac{2J_0}{c}\int_Z^{\sqrt{a^2+Z^2}}\frac{Z}{R}\frac{1}{R^2}RdR;$$

so that,

$$E(Z)=\frac{2J_0}{c}\left[1-\frac{Z}{a\sqrt{1+\frac{Z^2}{a^2}}}\right]. \tag{25}$$

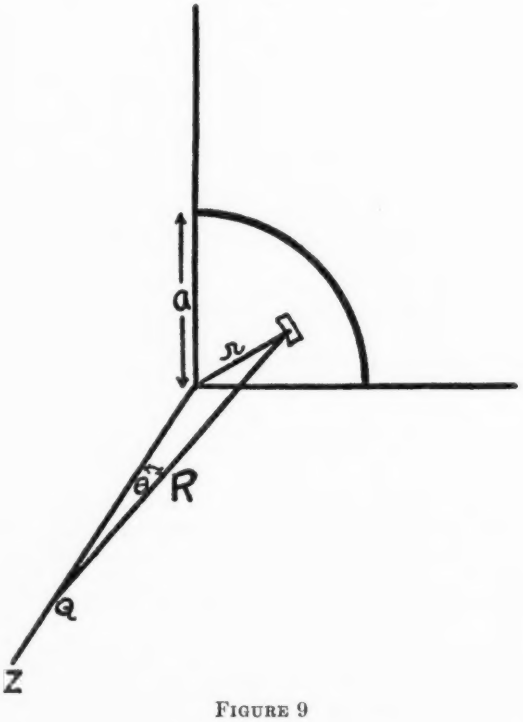

FIGURE 9

For $Z\ll a$, corresponding to measuring E immediately next to the panel, or having the disk much larger than the distance from the panel to the observation point,

$$E_0=\frac{2J_0}{c},$$

which is identical with eq 17. If the energy density is measured at $Z=0$, the result may be expected to be the same no matter what the

boundary is—circular, rectangular, or otherwise. Also, positions not too far removed from the polar axis should give approximately the same value for E_0.

For high-frequency excitation of the panel, in the neighborhood of 4,000 c/s, it was found that the Lambert law does not hold. To get agreement with experiment, it was found necessary to assume that the radiation follows a more directional law, the directionality factor being $\cos^2\theta$, instead of $\cos\theta$. Equations analogous to those derived for the Lambert source (eq 19 to 25) will be derived now.

The amount of energy radiated per second per unit area in the solid angle between Ω and $\Omega+d\Omega$ is given by

$$J_\Omega d\Omega = 2\pi B \cos^2\theta \sin\theta \, d\theta \tag{26}$$

$$J_0 = 2\pi B \int_0^{\pi/2} \cos^2\theta \sin\theta \, d\theta$$

Whence

$$B = \frac{3}{2\pi} J_0, \tag{27}$$

or

$$J_\Omega d\Omega = 3J_0 \cos^2\theta \sin\theta \, d\theta. \tag{28}$$

So

$$E_{dS}(R, \theta) = \frac{3J_0}{2\pi c} \frac{\cos^2\theta}{R^2} dS. \tag{29}$$

For a circular plate of radius a, there is obtained for the energy density at a distance Z measured along the polar axis

$$E(Z) = \frac{3J_0}{c} \int_Z^{\sqrt{a^2+Z^2}} \frac{\cos^2\theta}{R^2} R dR = \frac{3}{2} \frac{J_0}{c} \left[1 - \frac{Z^2}{a^2+Z^2}\right]. \tag{30}$$

If the measurements be confined to distances Z, such that $Z \ll a$, then

$$E_0 = \frac{3}{2} \frac{J_0}{c}. \tag{31}$$

To recapitulate, if the vibrating panel is considered as a collection of simple sources, which radiate directionally according to a $\cos\theta$ law, then $E_0 = 2J_0/c$. If the radiation is even more directional, that is, the proportionality factor is $\cos^2\theta$, $E_0 = (3/2)(J_0/c)$. It is to be noted that for the most directional type of wave possible, that is, a plane wave, $E_0 = J_0/c$.

So far the discussion has been limited to the direct component only. The reverberant or diffuse component has the energy density, E_2, given by eq 14. This diffuse energy, E_2, exists throughout the whole room. Hence at the panel face the energy density would be E_0+E_2. However, it has been shown in section III–1 that the pressure level at the panel face on the noisy side is roughly 3 db higher than the pressure level out in the center of the same room (fig. 5). Hence, if the pressure-microphone readings out in the center of the room are proportional to the energy density, then at the panel face its readings are proportional to twice the actual energy density. This is also true for the diffuse component on the quiet side. Hence if E_{20} is the

energy density *indicated* by the pressure microphone at the panel face on the quiet side, one obtains

$$E_{20}=E_0+2E_2. \tag{32}$$

Thus, for the Lambert region where eq 17 holds,

$$E_{20}=\frac{2J_0}{c}+2E_2. \tag{33}$$

But J_0, the amount of energy emitted per unit area per second from the radiating surface, is given by

$$J_0=\frac{\tau E_1 c}{4} \tag{34}$$

where $E_1c/4$ is the rate at which energy is incident on unit area of the panel on the noisy side. Substituting for J_0, and for E_2 from eq 14, one gets

$$E_{20}=\frac{\tau E_1}{2}+\frac{2\tau S}{A_2}E_1,$$

or

$$\frac{1}{\tau}=\frac{E_1}{E_{20}}\left(\frac{1}{2}+\frac{2S}{A_2}\right). \tag{35}$$

Taking 10 $\log_{10}$ of both sides, there is obtained

$$10\log_{10}\left(\frac{1}{\tau}\right)=10\log_{10}\left(\frac{E_1}{E_{20}}\right)+10\log_{10}\left(\frac{1}{2}+2\frac{S}{A_2}\right). \tag{36}$$

$10\log_{10}(1/\tau)$ is the transmission loss, and $10\log_{10}(E_1/E_{20})$ is the observed difference in pressure level $(PL)_1-(PL)_{20}$. Hence eq 36 is identical with eq 3. For the $\cos^2\theta$ region where eq 31 is valid, the microphones are too large to be able to get sufficiently close to the panel to have the sound level of the diffuse component increase by 3 db (Compare $\nu=4{,}096$ c/s of fig. 5). Therefore,

$$E_{20}=\frac{3}{2}\frac{J_0}{c}+E_2 \tag{37}$$

and

$$\frac{1}{\tau}=\frac{E_1}{E_{20}}\left(\frac{3}{8}+\frac{S}{A_2}\right). \tag{38}$$

Taking 10 $\log_{10}$ of both sides of eq 38, eq 4 is obtained. As already indicated in section III–1, best agreement is obtained with experiment by using eq 3 at frequencies ranging from 192 to 2,048 c/s, and eq 4 at the frequency of 4,096 c/s.

The lowest frequency, $\nu=128$ c/s, is in a difficult region where the radiated wavelength is comparable to the dimensions of the panel and the dimensions of the room. The wavelength at 128 c/s is 8.8 ft; dimensions of the sound-transmitting surface about 6½ by 5 ft; dimensions of the receiving room about 9 by 12 by 16 ft. The mean free path $\left(4\frac{\text{volume of room}}{\text{total wall area}}\right)$ is thus less than the wavelength, being 7.7 ft.

One might, therefore, expect very little randomness in the resultant steady state in the room. In deriving eq 2, it is assumed that conditions deviate from random to such an extent that the pressure wave radiated from the panel is in phase with the pressure wave which originates in the room proper. If P_R is the pressure amplitude at the panel face of the resultant wave, P that of the direct wave, and p that of the "diffuse" wave, then

$$P_R^2=(P+\sqrt{2}p)^2. \tag{39}$$

The factor $\sqrt{2}$ in front of p is in accord with Kellogg's [10] result that for a diffuse component the square of the pressure amplitude is twice as great at the wall as that at a position away from the wall. It is assumed that P_R^2 is proportional to E_{20}, P^2 to $E_0=\tau E_1/2$ of the direct component and p^2 to $E_2=\tau E_1 S/A_2$ of the diffuse component, the proportionality constant being the same for all three.

Thus,

$$E_{20}=\left(\sqrt{\frac{\tau E_1}{2}}+\sqrt{2\tau E_1\frac{S}{A_2}}\right)^2$$

or

$$\frac{1}{\tau}=\frac{1}{2}\frac{E_1}{E_{20}}\left(1+2\sqrt{\frac{S}{A_2}}\right)^2. \tag{40}$$

Equation 40 is to be considered as an attempt to weight properly the relative influence of the standing wave system in the room and the diffusing nature of the many reflections the sound experiences at the walls of the room. Other attempts to take into account these two factors were not as successful as eq 40 insofar as agreement with experiment is concerned.

Upon taking 10 $\log_{10}$ of both sides of eq 40, eq 2 is obtained. It is to be remembered that in accordance with its method of derivation, eq 2 only holds when the mean free path of the receiving room is of the same order of magnitude as the wavelength of the sound emitted; if the room is quite large, it is probable that eq 3 should be used.

Substituting for E_1 in terms of E_2 from eq 14, one obtains from eq 40

$$\frac{E_{20}}{E_2}=\frac{1}{2}\frac{A_2}{S}\left(1+2\sqrt{\frac{S}{A_2}}\right)^2, \tag{41}$$

which is simply a different form of eq 5. Similarly, eq 6 and 7 may be obtained by using eq 14 to eliminate τE_1 from eq 35 and 38, respectively.

If S/A_2 is eliminated from eq 40 with the aid of eq 14, one obtains an expression for $1/\tau$ (eq 42) which is a function of two readily observable ratios, namely, E_1/E_{20} and E_2/E_{20}. Similarly, from eq 35 and 38, eq 43 and 44, respectively, are obtained.

$$\frac{1}{\tau}=\frac{1}{2}\frac{\dfrac{E_1}{E_{20}}}{\left(1-\sqrt{\dfrac{2E_2}{E_{20}}}\right)^2} \qquad \nu=128\ c/s. \tag{42}$$

[10] J. Acous. Soc. Am. 4, 61 (1932).

$$\frac{1}{\tau}=\frac{1}{2}\frac{\frac{E_1}{E_{20}}}{\left(1-2\frac{E_2}{E_{20}}\right)} \qquad \nu=192 \text{ to } 2{,}048 \ c/s. \tag{43}$$

$$\frac{1}{\tau}=\frac{3}{8}\frac{\frac{E_1}{E_{20}}}{\left(1-\frac{E_2}{E_{20}}\right)} \qquad \nu=4{,}096 \ c/s. \tag{44}$$

Equations 42, 43, and 44 are the analytic formulation of the experiments in section III–1, in which it is pointed out that transmission-loss measurements could be made without a knowledge of A_2/S if, in addition, the quantity $(PL)_{20}-(PL)_2$ is measured.

2. RIBBON-MICROPHONE ALTERNATE METHOD

The fundamental problem here is to calculate the correction terms given in table 6. Is it possible to compute the correction terms by a procedure analogous to that used in deriving eq 2, 3, and 4? Such a calculation must first compute the response of a ribbon microphone when used in a reverberant room, and second, its response when used in a position adjacent to the panel on the quiet side.

The first calculation has appeared elsewhere in several places.[11] The essential point is that for sound originating at an angle θ, the ribbon microphone will generate a voltage proportional to $\cos\theta$. The response of the ribbon to the energy in the wave will therefore be proportional to $\cos^2\theta$, since the energy in the wave is proportional to the square of the particle velocity. Hence, if the energy density in the room is E, the rate at which energy is indicated by the ribbon as striking the ribbon area dS, is

$$\frac{E dS}{4\pi}\int_0^c\int_0^{2\pi}\int_0^{\pi}\cos^2\theta\sin\theta\, d\theta\, d\phi\, dR=\frac{Ec}{3}\,dS \tag{45}$$

Hence, if the energy density E is measured by a nondirectional microphone, a ribbon microphone will record it as $E/3$.

For the second part of the calculation, reference is made to eq 23, which gives the energy density at a distance R and an inclination θ due to a radiating element dS. If a ribbon microphone is situated at the point (R,θ), it will indicate the energy density $\bar{E}_{dS}(R,\theta)$ where

$$\bar{E}_{dS}(R,\theta)=\cos^2\theta\ E_{dS}(R,\theta)=\frac{J_0\cos^3\theta}{cR^2}\,dS. \tag{46}$$

Consider now a vibrating circular plate. In a manner similar to eq 24, one obtains

$$\bar{E}(Z)=\frac{J_0}{\pi c}\int_Z^{\sqrt{a^2+Z^2}}\frac{\cos^3\theta}{R^2}\,2\pi R dR. \tag{47}$$

[11] See, for example, Olson and Massa, Applied Acoustics, 1st ed., p. 133 (P. Blakiston's Son & Co., 1012 Walnut St., Philadelphia, Pa., 1934).

For the position immediately next to the panel the energy density indicated by the ribbon is

$$\overline{E}_{20}=\frac{2}{3}\frac{J_0}{c} \tag{48}$$

From eq 34 $J_0=(\tau E_1 c/4)$.
Furthermore, the energy density $\overline{E}_1$ indicated by the ribbon on the noisy side is

$$\overline{E}_1=\frac{E_1}{3} \tag{49}$$

so that

$$\overline{E}_{20}=\frac{1}{2}\tau\overline{E}_1 \tag{50}$$

or

$$10\log_{10}\left(\frac{1}{\tau}\right)=10\log_{10}\left(\frac{\overline{E}_1}{\overline{E}_{20}}\right)+10\log_{10}\left(\frac{1}{2}\right) \tag{51}$$

The first term on the right-hand side of eq 51 is the actual difference in level observed, while the second term is a correction term and is equal to −3.0 db. Of course, this equation should be valid only for the Lambert frequency region; in the $\cos^2\theta$ region the correction term turns out to be $-10\log_{10}(16/9)=-2.5$ db. It will be observed that the figure −2.5 db agrees well with the −2.0 db given in table 6 for the frequency 4,096 c/s. However, in the Lambert region (the range from 128 to 2,048 c/s according to our pressure-microphone alternate-method measurements) there is only one frequency, 2,048 c/s, which agrees with the −3.0 db calculated. All of the other corrections of table 6 are definitely in disagreement with the theoretical values.

There are two possible sources of error in the above calculations. Equation 49, $\overline{E}_1=E_1/3$, may be in error. Fortunately, it is possible to check the validity of eq 49. The response of a nondirectional microphone, such as a sound-pressure microphone, may be compared to the response of the ribbon microphone, when both are placed in a reverberant room. If both microphones have the same response to a plane wave, the ribbon microphone should indicate the velocity level to be $10\log_{10}3=4.8$ db lower than the corresponding pressure level. The experiment was carried out by comparing the response of the ribbon microphone with a pressure microphone (Western Electric Type 633A) under free-field, plane-wave conditions in the dead room at the National Bureau of Standards. From this the relative frequency-response characteristic of the two was determined. The two microphones were then placed on the noisy side of our transmission rooms and the difference in sound level indicated by the two was measured. The number of decibels by which the ribbon read less than the pressure microphone after correction was made for the differing response-frequency characteristics is as follows:

Frequency, c/s	128	192	256	384	512	768	1,024	2,048	4,096
Decibels	2.8	4.5	3.0	4.5	5.2	4.8	3.6	2.2	2.5

Measurements at frequencies up to 384 c/s have a possible error of about ±1.5 db; while the possible error for the other frequencies is about ±0.5 db. Thus all the figures are in rough agreement with the value 4.8 db except those at 2,048 and 4,096 c/s. Best agreement is

to be anticipated at these higher frequencies, since it is then that the sound field approaches the diffuse condition most closely. The explanation may be that at these frequencies the pressure microphone is becoming directional and its response is 5 to 10 db down for waves too far off from normal incidence.

In attempting to account for the results in table 6, an impasse has been reached. While the sound-pressure data seem to be well-behaved (in the sense that they accord with our analysis), the same cannot be said of the particle velocity measurements. One qualitative explanation is suggested by a perusal of table 6. The correction factor diminishes with increasing frequency, which corresponds to the fact that the velocity level as indicated by the ribbon when placed adjacent to the panel on the quiet side is greater than it should be, its excessive value also diminishing with increasing frequency. This is just the behavior one gets from a ribbon microphone when one approaches a point source with it. There is an inordinate increase in the particle velocity of a spherical wave over the pressure in the wave for positions close to the source, especially for the low frequencies.[12] It is thought that possibly a similar phenomenon is occurring here, even though the source is of such an extended nature as a wall. Different elements of the panel emit spherical waves, but the vibration of the panel is of such a complex nature that a quantitative elaboration of this idea would seem to be difficult.

V. FURTHER APPLICATIONS OF THE RIBBON-MICROPHONE ALTERNATE METHOD

From the discussion in section IV, it will be evident that of the two components, direct and diffuse, only the latter depends on the ratio A_2/S, the former being independent of this ratio. Since in the ribbon-microphone alternate method the response of the ribbon on the quiet side depends only on the direct sound, it follows that by this method it is possible to make transmission-loss measurements without considering complications arising from the size of the wall or the nature of the receiving room. The room may be extraordinarily large, say the size of a large auditorium, in which case the wall under test will be large also. The wall may be even discontinuous in nature with different sections differing in construction. It will still be possible to determine the transmission loss, but the different sections will give different results.

It is necessary to qualify the last statement somewhat. If two adjacent sections are too different in insulating efficiency, it is possible to obtain erroneous results. For example, suppose the energy radiated from one area is 30 db greater in level than that from another area. The energy radiated from the wall forms a reverberant sound field out in the center of the room, which, let us say, is 5 db less in level than the direct component. This means that at the face of the section which is a poorer radiator, the reverberant energy will be 25 db larger than the direct energy. If the ribbon microphone attenuates the reverberant component to the extent of 20 db, the result is that there will be a 5-db error in the transmission loss for the poorer section. In case the room is relatively bare, the error will be even greater.

[12] Olson and Massa, Applied Acoustics, 1st ed., p. 9 (P. Blakiston's Son & Co., 1012 Walnut St., Philadelphia, Pa., 1934).

The decibel difference between the direct and reverberant component may be readily shown to be 10 $\log_{10}$ ($A_2/2S$). With the aid of this formula it is possible to determine the difference in level between different sections whose transmission losses may be ascertained without error. The more absorbent the room or the smaller the area in question, the larger the difference in transmission loss which can be measured. For an untreated room a common condition is one in which the ratio of absorption to surface area is equal to 1. In this case the direct component is 3 db less than the reverberant component. If the ribbon microphone discriminates against reverberant energy to the extent of 20 db, the resultant discrimination will be 17 db. This means that the transmission loss of sections differing by as much as 17 db may be determined. This figure holds only where there is no appreciable direct feeding of sound into the microphone from the poorer section. These quantitative calculations will be wrong to the extent to which this phenomenon takes place.

All of the above figures have to be modified because of a factor which has not yet been taken into account, namely, the fact that the discrimination of the ribbon microphone in favor of the direct sound is increased even more because the velocity level due to the direct sound is considerably greater than it should be, as the figures in table 6 show. Since the theoretical value of these corrections in table 6 is -3.0 db ($\nu=128$ to 2,048 c/s), the velocity level indications at the panel face on the quiet side are $+3.0$ db higher than the correction terms given in table 6 (relative to the predicted velocity level). Thus at 128 c/s there is an additional discrimination in favor of the direct sound of 11.2 db, which must be added to 15 db obtained at 128 c/s from figure 6, making a total discrimination of about 26 db. Similarly, at the other frequencies, 192, 256, 384, 512, 768, 1,024, 2,048, and 4,096 c/s, the discrimination in favor of the direct sound is 28, 27, 25, 28, 24, 21, 16, 12 db, respectively. No experiments have been carried out as yet to check these figures.

Within the limitations indicated in the foregoing, the ribbon microphone may be used as a radiation pickup,[13] with certain obvious advantages over a vibration pickup. At no time does the microphone touch the radiator, so that the vibration characteristics of the body are not disturbed as sometimes happens in using a vibration pickup. What is measured is the sound radiated directly from the vibrating body, which is usually a quantity of primary interest. On the other hand, a determination of the vibration amplitude, velocity, or acceleration has an uncertain relationship to the sound which is radiated.

The ribbon microphone when used as a radiation pickup has one other advantage over a vibration pickup. The variation in velocity level between different positions over the panel face is much less than variations in level indicated by a vibration pickup. Thus, as a general observation, it may be stated that over the whole frequency range the maximum spread in velocity level obtained at the panel face with the ribbon microphone was usually less than 4 db but sometimes as large as 6 or 7 db. This is to be compared with the vibration pattern obtained on a 9-in. brick wall by Constable and Aston [14] with

[13] Paul Huber, of the General Motors Corporation, in an oral observation at the 23d meeting of the Acoustical Society indicated a similar use for a ribbon microphone in studying the radiation from the panels of automobile bodies.

[14] Proc. Phys. Soc. (London) **48**, 919 (1936).

a vibration pickup. Using a warble tone, the maximum spread in results was 13 db at 100 c/s, 12 db at 500 c/s, 21 db at 1,600 c/s, and 16 db at 4,000 c/s. The ribbon microphone thus acts somewhat like an averaging device in that its response depends on a region of the panel somewhat larger than that which influences the response of a vibration pickup.

One proposed application of the ribbon microphone is concerned with its use in evaluating the resistance of floor construction to transmitting impact noises. No completely satisfactory method of determining this physical quantity is now in use, as all measurements depend to some extent on room conditions. It is suggested that this type of measurement might rest on a more satisfactory basis if the ribbon microphone were used to measure the energy radiated directly from the panel, making appropriate use of the corrections of table 6. Of course, it would be necessary to take a frequency analysis of the noise resulting from the mechanical impact caused by the tapping machine, in order to use these correction terms. The efficiency of the panel might be defined in terms of the ratio of the sound energy emitted on the noisy side to the mechanical energy of the exciting hammer blow. Further work in this direction is contemplated. P. Haller [15] has given a discussion of this question along similar lines.

The development of the multiple loudspeaker unit and the commutating device used with the amplifier is due in large part to V. L. Chrisler and W. F. Snyder. S. Greenman assisted in carrying out some of the measurements.

WASHINGTON, January 31, 1941.

[15] Akustische Z. **4**, 370 (1939).

U. S. Department of Commerce National Bureau of Standards

RESEARCH PAPER RP1389

Part of Journal of Research of the National Bureau of Standards, Volume 26, May 1941

METASTABILITY OF CADMIUM SULFATE AND ITS EFFECT ON ELECTROMOTIVE FORCE OF SATURATED STANDARD CELLS

By George W. Vinal and Langhorne H. Brickwedde

ABSTRACT

Both solubility and electromotive force measurements are concordant in fixing the transition temperature of $CdSO_4.8/3H_2O$ to $CdSO_4.H_2O$, at 43.4°C. Previously the transition temperature was generally believed to be 74° C. Cells recently were made with each modification. Their respective electromotive forces differ except at the transition temperature, where they, as well as the solubilities, are equal. The temperature coefficient of cells containing $CdSO_4.H_2O$ was found to be positive, whereas the temperature coefficient for cells containing the ordinary salt $CdSO_4.8/3H_2O$ is negative, as is well known. Both hydrates tend to persist in a metastable state, and measurements can be made over a wide range of temperatures. The free energy changes of the cells are discussed, and some practical applications for the cells are described.

CONTENTS

	Page
I. Introduction	455
II. Experimental procedure	457
1. Solubility determinations	457
2. Construction of cells	457
3. Temperature control of the cells and measurement of electromotive force	458
III. Experimental results	458
1. Solubility measurements	458
2. Electromotive force	460
3. Temperature coefficient	461
IV. Thermodynamic discussion of the reaction	462
V. Hysteresis effects	463
VI. Conclusions	464
VII. References	465

I. INTRODUCTION

Contrary to the generally accepted opinion, the transition point of cadmium sulfate from $CdSO_4.8/3H_2O$ to $CdSO_4.H_2O$ occurs at a temperature much below that stated in the literature [1][1] dealing with standard cells. For more than 40 years this transition point was believed to be about 74° C, which is safely above any reasonable temperature at which standard cells might be used, and also above any necessary temperature for the preparation of the crystalline salt. Apparently the value 74° C, reported in 1897 by Mylius and Funk [1], is the basis for many of the statements made by other authors who wrote at a later date.

[1] Figures in brackets indicate the literature references at the end of this paper.

Other papers written without reference to standard cells have indicated anomalies in the behavior of cadmium sulfate. Thus Hofman and Wanjukow [2] concluded, as a result of heating cadmium sulfate in a muffle furnace, that some water is separated from $CdSO_4.8/3H_2O$ at 30° C or below and additional water is separated at 41° C. Carpenter and Jette [3] in the course of vapor-pressure measurements found indication of a discontinuity in their curve for the salt at about 41.5° C and concluded that this was a transition point.

Reasons can be advanced for the uncertainty in determining the transition temperature. They are based largely on the somewhat unusual properties of the salt in solution. Cadmium sulfate, $CdSO_4.8/3H_2O$, is slow to go into solution, although it is very soluble. The monohydrate, $CdSO_4.H_2O$, whose solubility decreases with rising temperature, is even slower in crystallizing out of solution. Both salts tend to form supersaturated solutions, and considerable time is required to attain saturation equilibrium. In the light of our present experience, we think that Mylius and Funk allowed insufficient time for the transition to occur. They reported agitating the solutions for 1 hour. We have found, however, that solutions containing the metastable phase may be agitated at 45° C for a week or more without the appearance of the stable form. The time required for the metastable form to be converted into the stable form decreases as the temperature is raised. At 74° or above, the time is probably reduced sufficiently for the transition to occur under conditions of their experiment.

Metastable states of the Clark standard cell (zinc cell) were recognized many years ago [4]. In this cell the transition from $ZnSO_4.7H_2O$ to $ZnSO_4.6H_2O$ occurs at about 39° C, as shown by both solubility and emf data. The fact that such a cell might have two differing electromotive forces at a specified temperature was considered an objection to its use as a standard of emf.

Several early investigators believed that irregularities which they observed in cadmium standard cells at about 15° C were caused by a transition of the cadmium salt. Subsequently, it was shown by others that this was the result of using too high percentages of cadmium in the amalgam, which undoubtedly consisted of the solid phase alone at this temperature. No further discussion of this point is warranted here, but reference may be made to a short summary given by Wolff and Waters [5]. Aside from this discussion about 40 years ago, it has generally been believed that the saturated Weston cell was not subject to irregularities resulting from metastable conditions of the cadmium salt.

The fact that the present work shows that the transition point for cadmium sulfate is only 4 or 5 degrees higher than for zinc sulfate should not be interpreted as being a serious objection to the use of the cadmium cells. The National Bureau of Standards has for years cautioned users of standard cells not to subject them to temperatures higher than 40° C. Forty degrees is above any ordinary operating temperatures for the cells; but what is more important, the newly determined transition temperature fixes an upper limit for the preparation of the crystallized salt. Exposure of cells to temperatures above the transition point does not necessarily mean that the cells will be seriously damaged. Experiments indicate that the usual form of crystallized salt persists in a metastable state considerably above the transition temperature. During the past 16 years several groups of saturated cells which had been grossly overheated have been tested.

Some of these had abnormal emf, while others were apparently not damaged.

Another hydrate of cadmium sulfate of somewhat uncertain composition was reported by Mylius and Funk to exist at temperatures of 0° C or below. They report this to be $CdSO_4.7H_2O$. We have made no study of it.

In this paper it is shown that solubility and emf measurements are concordant in fixing the transition temperature of $CdSO_4.8/3H_2O$ to $CdSO_4.H_2O$ at 43.4° C. Cells made with each of these hydrates are compared. Electromotive forces of such cells differ except at the transition point. The monohydrate salt produces cells with a positive temperature coefficient in contrast to the others which have a negative coefficient. Solubilities in the metastable condition are higher and resulting emf lower than when the cells contain the stable modifications. Free energy changes of the cells are discussed.

II. EXPERIMENTAL PROCEDURE

1. SOLUBILITY DETERMINATIONS

The solubility determinations are a part of a larger project involving the determination of solubilities in ordinary water and in deuterium oxide. These measurements were a necessary preliminary to the construction of cells containing high percentages of D_2O. The methods and results will be given in greater detail in another paper on the deuterium cells. For the present purpose, it is sufficient to state that widely different results for the solubility of cadmium sulfate in normal water at 50° C agreed no better after many repetitions in various temperature-controlled air and water baths. Samples of the crystals were examined microscopically by C. P. Saylor, who reported two modifications to be present. Throughout the course of the work Dr. Saylor kindly examined many samples for us, and his reports have been an indispensable guide in the conduct of this work.

Gravimetric determinations to identify the crystals of the solid phase were made, and the modification stable at the higher temperatures was found to be $CdSO_4.H_2O$, while that which is stable at the lower temperatures was found to be $CdSO_4.8/3H_2O$. By seeding the solutions with the proper kind of crystals, reproducible results could be obtained if certain obvious precautions were taken.

Analyses of the various solutions were made by evaporating samples to dryness and weighing the salt as $CdSO_4$ after it had been dehydrated at a temperature of 650° to 700° C in a muffle furnace. A trace of SO_3 was always present in the atmosphere of the furnace to prevent any possible decomposition.

2. CONSTRUCTION OF CELLS

The cadmium salt was a purified sample prepared for making standard cells. This was dehydrated in a muffle furnace, and subsequently the monohydrate crystals were grown in a solution at 85° C.

Some variations in the usual method of making the cells were necessary because of the metastability of $CdSO_4.H_2O$ at ordinary room temperatures. To have washed the mercurous sulfate in a Gooch crucible with the saturated solution of this hydrate might have re-

sulted in seeding the paste with the other kind of crystals. A procedure sometimes used by Wolff and Waters [6] many years ago was followed. Mercurous sulfate for all the cells was washed with absolute alcohol and then with dried ether. Paste for two cells containing $CdSO_4.8/3H_2O$ was then prepared in the ordinary manner at room temperature. For the two monohydrate cells it was necessary to keep the materials hot. This was done in an oven with the thermostat set for 85° C. The paste was prepared from the mercurous sulfate, the hot saturated solution, and crystals of $CdSO_4.H_2O$. The paste was introduced as quickly as possible into the cells, which also had been heated. Blanks with ground-glass stoppers were used, and these were sealed with collodion.

3. TEMPERATURE CONTROL OF THE CELLS AND MEASUREMENT OF ELECTROMOTIVE FORCE

The cells were placed in an oil bath with thermostatic control, variations from any specified temperature amounting to about ±0.05° C. The emf measurements at various temperatures were made directly against the Bureau's reference cell, which is a part of the primary standard of emf maintained always at 28° C. When the differences in emf of the cells under test from the reference cell were not more than 0.002 volt, the readings could be made on the comparator described by Brooks [7]. Otherwise, measurements were made on a Wolff potentiometer.

Because of slight variations in temperature of the oil bath and the large temperature coefficient of cells containing the high-temperature modification of $CdSO_4$, the emf readings are significant to about 10 microvolts. This, however, is sufficiently accurate for the present purpose.

Temperatures of the oil bath were read on a calibrated mercury thermometer which had a range of −11° to +53° C, graduated to tenths of a degree. All corrections, including that for the emergent stem, have been applied.

Successive measurements at decreasing temperatures could be made rather quickly as the cells had little hysteresis. Many exploratory observations were made, but these have been omitted from table 2, which is limited to the observations for which ample time was allowed for equilibrium conditions to be attained. Rising temperatures, however, resulted in considerable hysteresis of the cells containing the monohydrate salt. This is further discussed in later paragraphs.

III. EXPERIMENTAL RESULTS

1. SOLUBILITY MEASUREMENTS

Determinations of the solubility of both modifications of cadmium sulfate are plotted in figure 1, and values at regular temperature intervals read from the curves are given in table 1. All of the values are the result of measurements made during the present work, with the one exception of that at 10° C, which has been taken from the International Critical Tables [8]. This is marked ICT in the table and in the figure. No determination was made by us at this point

because of the difficulty in maintaining this temperature during the long period of shaking the solutions.

TABLE 1.—*Solubilities of cadmium sulfate*

Temperature	Solubility (mole of $CdSO_4$ per mole of H_2O)	
	$CdSO_4.8/3H_2O(s)$	$CdSO_4.H_2O(s)$
°C		
0	0.0655	----------
10 (ICT)	.06555	----------
15	.06566	----------
20	.06583	----------
25	.06607	----------
30	.06642	----------
35	.06693	----------
40	.06767	----------
43.4	.06828	0.06828
45	.06860	.06792
50	.06964	.06686
60	----------	0649

The solubilities are expressed as moles of $CdSO_4$ in 1 mole of H_2O. This is necessary as the other part of the work (not reported here) included similar determinations in D_2O. Saturation equilibrium

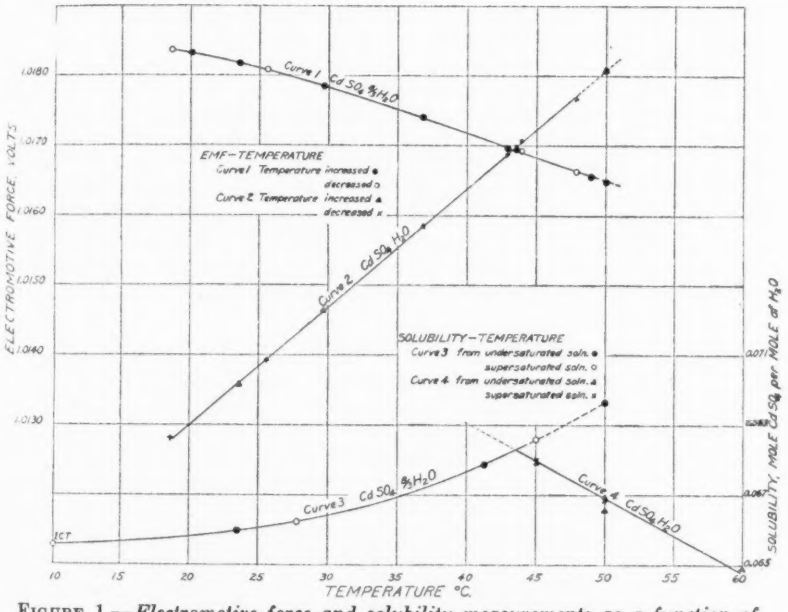

FIGURE 1.—*Electromotive force and solubility measurements as a function of temperature.*

Intersections at 43.4° C indicate a transition at this temperature.

was approached from undersaturated and supersaturated solutions, and care was taken to assure ourselves which crystalline form was present. This has necessitated discarding some of the earlier determinations, especially those at 50° C, when erratic values were undoubtedly caused by the presence of both crystalline forms.

Solubility curves of the two crystalline forms intersect at 43.4° C, which is therefore the transition temperature. This is confirmed by the measurements of emf. Measurements of the solubility of $CdSO_4.8/3H_2O$ have been extended above 43°, although the salt is metastable above this temperature. This can be done only under the condition that no other modification of the salt is present. Up to 50° C the results fall on an extension of the curve for the solubility of $CdSO_4.8/3H_2O$ below the transition temperature. Either metastable modification is more soluble than the stable modification at the same temperature.

Vosburgh and Eppley [9] determined the relation between emf and concentration of cadmium sulfate in unsaturated standard cells. By using their data, our observed differences in emf for the two kinds of cells, and the measured solubility of $CdSO_4.8/3H_2O$, it is possible to estimate the solubility of the metastable salt at temperatures below the transition point. For example, the calculated value at 25° C is 0.0726 mole of $CdSO_4$ per mole of water. This value lies on a linear extension of the monohydrate curve of figure 1. It appears to be entirely possible to make measurements of the solubility of this salt in the region of its metastability, but this has not been done.

2. ELECTROMOTIVE FORCE

Wide differences between the emf of the two kinds of cells are apparent, except at the transition point, 43.4° C, where the emf are equal. The observed values are given in table 2 and figure 1. Curve 1 in figure 1 is for cells containing the usual salt, $CdSO_4.8/3H_2O$. These cells are the ordinary saturated type. Above 43° C the cells are in a metastable condition. The general characteristic of these cells shows a decreasing emf with increasing temperature, that is, the temperature coefficient is negative. Particular values of emf read from the curve agree substantially with values computed from the international temperature formula [10]. These cells are, therefore, representative of Weston normal cells, and they provide a satisfactory criterion by which to judge the monohydrate cells.

TABLE 2.—*Observed electromotive forces*

[Values are given in the order in which they were taken]

Temperature	Cells with $CdSO_4.8/3H_2O$(s)			Cells with $CdSO_4.H_2O$(s)		
	No. 1028	No. 1030	Mean	No. 1026	No. 1027	Mean
°C	*Int. volts*	*Int. volts*	*Int. volts*	*Int. volts*	*Int. volts*	*Int. volts*
42.90	1.016986	1.017005	1.016996	1.016879	1.016871	1.016875
47.87	6619	6625	6622	7659	7693	7676
25.58	8082	8089	8086	3937	3932	3934
18.66	8369	8369	8369	2799	2824	2812
20.07	8323	8324	8324			
23.56	8173	8182	8178	3578	3569	3574
29.66	7850	7855	7852	4638	4637	4638
36.81	7408	7409	7409	5833	5849	5841
43.51	6940	6941	6941	6986	6956	6971
48.90	6550	6559	6555			
49.94	6475	6458	6467	8077		8077
43.90	6932	6921	6926	7078	7090	7084

Electromotive forces of the cells containing $CdSO_4.H_2O$, which is metastable at all temperatures below 43°, curve 2 of figure 1, are noticeably lower in this range. For these the temperature coefficient is positive. The measurements on these cells could not be extended above 50° C, because of limitations imposed by the cadmium amalgam employed in constructing them. This contained 10 percent of cadmium by weight. Such an amalgam at ordinary temperatures consists of both solid and liquid phases; but when the temperature is raised above 50° C, the solid phase is completely converted into the liquid phase, and the emf of the cells begins to fall rapidly.

Electromotive forces at uniform temperature intervals read from the curves are given in table 3.

TABLE 3.—*Electromotive forces of cells containing* $CdSO_4.8/3H_2O$ *and* $CdSO_4H_2O$

Temperature	Electromotive force	
	$CdSO_4.8/3H_2O(s)$	$CdSO_4.H_2O(s)$
°C	*Int. volts*	*Int. volts*
20	1.01832	1.01300
25	810	384
30	783	468
35	751	553
40	718	638
43.4	695	695
45	682	723
50	649	808

3. TEMPERATURE COEFFICIENT

The change in emf per degree change in temperature can be obtained from the curves plotted in figure 1. For the cells made with the usual salt, $CdSO_4.8/3H_2O$, values of the coefficient change with temperature. The international formula for the relation of emf to temperature is

$$E_t = E_{20} - 0.0000406(t-20°) - 0.00000095(t-20°)^2 + 0.00000001(t-20°)^3.$$

Wolff's work [11], on which this formula was based extended from 0° to 40°C. It applies reasonably well, however, to 50° C. Beyond this point our values for the emf are not sufficiently reliable for a comparison to be made, the reason being uncertainty as to the condition of the amalgam.

The monohydrate cells have a linear relationship between temperature and emf in the range of the measurements. Between 20° and 50° C the formula can be expressed as

$$E_t = E_{43.4} + 0.000173(t-43.4°),$$

Where $E_{43.4}$ is the emf at 43.4° C, the equilibrium temperature for the two hydrates, and has the value 1.01695 international volts.

IV. THERMODYNAMIC DISCUSSION OF THE REACTION

The chemical reactions which take place in the two cells may be represented by the equations:

$$\mathrm{Cd(amalgam)}+\left(\frac{8/3}{m_1-8/3}\right)[\mathrm{CdSO_4}.m_1\mathrm{H_2O}](\text{saturated soln})+\mathrm{Hg_2SO_4(s)}\rightleftarrows\left(\frac{m_1}{m_1-8/3}\right)[\mathrm{CdSO_4}.8/3\mathrm{H_2O}](\mathrm{s})+2\mathrm{Hg(l)} \quad (1)$$

$$\mathrm{Cd(amalgam)}+\left(\frac{1}{m_2-1}\right)[\mathrm{CdSO_4}.m_2\mathrm{H_2O}](\text{saturated soln})+\mathrm{Hg_2SO_4(s)}\rightleftarrows\left(\frac{m_2}{m_2-1}\right)[\mathrm{CdSO_4}.\mathrm{H_2O}](\mathrm{s})+2\mathrm{Hg(l)}, \quad (2)$$

where m_1 and m_2 are the number of moles of H_2O associated with 1 mole of $CdSO_4$ in saturated solutions of the respective salts.

Since the free energy per mole of $CdSO_4$ is the same in the saturated solution as in the crystal in equilibrium with that solution, and since the free energy per mole of H_2O is the same in the solution as in the crystal, for considerations of *free energy changes* in the cells these complete equations may be simplified.

Reaction 1 may be written as

$$\mathrm{Cd(amalgam)}+\mathrm{Hg_2SO_4(s)}\rightleftarrows 2\mathrm{Hg(l)}+\mathrm{CdSO_4}\ (\text{in saturated } \mathrm{CdSO_4}.8/3\mathrm{H_2O}\ \text{soln}), \quad (1a)$$

and reaction 2 as

$$\mathrm{Cd(amalgam)}+\mathrm{Hg_2SO_4(s)}\rightleftarrows 2\mathrm{Hg(l)}+\mathrm{CdSO_4}\ (\text{in saturated } \mathrm{CdSO_4}.\mathrm{H_2O}\ \text{soln}). \quad (2a)$$

Equation 1a minus eq 2a gives

$$\mathrm{CdSO_4}\ (\text{in saturated } \mathrm{CdSO_4}.\mathrm{H_2O}\ \text{soln})\rightleftarrows\mathrm{CdSO_4}\ (\text{in saturated } \mathrm{CdSO_4}.8/3\mathrm{H_2O}\ \text{soln}). \quad (3)$$

The free energy changes accompanying these reactions are

$$\text{for eq 1, } \Delta F_1=-2\boldsymbol{F}\boldsymbol{E}_1$$

$$\text{for eq 2, } \Delta F_2=-2\boldsymbol{F}\boldsymbol{E}_2, \text{ and}$$

$$\text{for eq 3, } \Delta F_3=\Delta F_1-\Delta F_2=-2\boldsymbol{F}(\boldsymbol{E}_1-\boldsymbol{E}_2).$$

In these equations $\boldsymbol{F}$ is the value of the faraday and $\boldsymbol{E}_1$ and $\boldsymbol{E}_2$ are the emf of the $CdSO_4.8/3H_2O$ and $CdSO_4.H_2O$ cells, respectively. These are expressed as functions of the temperature in tables 2 and 3 and by the equations on page 461.

ΔF_3 is equal to the difference in the partial molal free energies of $CdSO_4$ in aqueous solutions, whose concentrations determined by the two hydrates in equilibrium with the solutions, are given in table 1 and figure 1.

At 43.4° C the emf of the two cells were found to be equal, that is $\boldsymbol{E}_1=\boldsymbol{E}_2$, which makes $\Delta F_3=0$ and the compositions of the two saturated solutions the same at this temperature. It follows, therefore, from electrochemical data that at 43.4° C the two crystalline modifications, $CdSO_4.8/3H_2O$ and $CdSO_4.H_2O$, are in equilibrium with each other. The transition temperature determined in this way agrees to 0.2° C with that determined directly by solubility measurements.

At temperatures below 43.4° C, E_1 is greater than E_2, and ΔF_3 therefore is negative. This means that at temperatures below 43.4° C, reaction 3 proceeds in the direction in which it is written and $CdSO_4.8/3H_2O$ is more stable than $CdSO_4.H_2O$.

Since E_1 is less than E_2 above the transition temperature, ΔF_3 in this range is positive and $CdSO_4.H_2O$ is more stable than $CdSO_4.8/3H_2O$.

V. HYSTERESIS EFFECTS

Hysteresis as a term applied to standard cells means abnormal temporary changes in emf resulting from abrupt changes in temperature. This defect, rarely serious in new cells of the ordinary type containing $CdSO_4.8/3H_2O$, may become a more serious source of error in old cells. On the other hand, the monohydrate cells exhibit large hysteresis effects even when new. When the temperature of the cells is increased, hysteresis effects are usually negligible in the ordinary type of cell, but a month or more may be required for the monohydrate cells to reach an equilibrium condition. When the temperature falls the monohydrate cells come to equilibrium more quickly, but several days may be required.

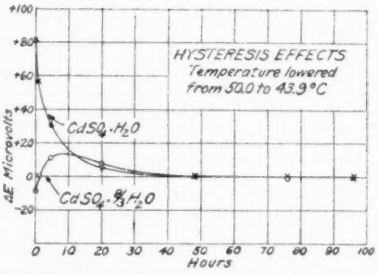

FIGURE 2.—*Comparison of hysteresis effects when temperature was decreased.*

ΔE represents the difference in electromotive force from the equilibrium value at the final temperature.

A comparison of the contrasting conditions of the two types of cells when subjected to changes of temperature is given in the following summary. It is evident that the larger hysteresis effect in both types of cells is associated with the temperature change which produces a precipitation of salt.

Temperature	Cells containing $CdSO_4.8/3H_2O$	Cells containing $CdSO_4.H_2O$
Increased	Salt dissolved. Emf decreased. Little or no hysteresis.	Salt precipitated. Emf increased. Large hysteresis effect.
Decreased	Salt precipitated. Emf increased. More hysteresis than above.	Salt dissolved. Emf decreased. Much less hysteresis effect than above.

The two types of cells contain identical materials except for the crystalline state of the cadmium salt, and it would seem that hysteresis, which has been attributed to many causes, is in part at least associated with the crystallization of the salt. New possibilities of studying the cause of hysteresis remain to be investigated.

Quantitative data on differences of emf, ΔE, from equilibrium values as a function of time are given in figures 2 and 3. The first of these compares values of ΔE for each type of cell when the tempera-

ture was decreased from 50° to about 44° C. Figure 3 shows values of ΔE of the same cells when the temperature was raised from about 37° to 43.5° C. In figure 3 it may be seen that much more time was required for cells containing $CdSO_4.H_2O$ to reach equilibrium than when the temperature was lowered, figure 2, by approximately the same number of degrees. Obviously, if the cells containing $CdSO_4.H_2O$ are to be of any practical value, hysteresis and the large temperature coefficient will necessitate good thermostatic control.

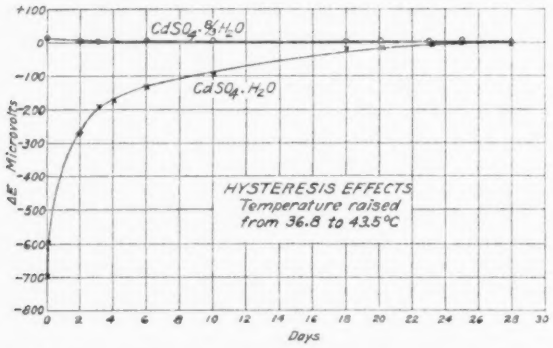

FIGURE 3.—*Comparison of hysteresis effects when temperature was increased.*

ΔE represents the difference in electromotive force from the equilibrium value at the final temperature.

VI. CONCLUSIONS

New lines of investigation on standards of emf are suggested by the results reported in this paper, but more work is needed before attempting to generalize too broadly. However, some of the more obvious practical considerations may be mentioned.

1. The stability of cells containing the metastable form of $CdSO_4$ at ordinary temperatures is sufficient to warrant a more careful study of these cells. They have been carried through a temperature cycle extending 25° below the transition point without indication of appreciable change, and they could of course be maintained indefinitely at a temperature of 43.4° C or more. Another form of saturated standard cell which has radically different properties from the customary Weston normal cell is therefore possible.

2. The transition temperature from $CdSO_4.8/3H_2O$ to $CdSO_4.H_2O$, which is 43.4° C, fixes an upper limit of temperature for the preparation of recrystallized salt to be used in the ordinary type of cell.

3. Since the temperature coefficient of the ordinary type of cell is negative and of the monohydrate type positive, it is possible to make combinations which would have very small values of $\Delta E/\Delta T$ over a limited range of temperatures. The value in volts of $\Delta E/\Delta T$ at the transition temperature is -0.000069 for the ordinary cells and $+0.000173$ for cells containing $CdSO_4.H_2O$. A series-connected combination of five of the former and two of the latter would have an emf which would change less than 1 part in 1 million per degree centigrade.

4. The contrasting hysteresis effects of the two types of cells suggest new methods of studying the causes of hysteresis. Obviously, close

regulation of temperature is necessary if satisfactory results are to be obtained with cells containing $CdSO_4.H_2O$.

5. The transition temperature, 43.4° C, between the two forms of cadmium sulfate is a fixed constant of nature which may ultimately be determined with greater accuracy than has been possible in the present work. At this transition temperature the emf of two differing types of cells containing the respective salts must be equal, assuming that the individual cells are not subject to secondary effects caused by impurities, variations in acidity, etc. The cells represented by eq 1 and 2 on page 462 are, for the present discussion, considered as ideal cells, differing only in the crystal structure of the cadmium sulfate. They are both in stable equilibrium at the transition temperature and should, therefore, be permanent. The numerical value assigned to the emf at this point depends on the units employed. In the present paper the results are given in terms of international volts, but whatever units may be chosen, equality of emf of the two systems at the transition temperature is independent of the units. One type of cell serves as a check on the other, and when equality of emf is obtained at the known transition temperature, the measurement carries the proof of its own validity. It might serve also as a means for judging the constancy of groups of cells over a period of time, since any variation of the temperature at which their respective emf are equal would mean that one or both of them were varying for reasons not expressed in eq 1 and 2 on page 462. On the other hand, if the two kinds of cells continued for a long period of time to have the same emf at the fixed transition temperature, it would be good evidence of the constancy of both, and the laboratory would have a new and radically different means of judging the constancy of its reference standard. Such a goal, however, could be attained only as a result of more precise work on the monohydrate cell than has been possible at this time.

VII. REFERENCES

[1] F. Mylius and F. Funk, Ber. deut. chem. Ges. **30,** 824 (1897).
W. Jaeger, Die Normalelemente, p. 83 (1902).
F. A. Wolff and C. E. Waters, Bul. BS **3,** 629 (1907) S67.
F. E. Smith, Phil. Trans. **207,** 396 (1908).
G. A. Hulett, Phys. Rev. **32,** 268 (1911).
[2] H. O. Hofman and W. Wanjukow, Trans. Am. Inst. Mining Engrs. **43,** 563 (1912).
[3] C. D. Carpenter and E. R. Jette, J. Am. Chem. Soc. **45,** 578 (1923).
[4] E. Wiedemann, Wied. Ann. **17,** 572 (1882).
Lord Rayleigh, Trans. Roy. Soc. (London) **176,** 781 (1885).
E. Cohen, Z. phys. Chem. **14,** 53 (1894).
H. L. Callendar and H. T. Barnes, Proc. Roy. Soc. (London) **62,** 150 (1897).
W. Jaeger, Wied. Ann. **63,** 354 (1897).
H. T. Barnes, J. Phys. Chem. **4,** 1 (1900).
[5] F. A. Wolff and C. E. Waters, Bul. BS **4,** 1 (1907) S70.
[6] Unpublished records of the NBS.
[7] H. B. Brooks, BS J. Research **11,** 211 (1933) RP 586.
[8] Int. Crit. Tables **4,** 222 (1928).
[9] W. Vosburgh and M. Eppley, J. Am. Chem. Soc. **45,** 2271 (1923).
[10] Report of London Conference on Electrical Units and Standards (1908).
[11] F. A. Wolff, Bul. BS **5,** 309 (1908) S104.

WASHINGTON, January 6, 1941.